CARBON NANOTUBE BASED POTENTIOMETRIC APTASENSORS FOR PROTEIN DETECTION

Ali Düzgün

Dipòsit Legal: T.616-2013

CARBON NANOTUBE BASED POTENTIOMETRIC APTASENSORS FOR PROTEIN DETECTION

DOCTORAL THESIS

Ali Düzgün

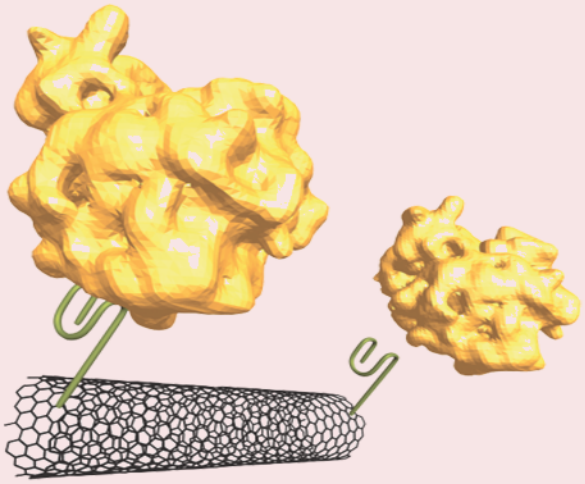

UNIVERSITAT ROVIRA I VIRGILI

2012

CARBON NANOTUBE BASED POTENTIOMETRIC APTASENSORS FOR PROTEIN DETECTION

DOCTORAL THESIS

Ali Düzgün

UNIVERSITAT ROVIRA I VIRGILI

2012

Ali Düzgün

CARBON NANOTUBE BASED POTENTIOMETRIC APTASENSORS FOR PROTEIN DETECTION

PhD Thesis

Supervised by Prof. Francesc Xavier Rius Ferrús

Departament de Química Analítica i Química Orgànica

UNIVERSITAT ROVIRA I VIRGILI

TARRAGONA, SPAIN

2012

UNIVERSITAT ROVIRA I VIRGILI
DEPARTAMENT DE QUÍMICA ANALÍTICA I QUÍMICA ORGÀNICA

Campus Sescelades
Carrer Marcel·lí Domingo s/n
43007 Tarragona
Tel. +34 977 55 97 69
Fax +34 977 55 84 46
e-mail: secqaqo@urv.cat

Prof. FRANCESC XAVIER RIUS FERRÚS, Professor at the Department of Analytical Chemistry and Organic Chemistry at the Universitat Rovira i Virgili

CERTIFIES THAT:

that the Doctoral Thesis entitled: "CARBON NANOTUBE BASED POTENTIOMETRIC APTASENSORS FOR PROTEIN DETECTION", submitted by ALİ DÜZGÜN to obtain the degree of Doctor by the Universitat Rovira i Virgili, has been carried out under my supervision, in the Department of Analytical Chemistry and Organic Chemistry at the Universitat Rovira i Virgili, and all the results presented in this thesis were obtained in experiments conducted by the above mentioned student.

Tarragona, December 12th, 2012

Prof. Francesc Xavier Rius Ferrús

ACKNOWLEDGMENTS

I would like to give my sincere thanks Prof. F. Xavier Rius for giving me the opportunity to conduct my PhD study in his group and for invaluable help and support throughout the PhD study. Both his scientific and personal experience have been really important in my personal development. I appreciate the active cooperation of Dr. Alicia Maroto, Dr.Pascal Blondeau, Dr. Santiago Macho, Dr. Francisco Andrade and Dr. Jordi Riu.

I would also like to acknowledge the Spanish Ministerio de Ciencia e Innovación (Research Projects CTQ2007-67570/BQU and CTQ2010-18717) and the Universitat Rovira i Virgili for providing a PhD fellowship.

Biggest special thanks to my family, my dad Vahid Düzgün, mum Nahiye Düzgün, sister Eylem Türkoğlu and brother Hakan Düzgün who has been always supporting me and respecting my decisions during the most difficult parts of life.

I would like to thank my close friends where we are always together in hearts; Mahir, Mehmet and Ali İmran Şirin, Talip Taş, Erkan Tahhuşoğlu, A. Kerem Subaşı, M. Özgen Paşa, Onur Bekçi, Selim Eşki, Yaser Çekmece and Talip Şirin from Hatay. Sevilay Karlık, Murat Altın, Onur Canlı, A. Özhan Aytekin and İsmail Sönmez from İzmir. I also would like to thank my Turkish friends that I met in Spain, especially for helping me not to forget speaking Turkish and of course for their support; Dr. Rükan Genç, Dr. Salih Özçubukçu, Erhan Özkal, Pınar Özkal, Sibel Demiroğlu, Sema Şirin, Ezgi Emre, Meriç Çağlar and all the rest.

I would like to thank Professor Kalle Levon being really wise and friendly towards me. Our meetings and table-hockey games at NYU-Poly have been fun and educative. I also give my sincere thanks to Professor Ciara O'Sullivan, and Dr. Teresa Mairal for their valuable scientific contribution. All present and past Chemometrics, Qualimetrics and Nanosensor group members, especially, Dr. Gaston A. Crespo who has always been helping me from the beginning of my PhD. In the same way, I thank my friends Dr. Enrique Parra, Dr. Xavi Rius-Ruiz, Dr. Gustavo A. Zelada, Jordi Ampurdanes and Ricardo Acosta for the good times.

I would like to express my deep and sincere gratitude to my wife, Dr. Nihal Ertürk Düzgün who has supported me in each moment of the thesis first as friend, and later as wife. Thank you for trusting me. And thank you for making me happy. I love you.

Table of Contents

SUMMARY

Rapid diagnosis of most illnesses has a vital importance for providing the appropriate cure and hence controlling public health concerns. Fast and accurate detection of large biomolecules, specifically proteins, is one of the major steps regarding the subject. Over recent years, several detection methodologies have been developed. However, almost all of the developed methods either required very complex techniques to be applied, or a long time to obtain the results. The most commonly used techniques were specific label requiring immunoassays. They generally require highly trained staff and complex equipment which results in an expensive and relatively slow methodology.

To improve performance characteristics and operational conditions such as obtaining higher limits of detection or faster detection time and even higher sensitivity, nanostructured materials have been incorporated to the mentioned biosensing platforms. Electrochemical methods, but especially potentiometry was among the simplest and fastest. Potentiometric solid-state electrodes have been one of the most promising candidates to date. They still are one of the best options to detect charged ions. However, they failed to detect relatively larger molecules due to the membrane based structure that does not allow any transport of large molecules through the solution-transducer interface. Due to the properties of the proteins, several challenges, mostly related to the analyte size and the recognition element structure, were still needed to overcome.

The main objective of the thesis was to develop, characterize and utilize a new type of direct potentiometric sensors based on a layer of single-walled carbon nanotubes (SWCNTs) as ion-to-electron transducers, and aptamers as recognition layer.

In the literature screening, we noticed that recent advances in biotechnology enabled scientists to design relatively short DNA/RNA fragments (aptamers) that were able to bind relatively large molecules such as proteins or even bacteria. They were highly selective and sometimes specific to the target molecules, and had better physical stability compared to antibodies. So we decided to choose aptamers as recognition elements to use in the developed sensors.

Carbon nanotubes were chosen as transducing materials as they were showing excellent electrochemical properties that we needed.

With the present thesis we report a new type of label-free potentiometric solid state carbon nanotube based aptasensors that can detect large analytes, as case example proteins, in a rapid (almost instantaneous), selective and sensitive way, for the first time. The developed sensors successfully responded to analyte protein (human α-thrombin) within physiological human serum levels.

Some drawbacks of the developed sensors are the reproducibility and stability issues. These are thought to be caused by the lack of proper blocking of the sensor surface. Introducing proper blocking methodology and a better deposition method for the transducer layer is also considered as a future development aspect.

The work done in the present doctoral thesis is structured into three main parts. The first part (Chapters 1 to 4) introduces recent advances in nanostructured material usage in potentiometry and explains the methodology. Second part (Chapter 5) shows proof of concept and optimized applications of the developed sensors. And lastly the third part (Chapters 6 and 7) focuses on characterization and comparison studies and finally summarizes the thesis.

The present thesis divided into 7 chapters with the following specific information regarding to each section:

Chapter 1 presents a brief review of the current state of the art in potentiometric sensors with a particular focus on protein detection. It also introduces the general and specific objectives of the present doctoral thesis.

Chapter 2 explains the fundamental concepts related to chemical and biosensors, and potentiometric electrochemical detection. It also gives detailed information of the produced sensor's main elements and the analyte.

Chapter 3 focuses on reflecting the recent trends in nanostructured material use in potentiometry in an explanative way giving detailed examples for basic sensor types that are used.

Chapter 4 includes a description of all the apparatus, materials, and reagents used along the experimental chapters of the thesis with corresponding procedures. Also, microscopic and electrochemical characterization techniques are described with their corresponding objectives.

Chapter 5 focuses on applications. Two sensors are developed where both sensors uses aptamers as recognition elements and SWCNTs as transduction elements to detect thrombin in aqueous solutions.

Chapter 6 focuses on characterization of the sensor by trying to determine the number of active aptamers on the surface. It also compares the developed carbon nanotube based sensor with a PANI based one in terms of characterization and sensitivity.

Chapter 7 introduces the conclusions have been made and points out some ideas about further development of the sensors.

Finally, annexes are introduced to complete the doctoral thesis.

RESUMEN

El diagnóstico rápido de la mayoría de las enfermedades tiene una importancia vital para proporcionar el remedio adecuado y, por lo tanto, el control de problemas de salud. La detección rápida y selectiva de biomoléculas grandes, específicamente proteínas, es uno de los objetivos importantes en este campo. Durante los últimos años se han desarrollado varias metodologías de detección, sin embargo, para poder aplicar casi todos los métodos descritos, se requieren técnicas complejas o bien un tiempo prolongado de análisis. Las técnicas basadas en inmunoensayo son las más comúnmente utilizadas, aunque requieren un marcaje específico. Por lo general, estos métodos también requieren personal altamente capacitado y equipos complejos que se traduce en una metodología relativamente cara y lenta.

Para mejorar las características de rendimiento y las condiciones operativas, tales como la obtención de mejores límites, mayor sensibilidad o menor tiempo de detección, a las plataformas biosensoras mencionadas se han incorporado materiales nanoestructurados. En cuanto a técnicas de detección, los métodos electroquímicos, sobre todo la potenciometría, se encuentran entre las más simples y rápidas. Los electrodos potenciométricos selectivos a iones de estado sólido han sido uno de los candidatos más prometedores hasta la fecha. Todavía son una de las mejores opciones para la detección de iones cargados. Sin embargo, no pueden detectar moléculas relativamente grandes debido a la estructura de la membrana que no permite ningún transporte de moléculas voluminosas a través de la interfase solución-transductor. Debido a las propiedades de las proteínas, aún se necesitan superar varios desafíos, la mayoría relacionados con el tamaño y la estructura del analito a reconocer y al elemento de reconocimiento.

El objetivo principal de la tesis ha sido desarrollar, caracterizar y utilizar un nuevo tipo de sensores potenciométricos directos basados de una capa de nanotubos de carbono de pared sencilla (SWCNT) como transductores ion-electrón, y aptámeros como capa reconocimiento.

En el estudio de la bibliografía científica hemos observado que los avances recientes de la biotecnología permiten desarrollar fragmentos de ADN/ARN relativamente cortos (aptámeros) que son capaces de unirse a moléculas relativamente grandes, tales como proteínas o incluso bacterias. Estos segmentos son muy selectivos, a veces específicos, a las moléculas objetivo y tienen una mejor estabilidad física frente a los anticuerpos. Por ello decidimos elegir los aptámeros como elementos de reconocimiento para utilizarlos en los sensores desarrollados.

Los nanotubos de carbono se eligieron como materiales de transducción ya que muestran propiedades electroquímicas excelentes para convertir el proceso de reconocimiento químico en una señal eléctrica medible.

En la presente tesis aportamos por primera vez un nuevo tipo de aptasensores potenciométricos de estado sólido basados en nanotubos de carbono que pueden detectar analitos grandes, como por ejemplo proteínas, de manera rápida (casi instantánea), selectiva, y sensible sin necesidad de marcaje químico. Los sensores desarrollados responden correctamente a la proteína analito *(α*-trombina humana) dentro de los niveles fisiológicos en el suero humano.

Las mejoras a introducir en el futuro en los sensores desarrollados se refieren principalmente a la reproducibilidad y la estabilidad. Los valores relativamente bajos de estos parámetros se cree que pueden estar causados por la falta de bloqueos adecuados de la superficie del sensor. También se consideran como aspectos a desarrollar en el futuro la introducción de la metodología apropiada de bloqueo y un método de deposición mejor para la capa de transducción.

El trabajo realizado en la actual tesis doctoral se estructura en tres partes principales. La primera parte (Capítulos 1 a 4) presenta los últimos avances en el uso de materiales nanoestructurados en potenciometría y explica la metodología empleada. La segunda parte (Capítulo 5) muestra la prueba de concepto y dos aplicaciones optimizadas de los sensores desarrollados. La tercera parte (Capítulos 6 y 7) se centra en la caracterización y estudios de comparación y el último capítulo corresponde a las conclusiones seguidas de los anexos.

La presente tesis está dividida en 7 capítulos con la siguiente información específica en cada sección:

Capítulo 1 presenta una breve revisión del estado actual de la técnica en los sensores potenciométricos con un enfoque particular en la detección de proteínas. También introduce los objetivos generales y específicos de la presente tesis doctoral.

Capítulo 2 explica los conceptos fundamentales relacionados con sensores químicos y biosensores, y la detección electroquímica potenciométrica. También da información detallada de los elementos principales del sensor producido y el analito.

Capítulo 3 se centra en reflejar las tendencias recientes en el uso de materiales nanoestructurados en la potenciometría de una forma pedagógica, dando ejemplos detallados para los tipos de sensores básicos que se utilizan.

Capítulo 4 incluye un descripción de todos los aparatos, materiales y reactivos utilizados a lo largo de los capítulos experimentales de la tesis con los procedimientos correspondientes. También, se describen la caracterización microscópica y electroquímica con sus objetivos correspondientes.

Capítulo 5 se centra en las aplicaciones. Se aportan dos sensores que utilizan aptámeros como elementos de reconocimiento y SWCNTs como elementos de transducción para detectar la trombina en soluciones acuosas.

Capítulo 6 se centra en la caracterización del sensor al tratar de determinar el número de aptámeros activos en la superficie. También compara el sensor desarrollado basado en nanotubos de carbono con otro de polianilina, PANI, en términos de caracterización y sensibilidad.

El capítulo 7 presenta las conclusiones que se han alcanzado y señala algunas ideas sobre el desarrollo ulterior de los sensores.

Por último, los anexos se presentan para completar la tesis doctoral.

CHAPTER 1

INTRODUCTION

1.1. State of the art

Potentiometry, although currently is one of the important analytical techniques in the daily practice in many laboratories, has been used since the early years of the last century [Hildebrand 1913, Bakker and Pretsch 2001, Pretsch 2007, De Marco and Clarke 2009]. Potentiometry is addressed mainly to charged small cations and anions. Potentiometric detection of large analytes, such as proteins, became a possibility by the introduction of the first potentiometric immunoelectrode by Janata et al [Janata 1975]. It was based on the electromotive force generated by the antibody-antigen interaction in the solution being analysed. This seminal work has been enlarged by the scientific community as briefly explained below. Throughout the years, the incorporation of different electrochemical sensing mechanisms and the development of appropriate measuring instruments have enabled the improvement of potentiometric methods to determine different types of analytes.

The first attempts addressed to the direct potentiometric detection of proteins, that is, the recording of the instrumental signal without any need of adding labels or further reagents, based on the potential generated by the interaction between receptor (linked to the electrode) and the proteins in the test solution, that also focused to explain the underlying phenomena, started in the mid-seventies [Janata 1975], but they could not correctly explain the sensing mechanism. Similar experimental results were obtained in the potentiometric detection of the protein concentrations, even when the research groups have a potentiometric signal which is usually a few mV, by using antibody-antigen couple in order to detect the potential difference originated in the immunoreactions events using chemically modified electrodes [Aizawa 1978, Yamamoto 1978, Aizawa 1979, Yamamoto 1980, Feng 2000]. The principles applied regarding the measurement of protein-related potentials were; charge redistribution, streaming potential, lipid membrane dipole potential and electrode surface potential. These principles later led to the construction of different variations of composite modified electrodes; a polypyrrole modified platinum electrode, on which the human immunoglobulin G (IgG) was immobilized, acts as an effective immunosensor for anti-IgG (from goat) [Taniguchi 1986]. A layer of plasma-

polymerized Nafion film (PPF) deposited on the platinum electrode surface, which was positively charged with tris(2,2'-bipyridyl)cobalt(III) ($Co(bpy)_3^{3+}$) and subsequently negatively charged with gold nanoparticles containing adsorbed hepatitis B surface antibody (HBsAb) assembled by layer-by-layer technique to detect hepatitis B surface antigen [Tang 2005a]. And finally, an integrated automatic electrochemical immunosensor array for the simultaneous detection of 5-type hepatitis virus antigens (i.e. hepatitis A, hepatitis B, hepatitis C, hepatitis D, and hepatitis E) where 5-type hepatitis virus antibodies were immobilized onto a self-made electrochemical sensor array using nanogold particles and protein A as matrices [Tang 2010]. But in most of these reported works, the charge transfer and/or redistribution could not clearly be explained not to mention the problems on slow response and/or low sensitivity. As a consequence, immunosensors were left apart in the field of biosensors. The Donnan equilibrium theory has been used to explain the phenomenon when the antibody and the antigen form a layer, similar to a semi permeable membrane, on the surface of the electrode [Bergveld 1991]. Some of the most remarkable works were published by Baumann, Pfeifer and Engel during the beginning of nineties at the same Mainz Institute in Germany. The selective binding of 3-indole acetic acid (IAA) alkali phosphatase (AP) to respective antibodies immobilized on pre-treated titanium wires were studied potentiometrically by Pfeifer et al [Pfeifer 1993]. They optimized and investigated the conditions with; which the antigen IAA-Me could be detected with good sensitivity, selectivity, and reproducibility and they showed for the first time for a small antigen that - when carefully controlling the conditions - this type of selective detector works indeed sufficiently well. Its limit of detection goes down to less than 100 pmol/ml and its selectivity is good, if cross-reacting compounds are excluded. They concluded that the unspecific binding of the IAA-AP, most probably through its enzyme part to the immobilized protein, as well as to the polystyrene layer, or even through holes therein to the titanium oxide, takes place to a large extent. Pfeifer et al used pencil tips as graphite polymer material in order to detect atrazine by direct potentiometric detection [Pfeifer 1993]. They tried several methods to immobilize the antibodies against atrazine but only one turned out to be useful for the preparation of graphite based immunoelectrode; that was the electrode that incorporates bound glutardialdehyde to active sites of the graphite surface and subsequent cross-linking of the antibodies with glutardialdehyde. They assumed the source of the potential as due to the charge equilibrium on a structurally complicated surface of the electrode which is severely changed when an antigen docks to the antibody since this reaction yields not only electronic but geometric structural changes in the area of the antigenic determinants of the antibody, which in turn then changes local charge densities which may even be near one elementary charge. Engel et al described a

method to determine atrazine and its cross-reacting relatives in water sample based on Pfeifer's method [Engel 1994]. They could obtain a 50 ng/L limit of detection. On another side, direct electron transfer to/from the active site of the proteins has been studied in order to demonstrate the applicability of the direct electron transfer (DET) effect [Varfolomeev 1996] to potentiometric, amperometric and semi conductive biosensors. Tunneling of electrons has been shown as a possible way for the explanation of DET effects.

Another remarkable strategy of potentiometric detection was the incorporation of the recognition layer in a classical membrane structure (albeit with higher pore size) to detect proteins. Yuan et al. [Yuan 2004] developed an ultrasensitive potentiometric immunosensor using colloidal gold and polyvinyl butyral (PVB) as sol-gel matrixes to detect hepatitis B surface antigen (HBsAg). Similarly, Tang et al. incorporated Nafion, colloidal Ag (Ag), and PVB as matrixes to potentiometrically detect hepatitis B surface antigen via immobilizing hepatitis B surface antibody [Tang 2004a], and again Nafion, colloidal gold, and gelatin as matrixes to potentiometrically detect diphtheria antigen (Diph) via immobilizing diphtheria antibody (anti-Diph) [Tang 2004b] both on a platinum electrode. They also created a membrane-like sol-gel methodology to detect adrenal cortical hormone [Tang 2005b] and again a potentiometric immunosensor where nanoparticles mixture (containing gold nanoparticles and silica nanoparticles) and PVB as matrix for detection of diphtherotoxin (D-Ag) [Tang 2005c]. A new type of potentiometric immunosensor for the determination of human α-fetoprotein (AFP) was developed by Qiang et al. [Qiang 2006] where gelatin–silver film as a gentle carrier was used to immobilize anti-AFP on the surface of platinum disk electrode and glutaraldehyde was employed to improve the character of complex film. Zhou et al. [Zhou 2007] developed a poly(vinylchloride) (PVC) membrane based potentiometric immunosensor for the direct detection of alphafetoprotein. They chemisorbed Au colloid particle onto amino groups of ophenylenediamine, which were dissolved in plasticized PVC membrane. Then they immobilized alpha-fetoprotein antibody (anti-AFP) onto the surface of the Au colloid particle to prepare the potentiometric AFP immunosensor. As it can be seen from the above examples, the target is limited to antibodies due to the size limit of the membrane transport.

From all the reports explained above, it can be inferred that there have been problems about the selectivity, stability and the sensitivity of the potentiometric sensors to detect proteins. Therefore, alternatives should be devised to overcome the present hurdles. After the great revolution into the materials science during 1990's, new materials were disseminated into

others field. These materials have been employed in many applications since the end of the 1990's until to date enabling to overcome previous obstacles successfully.

Field effect transistors (FETs) have been the most promising potentiometric devices to determine large analytes until the work performed in the present thesis. FETs often measure the current flow across the transistor that contains a semiconducting channel whose conductivity is affected by external fields. In the case of analytical sensors, these external fields have an electrochemical origin. Therefore, although these transistors are measuring the current, the origin of the current change is a variation in the potential, or field effect. This is the reason why FETs are classified as potentiometric devices. Kong et al [Kong 2000] reported the first chemical sensor based on a recently developed FET that in turn was based on a single semiconducting SWCNT. The conducting channel in carbon nanotube FETs (CNTFETs) can be made of a single SWCNT, a few interconnected SWCNTs, or a network of numerous SWCNTs. Although the first CNTFETs were initially developed for the sensitive detection of gaseous substances, most subsequent CNTFETs have been used to detect large biocompounds such as proteins, DNA sequences, immunoglobulins and bacteria [Kauffman 2008a 2008b, Stern 2008].

Meanwhile, our group also reported successful applications of CNTFETs for the detection of *Salmonella infantis* and *Candida albicans* [Villazimar 2008, 2009], trace levels of potassium in water using an ion-selective membrane [Cid 2008a], human immunoglobulin G both in aqueous and physiological conditions [Cid 2008b, 2008c], picomolar detection of bisphenol A in water [Sánchez-Acevedo 2009], and finally SO_2 at room temperature based on organoplatinum functionalized SWCNTs [Cid 2009]. The use of SWCNTs in FETs raised the idea to use them in solid contact ion-selective electrodes (SC-ISEs) as transducing elements. Crespo et al successively used them to detect potassium in aqueous solutions [Crespo 2008a]. It was the first application of SWCNTs in an SC-ISE as transducing element. Later the same team investigated the transduction mechanism of SWCNTs in order to understand the underlying phenomena of the generated EMF [Crespo 2008b]. Considering the transduction ability of the CNTs combined with their capability to be functionalized, we thought that a recognition element could be covalently linked to them. This concept made it possible to eliminate the ion-selective membrane since it would restrict the mobility of the large analyte.

During the literature scan, we noticed that aptamers, short DNA/RNA fragments (from about 15 to 100 nucleotides) which could be designed in a selective process, called SELEX, could be good candidates as recognition elements due to their specific binding abilities to their targets

[O'Sullivan 2002]. This led the research group to try and assess the possibilities to use aptamers directly linked to CNTs as new recognition and transducing elements. This strategy could eliminate the ion-selective membrane and thus to be able to detect larger analytes such as proteins by the help of aptamers.

As will be shown throughout this thesis, carbon nanotubes, polyaniline and aptamers can be successfully integrated to provide facile, rapid and cheap sensors to detect large analytes potentiometrically.

Very recently, works indirectly resulting from the present doctoral thesis using nanostructured materials have been reported regarding direct potentiometric sensors that are going to be detailed in chapter 3 [Zelada-Gullién 2009, Washe 2010, Zelada-Gullién 2010].

1.2. Objectives

The main objective of this thesis is the development, characterization and application of a new type of direct potentiometric sensors based on a layer of single-walled carbon nanotubes (SWCNTs) as ion-to-electron transducers, and aptamers as recognition layer. These sensors have been compared to those using the well-known conducting polymer, polyaniline (PANI), as transducer layer.

This general objective is detailed in the following specific objectives:

1. Demonstration that a layer of purified single wall carbon nanotubes can be employed as efficient ion-to-electron transducer in direct potentiometric sensors and aptasensors.
2. Explanation of the transduction mechanism involved in direct potentiometric aptasensors based on carbon nanotubes
3. Design, construction, validation and testing of a new aptasensor based on thrombin binding aptamers (TBAs) as recognition layer as well as SWCNTs as transducers to detect thrombin in aqueous samples.
4. Miniaturization of direct potentiometric sensor and aptasensors based on carbon nanotubes using filter paper as the substrate to increase the versatility and decrease the production costs.
5. Testing, comparison, and characterization of polyaniline based sensors to SWCNTs based ones in order to better understand the underlying phenomenon of the sensing mechanism.

The main added value of this thesis is the exploration of the capability of carbon nanotubes and aptamers to build membrane-less direct (i.e. direct contact between receptors and targets) potentiometric sensors that are capable of sensing large charge analytes as proteins without using any type of labels. The new sensors are comparable in terms of performance characteristics to the existing conventional ion-selective electrodes. This thesis attempts for the first time to implement and explain the use of nanostructured material as the transducer and aptamers as recognition layers in the direct potentiometric sensing of proteins.

1.3. References

Aizawa, M., Suzuki, S., Nagamura, Y., Shinohara, R., Ishiguro, I., Applied Biochemistry and Biotechnology 1979, 4, 25-31

Bakker, E., Pretsch, E., TrAC Trends in Analytical Chemistry 2001, 20, 11-19

Bergveld, P., Biosensors and Bioelectronics 1991, 6, 55-72

Cid, C. C., Riu, J., Maroto, A., Rius, F. X., Analyst 2008a, 133, 1001-1004

Cid, C. C., Riu, J., Maroto, A., Rius, F. X., Analyst 2008b, 133, 1005-1008

Cid, C. C., Riu, J., Maroto, A., Rius, F. X., Current Nanoscience 2008c, 4, 314-317

Cid, C. C., Jimenez-Cadena, G., Riu, J., Maroto, A., Rius, F. X., Batema, G. D., van Koten, G., Sensors and Actuators B: Chemical 2009, 141, 97-103

Crespo, G. A., Macho, S., Rius, F. X., Analytical Chemistry 2008a, 80, 1316-1322

Crespo, G. A., Macho, S., Bobacka, J., Rius, F. X., Analytical Chemistry 2008b, 81, 676-681

De Marco, R., Clarke, G., ELECTRODES | Ion-Selective Electrodes. In Encyclopedia of Electrochemical Power Sources, Jurgen, G., Eds. Elsevier: Amsterdam, 2009, pp 103-109

Engel, L., Baumann, W., Fresenius' Journal of Analytical Chemistry 1993, 346, 745-751

Engel, L., Baumann, W., Fresenius' Journal of Analytical Chemistry 1994, 349, 447-450

Feng, C. l., Xu, Y. H., Song, L. M., Sensors and Actuators B: Chemical 2000, 66, 190-192

Hildebrand, J. H., Journal of the American Chemical Society 1913, 35, 847-871

Janata, J., Journal of the American Chemical Society 1975, 97, 2914-2916

Kauffman, D. R., Star, A., Chemical Society Reviews 2008, 37, 1197-1206

Kauffman, D. R., Star, A., Angewandte Chemie International Edition 2008, 47, 6550-6570

Kong, J., Franklin, N. R., Zhou, C., Chapline, M. G., Peng, S., Cho, K., Dai, H., Science 2000, 287, 622-625

O'Sullivan, C., Analytical and Bioanalytical Chemistry 2002, 372, 44-48

Pfeifer, U., Baumann, W., Fresenius' Journal of Analytical Chemistry 1993, 345, 504-511

Pretsch, E., TrAC Trends in Analytical Chemistry 2007, 26, 46-51

Qiang, Z., Yuan, R., Chai, Y., Wang, N., Zhuo, Y., Zhang, Y., Li, X., Electrochimica Acta 2006, 51, 3763-3768

Sánchez-Acevedo, Z. C., Riu, J., Rius, F. X., Biosensors and Bioelectronics 2009, 24, 2842-2846

Stern, E., Vacic, A., Reed, M. A., Electron Devices, IEEE Transactions on 2008, 55, 3119-3130

Tang, D., Yuan, R., Chai, Y., Zhang, L., Zhong, X., Dai, J., Liu, Y., Journal of Biochemical and Biophysical Methods 2004a, 61, 299-311

Tang, D. P., Yuan, R., Chai, Y. Q., Zhong, X., Liu, Y., Dai, J. Y., Zhang, L. Y., Analytical Biochemistry 2004b, 333, 345-350

Tang, D., Yuan, R., Chai, Y., Fu, Y., Dai, J., Liu, Y., Zhong, X., Biosensors and Bioelectronics 2005a, 21, 539-548

Tang, D. Q., Tang, D. Y., Tang, D. P., Bioprocess and Biosystems Engineering 2005b, 27, 135-141

Tang, D., Ren, J., Electroanalysis 2005c, 17, 2208-2216

Tang, D., Tang, J., Su, B., Ren, J., Chen, G., Biosensors and Bioelectronics 2010, 25, 1658-1662

Taniguchi, I., Fujiyasu, T., Tomimura, S., Eguchi, H., Yasukouchi, K., Tsuji, I., Unoki, M., Analytical Sciences 1986, 2, 587-588

Varfolomeev, S. D., Kurochkin, I. N., Yaropolov, A. I., Biosensors and Bioelectronics 1996, 11, 863-871

Villamizar, R. A., Maroto, A., Rius, F. X., Inza, I., Figueras, M. J., Biosensors and Bioelectronics 2008, 24, 279-283

Villamizar, R. A., Maroto, A., Rius, F. X., Sensors and Actuators B: Chemical 2009, 136, 451-457

Washe, A. P., Macho, S., Crespo, G. n. A., Rius, F. X., Analytical Chemistry 2010, 82, 8106-8112

Yamamoto, N., Nagasawa, Y., Sawai, M., Sudo, T., Tsubomura, H., Journal of Immunological Methods 1978, 22, 309-317

Yamamoto, N., Nagasawa, Y., Shuto, S., Tsubomura, H., Sawal, M., Okumura, H., Clinical Chemistry 1980, 26, 1569-1572

Yuan, R., Tang, D., Chai, Y., Zhong, X., Liu, Y., Dai, J., Langmuir 2004, 20, 7240-7245

Zelada-Guillén, G. A., Riu, J., Düzgün, A., Rius, F. X., Angewandte Chemie International Edition 2009, 48, 7334-7337

Zelada-Guillén, G. A., Bhosale, S. V., Riu, J., Rius, F. X., Analytical Chemistry 2010, 82, 9254-9260

Zhou, L., Yuan, R., Chai, Y., Electroanalysis 2007, 19, 1131-1138

CHAPTER 2

FUNDAMENTAL CONCEPTS

2.1. Introduction

This chapter presents a short overview of the principles of classical potentiometry when using ion-selective membranes and aptamers as recognition layer and carbon nanotubes and polyaniline, acting as transducer layer.

2.2. Chemical sensors and biosensors

According to the IUPAC definition [Thevenot 1999], "A chemical sensor is a self-contained integrated device that transforms chemical information, ranging from the concentration of a specific sample component to total composition analysis, into an analytically useful signal. Chemical sensors usually contain two basic components connected in series: a chemical (molecular) recognition system (receptor) and a physicochemical transducer. This latter sends the signal to the detection system which converts it into measurable data containing information. Biosensors are chemical sensors in which the recognition system utilizes a biochemical receptor." Thus biosensors can be classified according to the type of their transducer, the detection system and the recognition element.

Electrochemical detection shows some characteristics that are advantageous compared to other detection techniques such as optical, thermal or mass detection. For instance, electrochemical techniques are easy to miniaturize and display a low cost. Therefore, they can be applied to portable instruments. In addition, many electroanalytical methods can be applied in turbid solutions and, in many cased, show performance parameters comparable to other techniques.

Electrochemical sensors, which share the common characteristic of having an electrochemical detection system, can be classified according their transducing and recognition elements. The electrochemical signal can be generated by detecting the current (amperometry) or the potential in the absence of the current (potentiometry). Also; conductance and impedance, among other parameters, can be used for the detection. The amperometric and voltammetric sensors are characterized by their current-potential relationship with the electrochemical

system. Amperometric sensors can also be viewed as a subclass of voltammetric sensors. The general principles of electrochemical sensors have been extensively discussed [Janata 2009]. Commonly used electrochemical transducers are based on amperometry [Liu 2012], potentiometry [Vincke 1985, Musa 2011], conductometry [Watson 1987, Soldatkin 2012] and impedance spectroscopy [Keese and Giaever 1990, Ismail 2011]. Optical sensors are based on the detection of luminescence whether as a result of the generation of luminescent centers or by quenching them [Xia 2012]. Moreover, piezoelectric transducers are used in biosensors such as the quartz crystal microbalance (QCM) [Tessier 1993, Wang 2011], mechanical such as cantilevers [Florin 1995, Mostafa 2011] and temperature [Danielsson 1992], or magnetic [Kindavater 1990, Sinn 2011]. Biosensors that incorporate aptamers as recognition elements are named as “aptasensors” [O’Sullivan 2002].

Electrochemical sensors are frequently reviewed by many authors [Zhang 2008, Jacobs 2010, Carrara 2011, Ju 2011, Albrecht 2012, Malitesta 2012].

2.3. Potentiometry

Potentiometry is an electroanalytical technique which is based on measurement of potential generated in an electrochemical cell in absence of current. This measured electromotive force is primarily related to the activity of the target ion in solution. Potentiometric measurements enable selective detection of ions in presence of multitude of other substances. Classical potentiometric measurement system consists of two electrodes (working or indicator electrode and reference electrode), a potentiometer and a solution containing the analyte. In a system like the one depicted on Figure 2.3-1, the potential is measured by a high impedance voltmeter placed between a reference electrode e.g. Ag/AgCl electrode, and the ion-selective electrode. Reference electrode is an electrode with potential which is

a) Independent of the analyte and other ions in solution, and their activity,

b) Independent of temperature.

The potential of an indicator electrode depends on the concentration of the target analyte ion. This dependence is not absolute, so there is always a certain degree of selectivity. Here the classical potentiometric electrodes are names ion-selective electrodes (ISEs).

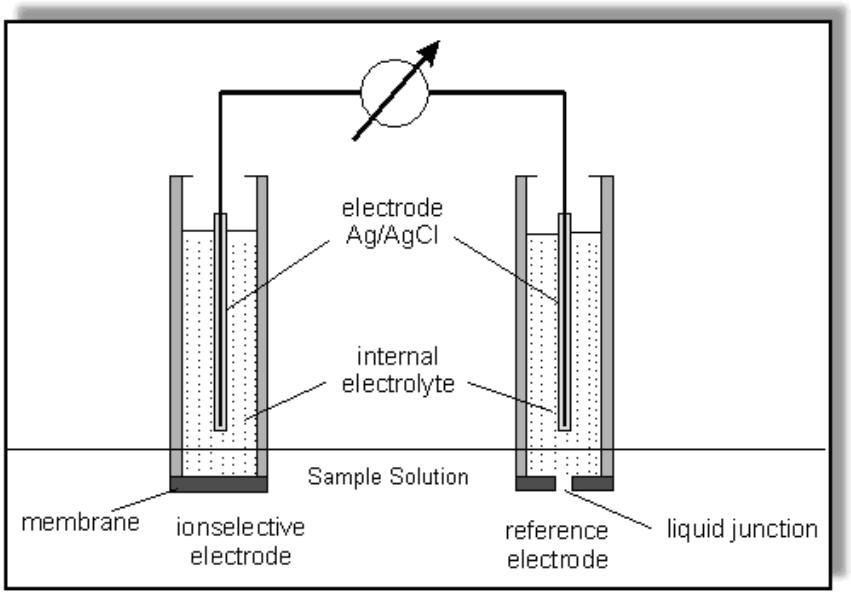

Figure 2.3-1 Conventional electrochemical cell.

The sensing mechanism in the ion-selective electrodes has been the source of a large discussion for over 30 years since there are several models that attempt to explain the mechanism using different factors and suppositions. Several models ranging from basic ones to others showing a high degree of complexity have been proposed. Bobacka *et al* [Bobacka 2008] summarize in his review the advantages and drawbacks of each model. To summarize, the most accepted theory is the phase-boundary potential model suggested by Bakker *et al* [Bakker 2004] that is based on the assumption of local equilibria at the aqueous/polymeric membrane interface.

Due to this detection system, optimized potentiometric ISEs can detect very low amounts of ions up to picomolar levels [Skokalski 1997]. Also they are not affected from the change of the solutions color or transparency. Therefore the ion-selective electrodes are widely applied in biological, industrial and environmental fields [Dimeski 2010]. Furthermore, the interest in developing small sensing devices for biomedical use is a promising trend [Wang 1999, Pretsch 2007].

The conventional ion-selective electrodes use an internal reference solution that is able to transduce the 'ionic current' in the membrane into the 'electronic current' in the conducting wire of the electrode. However, these classical ion-selective electrodes are not well suited for some applications. Although this type of ISEs are the most commonly used due to their high selectivity and reliability for the pH or other ions (e.g. Ca^{2+}, Cl^{-}, K^{+}), they display some disadvantages such as high ohmic resistance, the need for internal solution, the fragility of the membrane and vertically usage obligation [Michalska 2006]. Also they should be simpler, have

better mechanical flexibility and allow the miniaturization of the devices. Most of these disadvantages are overcome with the use of all-solid-state electrodes, specifically, solid state potentiometric electrodes that do not contain an internal reference solution.

2.3.1. Solid-state potentiometry

Solid-state potentiometry, as a subsection of potentiometry, emphasizes phenomena in which the properties of solids play a dominant role. This includes phenomena involving ionically and/or electronically conducting phases. The initial aims were the elimination of the liquid parts and change them with appropriate solid transducer as conductive polymers. Thus, designing much smaller and more rigid sensors would be possible. Many attempts [Michalska 2006] resulted in relative success but with some drawbacks such as high drift, low response stability and relatively higher limit of detection.

The main sensor types that use solid state potentiometry are built in a way that no liquid junction plays a role in the construction. Polymeric membrane ion-selective electrodes (ISEs) are currently one of the most widely applied chemical sensors [Zhu 2009, Anastasova-Ivanova 2010]. New theory and more applications of potentiometric ion sensors have been exploited after the detection limit of ISEs was pushed to trace levels [Bakker 2001]. Solid-contact ISEs have drawn much attention in this direction, since the solid inner contact eliminates ion flux in the membrane from inner filling solution [Sutter 2004]. As an excellent conductor, carbon nanotubes (CNTs) have been firstly used as the ion-to-electron transducer in solid-state ISEs by Crespo *et al* [Crespo 2008] to detect K^+ ions. Following this pioneering work, our group has used the concept for different applications such as: detection of perchlorate [Parra 2009], choline and derivatives [Ampurdanés 2009], Ca^{2+} in sap [Hernández 2010] and even as solid state reference electrodes [Rius-Ruiz 2011].

2.4. Direct potentiometric chemical sensors

Direct potentiometric chemical sensors are self-contained integrated devices that record the instrumental signal without any need of adding labels or further reagents. They are based on the potential generated by the direct interaction between the recognition element (usually linked to the transducer layer of the electrode) and the analyte. Depending on the transducing or recognition element as well as their basic construction, they can be named using different names such as carbon nanotube field effect transistors (CNT-FETs) or potentiometric aptasensors.

2.4.1. Carbon nanotube based sensors

Carbon nanotube based sensors are chemical sensors that incorporate CNTs mainly as transducing elements although, in some specific cases, they can also act as recognition elements.

2.4.1.1.Carbon nanotubes

CNTs are grapheme sheets rolled up into a nanoscale-tube [Saito 1998], which were rediscovered by Sumio Iijima [Iijima 1991]. A single sheet generates single-walled carbon nanotubes (SWCNTs) while multiple concentric sheets produce multi-walled carbon nanotubes (MWCNTs) (see figure 2.4-1). SWCNTs have a minimum diameter of about 0.4 nm and can reach up to 2 nm. Also lengths up to 1.5 cm have been reported [Huang 2004]. Such dimensions give rise to aspect ratios (length/diameter) of over ten million [Raffaellea 2005]. SWCNTs can be either metallic or semiconducting [Fischer 2006] depending on their chirality and diameter.

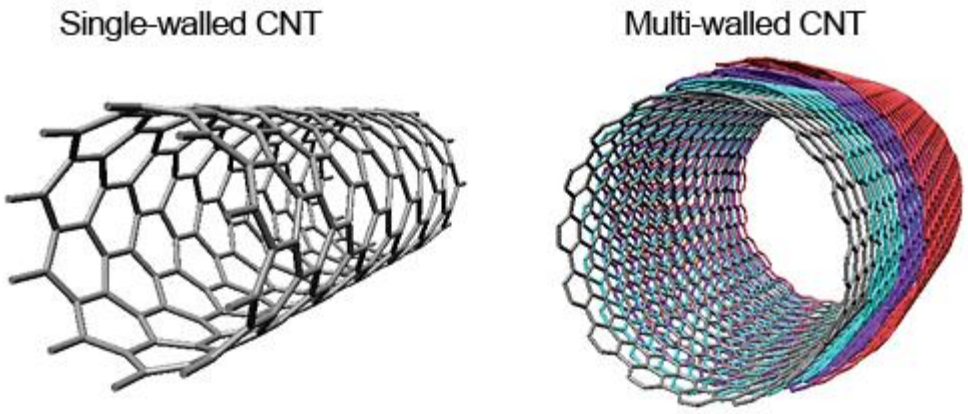

Figure 2.4-1 Schematic representation of the CNTs. A single-walled carbon nanotube (left) and a multi-walled carbon nanotube (right)

Noriaki *et al*, at the NEC Laboratory in Tsukuba have calculated dispersion relations for small-diameter nanotubes showing that about one-third of small-diameter nanotubes are metallic, while the rest are semiconducting, depending on their diameter and chiral angle [Noriaki 1993]. By contrast, MWCNTs have diameters from 10 to 200 nm and lengths up to hundreds of microns with an adjacent shell separation of 0.34 nm [Khare, R., and Bose, S. 2005]. They usually display a metallic character.

The properties of CNTs are very different depending on whether they are SWCNTs or MWCNTs [Saito 1998]. SWCNTs are stable up to 750 °C in air (but in an oxidizing atmosphere they start to

become damaged earlier) and up to 1.500 °C in an inert atmosphere. They have half the mass density of aluminum. Their unique structural features give SWCNTs exceptional physical and chemical properties [Dresselhaus 2001, Dai 2002, Zhou 2002]. Their incredibly high surface/volume ratio and their capacity for charge transfer makes them very important candidates for sensor applications. In addition to this feature, chemically inertness, functionalizability of carboxylated CNTs are the other essential properties. Furthermore due to the sp^2-hybridized carbon atoms in CNTs, a free electron cloud exists on the surface which enables rapid mobility of electrons.

There are many ways to roll a graphene structure to form a SWCNT, resulting in structural variations. These variations, as well as the tube diameter, determine the electrical properties displayed by the various types of tubes. The most fundamental of these properties is whether the tube will behave as a metal or as a semiconductor.

Although CNTs are not actually synthesized by rolling graphite sheets, it is possible to explain the different structures by considering the way graphite sheets might be rolled into tubes. An SWCNT can be formed by rolling a sheet of graphene into a cylinder along an (*n*,*m*) lattice vector in the graphene plane, where *n* and *m* are integers of the vector equation $OA = C_h = na_1 + ma_2$, which is known as the Hamada vector[Kim 2007]. The chiral angle (Θ) is formed between the Hamada vector and the unit lattice vector a1. The values of *n* and *m* determine the chirality and the diameter of a CNT (Figure 2.4-2, Table 2.4-1). The chirality in turn affects the conductance of the nanotube, its density, its lattice structure, and other properties. An SWCNT is considered metallic if the value resulting from (*n*-*m*)/3 is an integer. Otherwise, the nanotube is semiconducting [Dekker 1999]. Consequently, when tubes are formed with random values of *n* and *m*, we would expect two-thirds of nanotubes to be semi-conducting, and one third to be metallic [Saito 1998, Dai 2002].

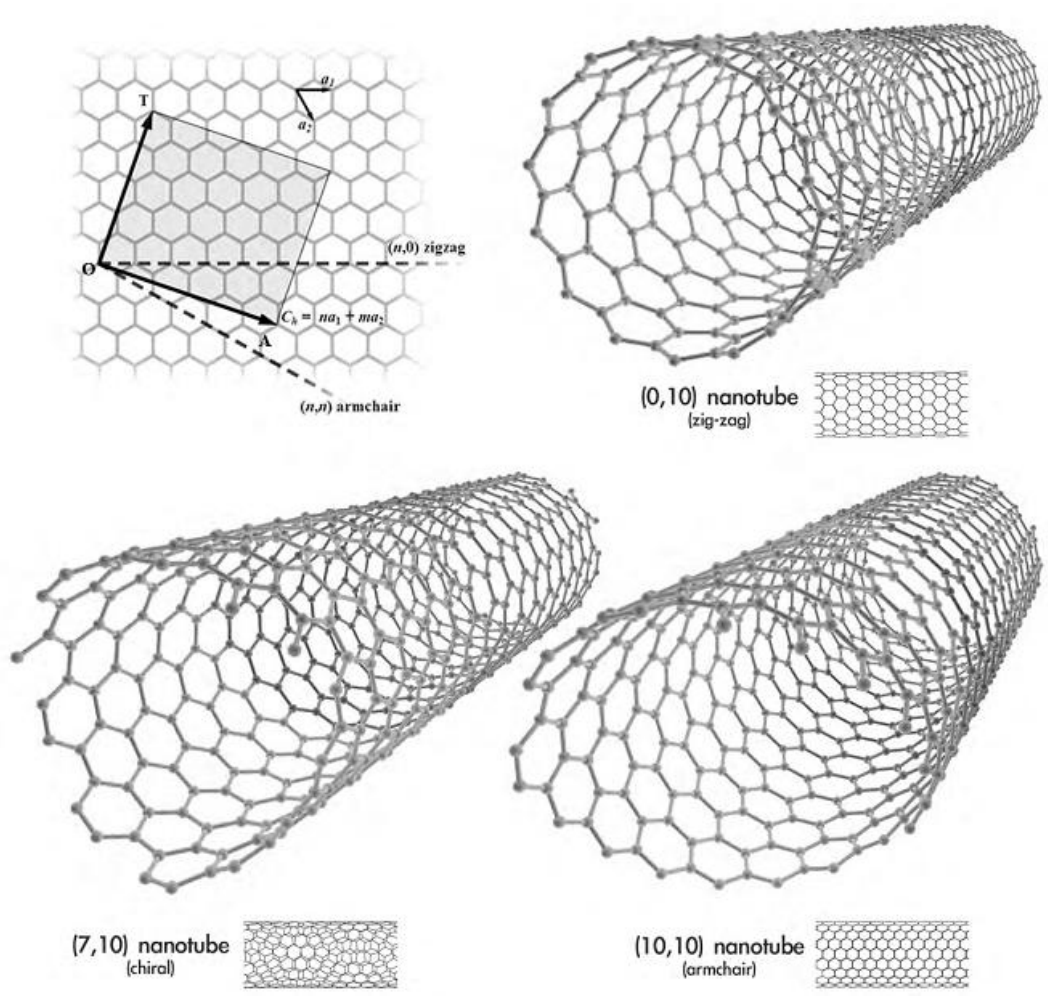

Figure 2.4-2 Diagram depicting different directions to roll a graphene sheet to create an SWCNT. Three different SWCNT structures resulting in graphene sheets rolled differently, a zigzag-type nanotube, an armchair type nanotube, and a chiral nanotube.

Table 2.4-1 Effect of integer coefficients on electric behavior and morphology of the carbon nanotubes.

Type	Integer coefficients	Chiral angle	Morphology	Electrical characteristics
Armchair	*n*=*m*	30°	No twist with respect to tube axis	100% metallic
Zigzag	*n*=0 or *m*=0	0°	Maximum twist angle	25% metallic 75% semiconducting
Chiral	Both *n* and *m* vary in value	Angle varies between 0° and 30°	Twist angle between no twist and maximum twist	

2.4.2. Carbon nanotube based aptasensors

CNT based aptasensors incorporate CNTs as transducers and aptamers as recognition elements.

2.4.2.1. Aptamers

Aptamers are small nucleotide fragments (approx. 15-100 bases) that are purposely isolated from random combinatorial libraries most commonly by an exponential enrichment method called SELEX (Systematic evolution of ligands by exponential enrichment). As a result, the unique three-dimensional structure for the binding of their target can be determined and synthetised. Aptamers can selectively or specifically recognize and bind virtually to any kind of targets. Those including, ions [Smironov and Shafer 2000], whole cells [Famulok 2000], drugs [Varani and Gallego 2001], toxins [Jayasena 1999], low molecular weight ligands [Famulok 1999], peptides [Wilson and Szostak 1999] and proteins [Mc Cauley 2003]. Many recent reviews about the therapeutic character of sensors, where aptamers are used as sensing elements, can be found in the literature [Hage 2010, Xu 2010, Hamula 2011, Citartan 2012, and Palchetti 2012].

As well as high affinity, aptamers also demonstrate high specificity. Using aptamers, targets can be discriminated on the basis of subtle structural differences such as the presence or absence of a hydroxyl group [Sassanfar and Szostak 1993] or a methyl [Haller and Sanow 1997]. Enzymes with similar activity and structure can be distinguished, as is demonstrated with the detection of a-thrombin and y-thrombin [Paborsky 1993]. More impressive is the ability of aptamers to distinguish between enantiomers, as was reported by Geiger *et al* [Geiger 1996], when L and D-arginine were discriminated. The high degree of specificity often seen in aptamers, sometimes even better than antibodies [Jenison 1994], is a result of the selective process in the SELEX.

The aptamer generation emerged from the experimentation of three independent groups, all of whom published their work in 1990. First, the Joyce group [Robertson and Joyce 1990] was looking for a new enzymatic activity of RNA. They used in vitro mutation, selection and amplification to isolate the enzymatic RNA, which became the basis for the current in vitro selection of aptamers. Then the Gold group was trying to identify in vitro the sequences of T4 DNA polymerase [Tuerk and Gold 1990]. The library they created was based on the natural structure but with the eight-loop randomized. They were the first to baptize the process of in vitro selection as SELEX, and the process was able to identify the natural target of the enzyme as the predominant. The authors patented their process. A month later Szostak and Ellington reported the use of in vitro selection to isolate molecules with specific ligand binding activities

[Ellington and Szostak 1990]. They created a library with 100 nucleotides of randomized sequences, related to any known oligonucleotide sequence. The targets had no previously identified nucleic acids ligand. This group coined the term aptamer, which comes from the Latin *aptus* meaning "to fit" and Greek *meros,* "region".

2.4.2.2.Target-aptamer interaction

The affinity of aptamers depends on the kind of target. Aptamers against small molecules have affinities in the micromolar range, as in the case of dopamine, 2.8 μM [Lorsch and Szostak 1994] or ATP, 6 μM [Kiga 1998]. Affinities in the nanomolar and sub-nanomolar range are found against some large molecules as proteins, for example, vascular endothelial growth factor (VEGF) with an affinity of 100 pM [Ruckman 1998], and keratinocyte growth factor, 1pM [Pagratis 1997].

The interactions between protein and aptamers include Van der Waals, hydrogen bonds and water mediated contacts [Gutfreund 1995]. About 30% of all interactions are non-specific bonds, mediated through Van der Waals forces; however, they are extremely important for the stability of the complex. The majority of the specific interactions involves hydrogen bonds [Schwabe 1997] and demonstrates some amino acid-base preferences. Cowan *et al* [Cowan 2000] demonstrated that 80 % of the binding energy was contributed by hydrogen bonds. The relative contributions of these and other forces, such as interaction with aromatic rings and Van der Waals forces have been also reported [Hermann and Patel 2000]. Water molecules also facilitate the contact by filling the empty spaces at the protein-aptamer interface and play an important role in complex formation [Tuerk and Gold 1990].

The Ellington Lab. in University of Texas at Austin introduced an aptamer database where it can be found the appropriate aptamers with their corresponding target interaction in selected scientific journals [http://aptamer.icmb.utexas.edu/].

2.4.2.3.Thrombin

Thrombin (commonly α -thrombin) is a pluripotent serine protease enzyme that plays a central role in homeostasis following tissue injury. It selectively cleaves the Arg-Gly bonds of fibrinogen to form fibrin and release fibrinopeptides A and B. The predominant form of thrombin in vivo is the zymogen, prothrombin (factor II), which is produced in the liver. The concentration of prothrombin in normal human plasma is 5-10 mg/dL. Prothrombin is a glycoprotein with a glycan content of ~12%. Prothrombin is cleaved in vivo by activated factor X releasing the activation peptide and cleaving thrombin into light and heavy chains yielding catalytically active

α-thrombin. α-Thrombin is composed of a light chain (A chain, MW ~ 6,000) and a heavy chain (B chain) (~31,000). These two chains are joined by one disulfide bond as can be seen in Figure 2.4-3 [Sigma-Aldrich Biofiles © 2012, Lundblad 1976].

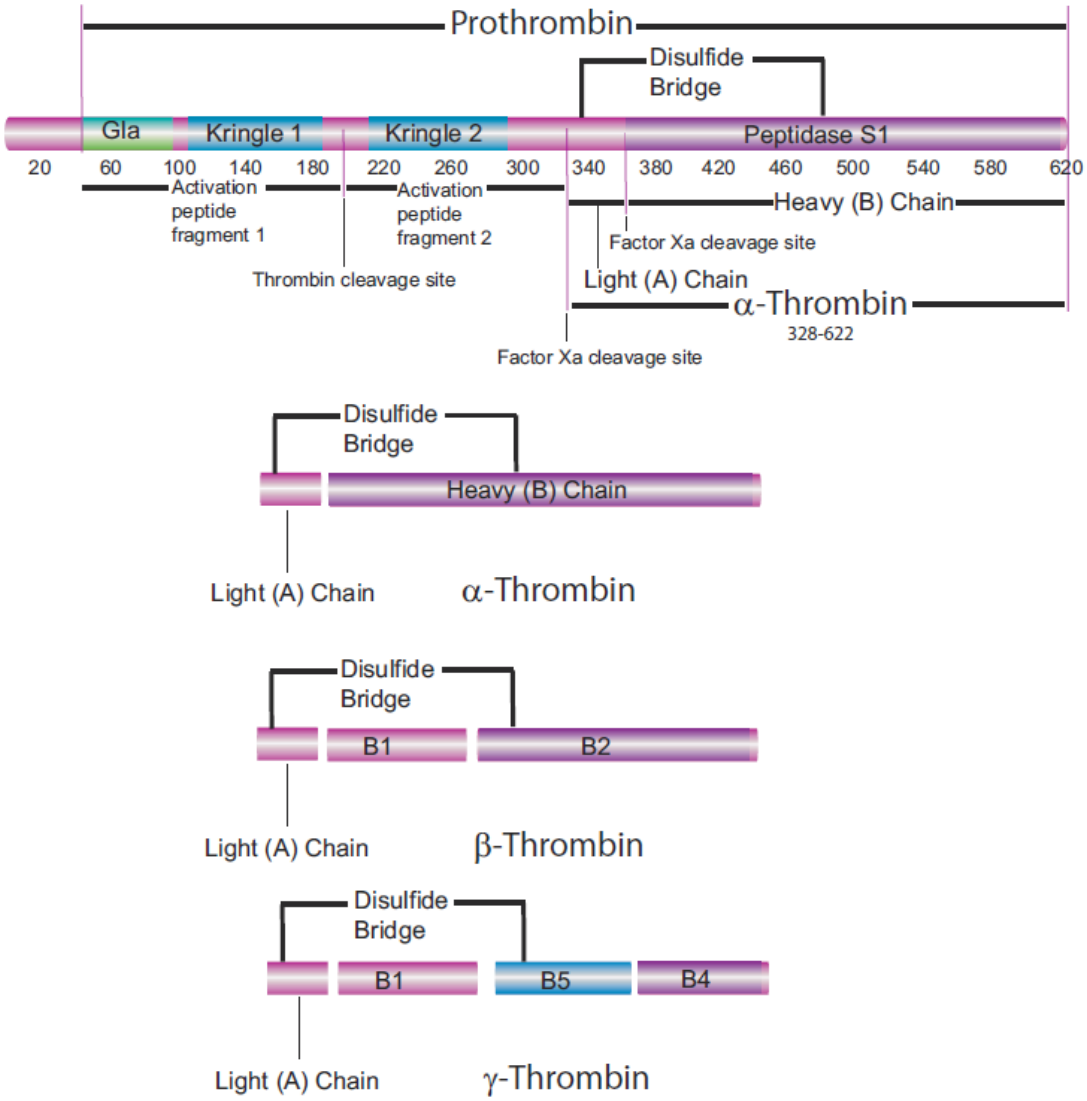

Figure 2.4-3 Diagram depicting different structural regions of thrombin protein [Sigma-Aldrich Biofiles © 2012].

There is not any known naturally occurring nucleic acid sequence that binds thrombin. One of the anti-thrombin aptamer sequences that shows a higher affinity constitutes the first example of an in vitro designed oligonucleotide targeted towards protein binding. The identified thrombin binding aptamer has a well-defined folded structure in solution [Bock 1992, Fukusaki 1993, Russo Krauss 2012]. α-thrombin binding affects two electropositive parts of the molecule, the fibrinogen-recognition and heparin-binding exosites. When thrombin is in contact with the aptamer, the aptamer adopts folded G-quadruplex structure [See Figure 2.4.4], the central part

of the structure is formed by two guanine quartets. The quartets are connected at one end by two TT loops, which span the two narrow grooves and at the other end by a TGT loop, which spans a wide groove of the mini-quadruplex.

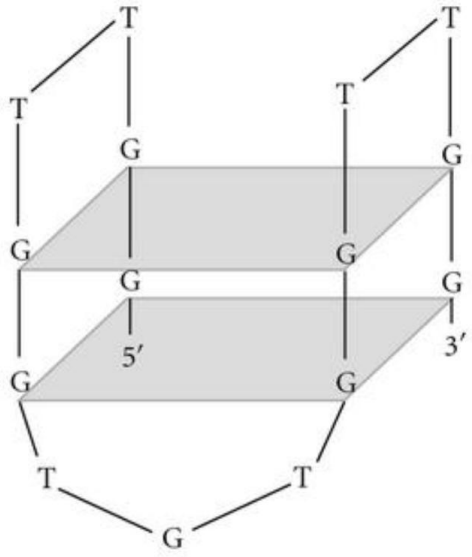

Figure 2.4-4 Schematic of thrombin binding aptamer.

The anti-thrombin aptamer can be applied as an inhibitor of thrombin activity [Tasset 1997, Bock 1992, Holland 2000]. The aptamer drug ARC183 from Archemix Corporation is a thrombin inhibitor for use as an anticoagulant during coronary artery bypass graft procedures. Currently, herapin is used for this aim. However, the herapin treatment has serious side effects and requires a separate reversing agent. These limitations could be overcome with the use of the anti-thrombin aptamer. A further application of anti-thrombin aptamers is as an imaging agent to detect thrombus, since it distinguishes between actively growing clots and inactive clots. The thrombus imaging permits an accurate identification of pulmonary embolism, calf veins thrombi, vascular thrombus and other thrombotic disorders [Goldhaber 1998, Knight 1993, Worsley and Alavi 2001]. More recently, anti-thrombin aptamers have been used as biorecognition elements for thrombin detection in biosensors [Xu 2001, Schlensog 2004, Fan 2012, Rotem 2012, Tang 2012].

2.4.3. Conductive polymer based aptasensors

Molecular imprinting polymers (MIPs) and conducting polymers (CPs) are the two types of polymers that are commonly used in biosensing applications [Hahm 2011]. Conductive polymer

based aptasensors are composed of a conducting polymer, as the transducing element, while the aptamer is the recognition element.

2.4.3.1.Polyaniline

Polyaniline (PANI) is a conducting polymer of the semi-flexible rod polymer family. Although the compound itself was discovered over 150 years ago, only since the early 1980s polyaniline has captured the intense attention of the scientific community. This is due to the rediscovery of its high electrical conductivity. Amongst the family of conducting polymers and organic semiconductors, polyaniline is unique due to its ease of synthesis, environmental stability, and simple doping/dedoping chemistry. Although the synthetic methods to produce polyaniline are quite simple, its mechanism of polymerization and the exact nature of its oxidation chemistry are quite complex. Because of its rich chemistry, polyaniline is one of the most studied conducting polymers of the past 50 years.

Polymerized from the aniline monomer, polyaniline can be found in one of three idealized oxidation states [Feast 1996]:

leucoemeraldine – white/clear & colorless

emeraldine – green for the emeraldine salt, blue for the emeraldine base

(per)nigraniline – blue/violet

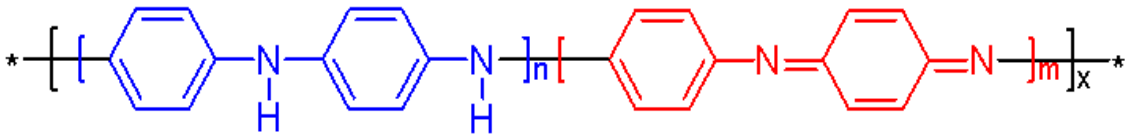

Figure 2.4-5 Main polyaniline structures n+m = 1, x = degree of polymerization

In figure 2.4-5, x equals half the degree of polymerization (DP). Leucoemeraldine with n = 1, m = 0 is the fully reduced state. Pernigraniline is the fully oxidized state (n = 0, m = 1) with imine links instead of amine links. The emeraldine (n = m = 0.5) form of polyaniline, often referred to as emeraldine base (EB), is neutral, if doped it is called emeraldine salt (ES), with the imine nitrogens protonated by an acid. Emeraldine base is regarded as the most useful form of polyaniline due to its high stability at room temperature and the fact that, upon doping with acid, the resulting emeraldine salt form of polyaniline is electrically conducting [Tzamalis 2003]. Leucoemeraldine and pernigraniline are poor conductors, even when doped with an acid.

The color change associated with polyaniline in different oxidation states can be used in sensors and electrochromic devices [Huang 2006]. Though color is useful, the best method for making a polyaniline sensor is arguably to take advantage of the dramatic conductivity changes between the different oxidation states or doping levels [Virji 2004].

PANI in its conductive form, the ES, can easily be functionalized with a thiolated molecule such as aptamers. This hybrid material can be employed as the basic component of the electrochemical aptasensor. Chapter 6 demonstrates a characterization and comparison study where the PANI is compared with SWCNTs as transducing element in electrochemical aptasensors.

2.5. References

Albrecht, T., Nature Communications 2012, 3, 829

Ampurdanés, J., Crespo, G. A., Maroto, A., Sarmentero, M. A., Ballester, P., Rius, F. X., Biosensors and Bioelectronics 2009, 25, 344-349

Anastasova-Ivanova, S., Mattinen, U., Radu, A., Bobacka, J., Lewenstam, A., Migdalski, J., Danielewski, M., Diamond, D., Sensors and Actuators B: Chemical 2010, 146, 199-205

Bakker, E., Pretsch, E., TrAC Trends in Analytical Chemistry 2001, 20, 11-19

Bakker, E., Bühlmann, P., Pretsch, E., Talanta 2004, 63, 3-20

Bhushan, B., “Springer Handbook of Nanotechnology” Springer (2004)

Bobacka, J., Ivaska, A., and Lewenstam, A., Chemical Reviews 2008, 108, 329-351

Bock, L. C., Griffin, L. C., Lathan J. A., Vermaas, E. H., Toole, J. J., Nature 1992, 355, 564-568

Bronzino, J. D., “The biomedical engineering handbook”, CRC Press (2000)

Carrara, S., “Nano-Bio-Sensing” Springer (2011)

Citartan, M., Gopinath, S. C. B., Tominaga, J., Tan, S. -C., Tang, T. -H., Biosensors and Bioelectronics 2012, 34, 1-11

Cowan, J. A., Ohyama, T., Wang, D., Natarajan, K., Nucleic acid Research 2000, 28, 2935-2942

Crespo, G. A., Macho, S., Rius, F. X., Analytical Chemistry 2008, 80, 1316-1322

Dai, H., Accounts of Chemical Research 2002, 35, 1035-1044

Danielsson, B., Hedberg, U., Rank, M., Xie, B., Sensors and Actuators, B 1992, 1-3, 138-142

Dimeski, G., Badrick, T., John, A. S., Clinica Chimica Acta 2010, 411, 309-317

Dekker, C., Physics Today 1999, 52, 22-28

Dresselhaus, M. S., Dresselhaus, G., and Avouris, P., "Carbon Nanotubes. Synthesis, Structure, Properties and Applications", Springer (2001)

Ellington, A. D., Szostak, J. W., Nature 1990, 346, 818-822

Famulok, M., Current Opinion in Structural Biology 1999, 9, 324-329

Famulok, M., Mayer G., Blind, M., Accounting Chemical. Research 2000, 33, 591-599

Fan, H., Li, H., Wang, Q., He, P., Fang, Y., Biosensors and Bioelectronics 2012, 35, 33-36

Feast, W. J., Tsibouklis, J., Pouwer, K. L., Groenendaal, L., Meijer, E. W., Polymer 1996, 37, 5017-5047

Fischer, J. E., "Nanotubes and Nanofibers", Taylor & Francis Group, (2006)

Florin, E. L., Rief, M., Lehmann, H., Ludwig, M., Dornmair, C., Moy, V. T., Gaub, H. E., Biosensors and Bioelectronics 1995, 10, 895-901

Fukusaki, E., Hasunuma, T., Macaya, R. F., Schultze, P., Smith, F. W., Roe, J. A., Feigon, J., Proceedings of the National Academy of Sciences 1993, 90, 3745-749

Geiger, A., Burgstaller, P., von der Eltz, H., Roeder, A., Famulok, M., Nucleic Acids Research 1996, 24, 1029-1036

Goldhaber, S. Z., New England Journal of Medicine 1998, 339, 93-103

Gutfreund, M. Y., Schueler, O., Margalit, H., Journal of Molecular Biology 1995, 253, 370-382

Hahm, J. -i., Sensors 2011, 11, 3327-3355

Hage, D. S., Bioanalysis 2010, 2, 719-720

Haller, A. A., Sarnow, P., Proceedings of the National Academy of Science USA 1997, 94, 8521-8527

Hamula, C. L. A., Zhang, H., Li, F., Wang, Z., Chris, Le X., Li, X. -F., TrAC Trends in Analytical Chemistry 2011, 30, 1587-1597

Hermann, T., Patel, D. J., Science 2000, 287, 820-825

Hernández, R., Riu, J., Rius, F. X., Analyst 2010, 135, 1979-1985

Holland, C. A., Henry, A. T., Whinna, H. C., Church, F. C., FEBS Letters 2000, 484, 87-91

Huang, L. M., Chen, C. H., Wen, T. C., Electrochimica Acta 2006, 51, 5858-5863

Huang, S., Woodson, M., Smalley, R., Liu, J., Nano Letters 2004, 4, 1025-1028

Iijima, S., Nature 1991, 354, 56-58

Ismail, A. H., Schäfer, C., Heiss, A., Walter, M., Jahnen-Dechent, W., Leonhardt, S., Biosensors and Bioelectronics 2011, 26, 4702-4707

Jacobs, C. B., Peairs, M. J., Venton, B. J., Analytica Chimica Acta 2010, 662, 105-127

Janata, J., "Principles of Chemical Sensors", Springer (2009)

Jayasena, S. D., Clinical Chemistry 1999, 45, 1628-1650

Jenison, R. D., Gill, S. C., Pardi, A., Polisky, B., Science 1994, 263, 1425-1434

Ju, H., Zhang, X., Wang, J., "Nanobiosensing Principles, Development and Application" Springer (2011)

Keese, C. R., Giaever, I., Proceedings of the Annual Conference on Engineering in Medicine and Biology 1990, 2, 500-501

Khare, R. and Bose, S., Journal of Minerals & Materials Characterization & Engineering 2005, 4, 31-46

Kiga, D., Futamura, Y., Sakamoto, K., Yokoyama, S., Nucleic Acids Research 1998, 26, 1755-1760

Kim, S. N., Rusling, J. F., Papadimitrakopoulos F., Advanced Materials 2007, 19, 3214-3228

Knight, L. C., Journal of Nuclear Medicine 1993, 34, 554-561

Liu, X., Feng, H., Zhao, R., Wang, Y., Liu, X., Biosensors and Bioelectronics 2012, 31, 101-104

Lorsch, J. R., Szostak, J. W., Biochemistry 1994, 33, 973-982

Lundblad, R. L., Kingdon, H. S., Mann, K. G., Methods of Enzymology 1976, 45, 156-176

Malitesta, C., Mazzotta, E., Picca, R., Poma, A., Chianella, I., Piletsky, S., Analytical and Bioanalytical Chemistry 2012, 402, 1827-1846

McCauley, T. G., Hanaguchi, N., Stanton, M., Analytical Biochemistry 2003, 319, 244-250

Michalska, A., Analytical and Bioanalytical Chemistry 2006, 384, 391-406

Mostafa, S., Lee, I., Islam, S. K., Eliza, S. A., Shekhawat, G., Dravid, V. P., Tulip, F. S., Electron Device Letters, IEEE 2011, 32, 408-410

Musa, A. E., del Campo, F. J., Abramova, N., Alonso-Lomillo, M. A., Domínguez-Renedo, O., Arcos-Martínez, M. J., Brivio, M., Snakenborg, D., Geschke, O., Kutter, J. P., Electroanalysis 2011, 23, 115-121

Noriaki, H., Materials Science and Engineering: B 1993, 19, 181-184

O'Sullivan, C., Analytical and Bioanalytical Chemistry 2002, 372, 44-48

Paborsky, L. R., McCurdy, S. N., Griffin, L. C., Toole, J. J., Leung, L. L., The Journal of Biological Chemistry 1993, 268, 0808–20811

Pagratis, N. C., Fitzwater, T., Jellinek, D., Dang, C., Nature Biotechnology 1997, 15, 68-73

Palchetti, I., Mascini, M., Analytical and Bioanalytical Chemistry 2012, 402, 3103-3114

Parra, E. J., Crespo, G. A., Riu, J., Ruiz, A., Rius, F. X., Analyst 2009, 134, 1905-1910

Pretsch, E., Trends in Analytical Chemistry 2007, 26, 46-51

Raffaellea, R. P., Landia, B. J., Harrisb, J. D., Baileyb, S. G., Hepp, A. F. Materials Science and Engineering B. 2005, 116, 233-243

Rius-Ruiz, F., Kisiel, A., Michalska, A., Maksymiuk, K., Riu, J., Rius, F., Analytical and Bioanalytical Chemistry 2011, 399, 3613-3622

Robertson, D. L., Joyce, G. F., Nature 1990, 344, 467-468

Rotem, D., Jayasinghe, L., Salichou, M., Bayley, H., Journal of the American Chemical Society 2012, 134, 2781-2787

Ruckman, J., Green, L. S., Waugh, S., Gillette, W. L, Henninger, D. D, Claesson-Welsh, L., Janjic, N., Journal of Biological Chemistry 1998, 273, 20556-20567

Russo Krauss, I., Merlino, A., Randazzo, A., Novellino, E., Mazzarella, L., Sica, F., Nucleic Acids Research, Article In Press, doi: 10.1093/nar/gks512

Saito, R., Dresselhaus, G., Dresselhaus, M. S., "Physical Properties of Carbon Nanotubes, Imperial College Press", London (1998)

Sassanfar, M., Szostak, J. W., Nature 1993, 364, 550-553

Schlensog, M. D., Gronewold, T. M. A., Tewes, M., Famulok, M., Quandt, E., Sensors and Actuators, B: Chemical 2004, 101, 308-315

Schwabe, J. W., Current Opinion on Structural Biology 1997, 7, 126-34

Sinn, I., Kinnunen, P., Albertson, T., McNaughton, B. H., Newton, D. W., Burns, M. A., Kopelman, R., Lab on a Chip 2011, 11, 2604-2611

Smironov, I., Shafer, R. H., Biochemistry 2000, 39, 1462-68

Sokalski, T., Ceresa, A., Zwickl, T., Pretsch, E., Journal of the American Chemical Society 1997, 119, 11347-11348

Soldatkin, O. O., Kucherenko, I. S., Pyeshkova, V. M., Kukla, A. L., Jaffrezic-Renault, N., El'skaya, A. V., Dzyadevych, S. V., Soldatkin, A. P., Bioelectrochemistry 2012, 83, 25-30

Sutter, J., Radu, A., Peper, S., Bakker, E., Pretsch, E., Analytica Chimica Acta 2004, 523, 53-59

Tang, J., Tang, D., Niessner, R., Knopp, D., Chen, G., Analytica Chimica Acta 2012, 720, 1-8

Tasset, D. M., Kubik, M. F., Steiner, W., Journal of Molecular Biology 1997 272, 688-698

Tessier, L., Patat, F., Schmitt, N., Pourcelot, L., Frangin, Y., Guilloteau, D., Proceedings of the Ultrasonics International Conference 1993, 627-630

Thevenot, D. R., Toth, K., Durst, R. A., Wilson, G. S., Pure Applied Chemistry 1999, 71. 12, 2333-2348

Tuerk, C., Gold, L., Science 1990, 249, 505-510

Tzamalis, G., Zaidi, N. A., Monkman, A. P., Physical Review B 2003, 68, 245106

Varani, G., Gallego, J. A., Accounting Chemical Research 2001, 34, 836-843

Vincke, B. J., Devleeschouwer, M. J., Patriarche, G. J., Analytical Letters 1985, 18, 593-607

Virji, S., Huang, J., Kaner, R. B., Weiller, B. H., Nano Letters 2004, 4, 491-496

Wang, G., Dewilde, A., Zhang, J., Pal, A., Vashist, M., Bello, D., Marx, K., Braunhut, S., Therrien, J., Particle and Fibre Toxicology 2011, 8, 4

Wang, J., Analytical Chemistry 1999, 71, 328-332

Wilson, D. S., Szostak, J. W., Annual Review of Biochemistry 1999, 68, 611-647

Worsley, D. F., Alavi, A., Radiologic Clinics of North America 2001, 39, 1035-1052

Xia, J., Rossi, A. M., Murphy, T. E., Optical Letters 2012, 37, 256-258

Xu, S., Cai, X., Tan, X., Zhu, Y., Lu, B., Proceedings of SPIE - The International Society for Optical Engineering 2001, 4414, 35-37

Xu, Y., Yang, X., Wang, E., Analytica Chimica Acta 2010, 683, 12-20

Zhang, X., Ju, H., Wang, J., "Electrochemical Sensors, Biosensors and Their Biomedical Applications", Elsevier (2008)

Zhou, O., Shimoda, H., Gao, B., Oh, S. J., Fleming, L., Yue G. Z., Accounts of Chemical Research 2002, 35, 1045-1053

Zhu, J., Qin, Y., Zhang, Y., Electrochemistry Communications 2009, 11, 1684-1687

http://www.sigmaaldrich.com/life-science/learning-center/biofiles/biofiles-issue-5.html Last connection 15.11.2012

http://aptamer.icmb.utexas.edu Last connection 15.11.2012

CHAPTER 3

NANOSTRUCTURED MATERIALS IN POTENTIOMETRY

3.1. Introduction

This chapter reflects an overview of the current trends of the nanostructured material use in the potentiometry field in an explanative way. It introduces the two main well known types of potentiometric sensors, the field effect transistors (FETs) and ion selective electrodes (ISEs), and new types of potentiometric sensors where the polymeric membrane in ISEs has been replaced by receptors linked directly to the transducers. The functionalization of some of these materials, particularly carbon nanotubes and graphene, which has been extensively reported [Ahammad 2009, Jacobs 2010, Shao 2010], investigates the possibility of directly linking the receptor molecules to carbon nanotubes instead of entrapping them in the ion-selective polymeric membranes.

Later it focuses on potentiometry as a tool for analyzing nanostructured materials by introducing different advances in the field. Also it gives a brief introduction on a different type of potentiometric approach that relies on porous nanostructures in a way that the nanopore, and the interactions within it, modulating the transport characteristics of the target analytes. Lastly, it gives a brief outlook on the advances and discusses them.

The contents of this chapter has been published as a trend article in the journal *Analytical and Bioanalytical Chemistry,* year 2011, volume 399, pages 171-181, and co-authored by Gustavo A. Zelada-Guillén, Gastón A. Crespo, Santiago Macho, Jordi Riu and F. Xavier Rius. Recent advances during and after the publication of the article are also introduced and discussed in section 3.3.

3.2. "Nanostructured materials in potentiometry"

Analytical and Bioanalytical Chemistry 2011, 399. 171-181

Ali Düzgün, Gustavo A. Zelada-Guillén, Gastón A. Crespo, Santiago Macho, Jordi Riu and F. Xavier Rius*

Department of Analytical and Organic Chemistry, Rovira i Virgili University,

43007 Tarragona, Spain.

3.2.1. Abstract

Potentiometry is a very simple electrochemical technique with extraordinary analytical capabilities. It is also well known that nanostructured materials display properties which they do not show in the bulk phase. The combination of the two fields of potentiometry and nanomaterials is therefore a promising area of research and development. In this report, we explain the fundamentals of potentiometric devices that incorporate nanostructured materials and we highlight the advantages and drawbacks of combining nanomaterials and potentiometry. The paper provides an overview of the role of nanostructured materials in the two commonest potentiometric sensors: field-effect transistors and ion-selective electrodes. Additionally, we provide a few recent examples of new potentiometric sensors that are based on receptors immobilized directly onto the nanostructured material surface. Moreover, we summarize the use of potentiometry to analyze processes involving nanostructured materials and the prospects that the use of nanopores offer to potentiometry. Finally, we discuss several difficulties that currently hinder developments in the field and some future trends that will extend potentiometry into new analytical areas such as biology and medicine.

3.2.2. Keywords

Potentiometry – Nanostructured materials – Sensors – Field-effect transistors – Ion-selective electrodes – Nanoparticles – Nanotubes – Nanowires – Graphene

3.2.3. Introduction

Potentiometry is one of the simplest electrochemical techniques. It is a very attractive option for numerous analyses owing to the low cost and ease of use of the instruments employed. Potentiometry also has other interesting properties, such as short response times, high selectivity, and very low detection limits. Moreover, the instrumental response does not depend on the area of the electrode. Therefore, potentiometric devices could be readily miniaturized

without, in theory, losing their determination capabilities. In this way, the inherent portability of the electrochemical sensors could be added to the already numerous performance characteristics of potentiometry.

On the other hand, nanomaterials display new properties not shown in the bulk material. Their extremely high surface-to-volume ratio promotes a greater interaction with targets when nanostructures are part of the recognition layer. Moreover, the exceptional electrical properties, such as the high charge transfer and the extraordinary electrical capacities generated at the interfaces of some nanostructured materials, are of paramount importance when nanomaterials are used as the transducing components in potentiometric sensors.

Can we combine the simplicity of the potentiometric technique with the new characteristics provided by nanostructured materials? Can we devise new devices that take advantage of both complementary aspects? What role do nanostructured materials play in the new potentiometric measurements? We will try to answer these questions in the present report while also explaining to the nonspecialist reader the advantages and drawbacks encountered when merging the two fields.

Two main devices fall within the category of potentiometric sensors: field-effect transistors (FETs) and ion-selective electrodes (ISEs). Both have been successfully used for many years. In 2004, Janata [*1*] wrote a paper to commemorate 30 years of chemical FETs (CHEMFETs), a particular type of FET acting as a chemical sensor. Since then, the introduction of nanomaterials in FETs has not only brought about a change in their architecture, but has also extended the type and number of analytes that can be detected and quantified. The development of FETs based on nanostructured materials is well established. In fact, FETs were the first type of electrochemical sensors incorporating a single semiconducting carbon nanotube [*2*]. On the other hand, several breakthroughs have revitalized the field of ISEs since their original conception [*3*, *4*]. Moreover, the introduction of nanomaterials as transducing elements or as part of the recognition layer is opening the field to the determination of species other than small ions. New potentiometric sensors are emerging that are based on different sensing mechanisms and which are able to determine large molecules such as proteins or even much more complex targets such as microorganisms, leading to a new wave of potentiometric sensors.

The paper is structured as follows. After this introduction, the most important characteristics of the two main types of potentiometric sensors, FETs and ISEs, are briefly reviewed. The

importance of introducing nanostructured materials is described for each sensor type. The nanomaterials are introduced according to their quantum confinement characteristics (zero-, one-, and two-dimensional nanostructures). In all cases, we have tried to stress the advantages and drawbacks of new devices that incorporate nanomaterials. We then discuss new potentiometric sensors using nanomaterials, potentiometry as a tool for analyzing nanostructured materials, and new potentiometric systems based on nanopores. The final section, the outlook, describes some of the future challenges and trends that will appear in the field.

3.2.4. Two main types of potentiometric sensors

3.2.4.1.Field-effect transistors

FETs often measure the current flow across the transistor that links the source and drain electrodes. These transistors always contain a semiconducting channel whose conductivity is affected by external fields. In the case of analytical sensors, these external fields have an electrochemical origin. Therefore, although these transistors are measuring the current, the origin of the current change is a variation in the potential, which in turn is affected by the analyte concentration in the test sample. This variation in the potential, or field effect, is the reason why FETs are classified as potentiometric devices. CHEMFETs are a particular type of FET that have traditionally been used for chemical sensing, but the incorporation of nanostructured materials in FETs has led to a new generation of nano-FETs displaying an architecture different from that of CHEMFETs. The theory and applications of CHEMFETs are well explained in reference books [5]. Their selectivity is provided by the polymeric membranes containing ionophores in a similar way to ISEs. With use of electronic circuits, the source–drain current may be kept at a constant value and, in this case, the changes at the solution membrane interface are reflected in changes in the potential difference between the source and gate electrodes (Fig. 4.1-1a). Therefore, the signal recorded in CHEMFETs is in this case a voltage that varies with the activity of the ion tested following the Nernst equation.

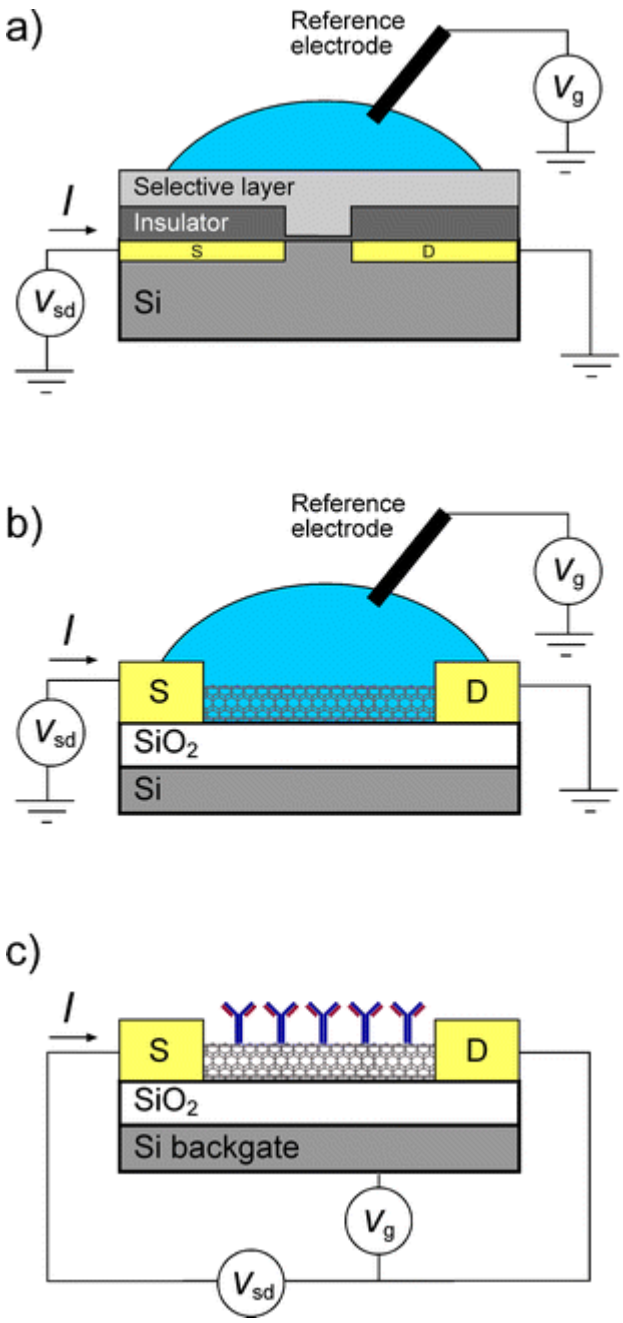

Figure 4.1-1 Different field-effect transistors (FETs): a chemical FET; b electrolyte-gated carbon nanotube field-effect transistor (CNTFET); c internally gated CNTFET showing the receptors directly contacting the carbon nanotubes

The introduction of nanostructured materials in the development of FETs represents an evolution of CHEMFETs that has contributed the following innovations:

1. The semiconducting channel is not made of doped silicon but of different semiconducting nanomaterials such as nanowires, nanoparticles, nanotubes, or thin films.

2. The ability of the sensor to detect very low amounts of the target analyte usually increases

when the size of the nanostructured material decreases, partly because to the very high surface-to-volume ratio of individual nanostructured materials. Moreover, some of the nanomaterials' charge-transfer properties play an additional role, compared to the bulk material, in detecting lower amounts of the target analyte.

3. The nanostructured channel connects the source and drain electrodes and is not buried under the dielectric layer but rather is in contact with the test sample containing the target analytes.

4. In a similar configuration to CHEMFETs, nanostructured FETs can be externally gated through an electrolyte solution [*6*] (Fig. 4.1-1b). These sensors are able to detect even lower amounts of the target analyte; however, they are difficult to miniaturize because of difficulties in reducing the size of the reference electrode.

5. Alternatively, the gate electrode can be integrated into the device as a back electrode, which obviates the need for an external electrode (Fig. 4.1-1c). Internally gated devices are a clear improvement over externally gated FETs when miniaturizing sensors.

6. The recognition layer is, in the vast majority of examples, directly immobilized into the nanostructured material, which acts as the semiconducting channel. This is a significant advantage over CHEMFETs (including ion-selective FETs, ISFETs, a specific case of CHEMFETs) because FETs based on nanostructured materials can take advantage of a wide range of molecular receptors (e.g., antibodies, nucleic acids, synthetic receptors, etc.) that are selective for different target analytes. This strategy has led to the development of new biosensors that are able to detect a large range of targets, from small molecules to microorganisms (Fig. 4.1-1c).

7. Alternatively, the recognition layer can be made of chemical receptors entrapped in a typical polymeric membrane, although very few examples of FETs based on nanostructured materials using this strategy can be found. Thus, these nano-FETs behave in a similar way to CHEMFETs/ISFETs. The electrochemical membrane potential is generated at the interface between the polymeric membrane and the solution and creates the electrical field that influences the potential difference between the source and gate electrodes.

These innovations overcome some of the drawbacks of CHEMFETs, such as unstable responses due to the lack of a thermodynamically reversible interface between the polymeric membrane

and the transducer elements or the presence of an inner water layer. However, some challenges still remain. The deposition of the semiconducting nanostructured material must be better controlled and the resistance between the metallic electrodes and the semiconducting material must be kept as low as possible, otherwise the high Schottky barrier influences the signal. Currently, the low control of these effects significantly influences the response signal's precision between devices. In the specific case of carbon nanotubes, only semiconducting carbon nanotubes should be present in order to prevent the damaging effect of metallic pathways. The most sensitive sensors are based on a single nanostructure (a sole nanotube, nanorod, etc.); however, the difficulties in properly handling these single structures and the lack of physical robustness of the resulting devices prevent this format from being generally applied in commercial devices.

Virtually all the examples of FETs using nanostructured materials directly link the molecular receptor, which is selective to the target analyte, to the nanostructures instead of using a polymeric membrane where the chemical receptors are entrapped (as is the case in CHEMFETs).

There are only a few examples of FETs where the semiconducting channel is made of quasi-zero-dimensional nanostructures applied to sensing applications. An interesting example that combines photonics and FETs involves the use of quantum dots. Quantum dots have recently been used as optically addressable floating gates in the development of optically gated FETs for photon-number discrimination [*7*]. These optically gated FETs could have many applications in the future both for quantum communications and for single-molecule detection if the FET is properly functionalized with molecular receptors so that it can selectively detect the target analyte.

Both nonmetallic and metallic nanoparticles are currently used as labels in combination with bioreceptors. An example of this is the FET developed by Luo *et al* [*8*] for detecting glucose by simultaneously immobilizing MnO_2 nanoparticles and the enzyme glucose oxidase on the gate of an ion-sensitive FET. In such a device, the MnO_2 nanoparticles enhance the dynamic range of the sensor, although the detection limit obtained (0.02 mM) is not particularly low. The MnO_2 nanoparticles act as an oxidant of H_2O_2 which is produced by the glucose oxidase driven catalytic reaction of glucose oxidation, instead of acting as a catalyst for H_2O_2 decomposition. Fullerenes have also been employed in FET technology since the middle of the 1990s as an n-type material that transports electrons [*9*]. Metals caged inside the fullerenes also represent an interesting option in the development of this family of FETs. Kobayashi *et al* [*10*] reported FETs that include

within their structure a thin film of a dimetallofullerene (two atoms of La caged in a C_{80} fullerene molecule) as the conducting channel, and these might be useful for determining the mechanism of the charge transport and carrier types in similar systems.

FETs made of quasi-one-dimensional nanostructures (i.e., mainly single-walled carbon nanotubes, SWCNTs, or nanowires) have been much more widely reported than quasi-zero-dimensional nanostructured FETs. Kong *et al* [*2*] reported the first chemical sensor based on a recently developed FET that in turn was based on a single semiconducting SWCNT. The conducting channel in carbon nanotube FETs (CNTFETs) can be made of a single SWCNT, a few interconnected SWCNTs, or a network of numerous SWCNTs. The first CNTFET-based sensing devices were reported for the detection of gases and were able to detect analytes at parts per trillion levels in samples containing a single gas in a few seconds. Selectivity is one of the most important performance characteristics in gas detection because of the small size of the gaseous interferences that are able to interact with the SWCNTs and nonselectively modify the electrical conductance of the CNTFET device. There have been recent promising advances in making CNTFETs selective for gas sensing [*11*, *12*], most of these involving coating the SWCNTs to isolate them from interferences. However, a CNTFET that can sense gases in complex real samples has yet to be reported. In most cases the process of functionalization increases the response time by up to a few minutes, probably owing to the specific response mechanism between the target analyte and the sensing layer attached to SWCNTs.

Although the first CNTFETs were initially developed for the sensitive detection of gaseous substances, most subsequent CNTFETs have been used to detect large biocompounds such as proteins, DNA sequences, immunoglobulins and bacteria [*13*, *14*]. Apart from the intrinsic interest of these biocompounds, there are probably two main reasons why there is such a high number of biosensing CNTFET devices: on one hand, the relatively high number of available molecular receptors (e.g., antibodies or synthetic nucleic acid segments) that selectively bind to the target analyte and that can be used to functionalize CNTFETs, and, on the other hand, the relatively large size of these biocompounds, meaning that the selectivity is tested against interfering biocompounds of similar size (e.g., a protein similar to the target protein to be detected), which makes it easier to isolate the SWCNT surface against nonspecific interactions caused by interferences. After functionalization of the SWCNTs (usually in a noncovalent way) with a suitable molecular receptor for the target analyte, a blocking agent [e.g., Tween 20, gelatine, poly(ethylene glycol) or pyrene] is used to coat the SWCNTs to prevent nonspecific binding. These CNTFETs are able to detect very low concentrations of the target analyte, on the

order of picomolar concentrations for proteins or 100 cfu/mL for *Salmonella infantis* [*15*], usually in short response times ranging from a few seconds to 1 h in the case of bacteria. The affinity between the target analyte and the molecular receptor is often very high, making it difficult to regenerate the sensing device in some cases. However, for safety reasons, the future commercialization of these sensors would probably be as disposable devices.

In addition to detecting biocompounds in a solution, CNTFETs are also able to detect small molecules. Very recently, a microfluidic-based CNTFET was reported as being able to detect 500 fmol·L^{-1} of a single herbicide [*16*].

Although the chemical sensing principles of CNTFETs have been well established, many articles fail to report their most suitable performance parameters. CNTFETs are sensing devices with a lot of potential but their accuracy, selectivity, stability, and precision are often not described in sufficient depth. Consequently, the potential of CNTFETs needs to be confirmed through empirical studies of the devices' performance parameters and their application to real samples. Another problem regarding CNTFETs is their lack of reproducibility. There is a significant current variation between CNTFETs that are made identically from a single carbon nanotube, and this is mainly caused by variations in nanotube diameters and chiralities and the different contacts with the metallic electrodes.

Nanowires are made mainly of Si, but InAs, GaN, Ge, and metal oxides have also been incorporated into FETs to create nanowire FETs (NWFETs) [*17*]. Some of these devices, despite having the classic FET configuration, apparently work at zero gate potential, i.e., they work as resistors rather than FETs. These NWFETs have characteristics similar to those of CNTFETs and have also been mainly used for detecting different biocompounds [*18*]. A particular advantage of NWFETs is that they are exclusively semiconducting, unlike carbon nanotubes, which are both metallic and semiconducting. Moreover, NWFETs are highly reproducible because the nanowire growth process can be controlled without difficulty. NWFETs are mainly functionalized with covalent bonds, a process which takes advantage of current knowledge regarding the chemical modification of oxide surfaces. A particular feature of NWFETs is that nonselective binding seems to be much less of a problem than it is for CNTFETs, which means that nanowires are not commonly protected with a blocking agent after functionalization. Other quasi-one-dimensional nanostructured FET devices include nanobelts and nanorods mainly made of different metal oxides [*19*], although these have yet to be widely applied as potential chemical sensors.

Quasi-one-dimensional nanostructured FETs (i.e., FETs that contain just a few SWCNTs or nanowires) have several better intrinsic properties than traditional FETs based on the metal oxide semiconductor technology. In addition to the semiconductor channel being in direct contact with the target analytes, they have either a larger on-state current and transconductance or a smaller off-state current, which makes these FETs better suited for sensing applications. However, from an operative point of view these FETs are expensive devices because they depend heavily on costly lithographic techniques. A few devices have been built using less costly screen-printing techniques that deposit silver conductive paint as the source and drain electrodes, but the reproducibility of these devices is worse than when lithographic techniques are used.

Graphene is a nanomaterial that could soon provide ultrafast electronics, and is the best example of a two-dimensional nanostructured material used as the conducting channel in FETs. The two-dimensional nature of graphene combined with its quantum properties and high carrier mobilities make it a promising material for use in the next generation of sensors, particularly those based on the field effect, although graphene-based FETs cannot be turned off owing to the absence of a band gap, leading to an on/off ratio of around 5. Recent FETs using bilayer graphene in a dual-gate FET have been reported as having on/off ratios of between 100 and 2,000 [*20*], although the construction of these devices involves complicated and lengthy steps such as identification of bilayer flakes using optical and Raman spectroscopies or the use of different lithographic techniques. One of the main obstacles so far to using graphene is probably the construction of reproducible FETs. Mechanical exfoliation from natural graphite is probably the most widely used method for obtaining single- and multilayer graphene films. Other tedious and complicated methods can be used to obtain high-quality graphene sheets, for example, one recently reported method obtains high-quality graphene sheets in only 10 min by quenching hot graphite in an ammonium hydrogen carbonate aqueous solution [*21*]. Although graphene FETs are a very recent development and have not been as widely applied as CNTFETs or NWFETs, each year they are applied in an increasing number of applications and for different analytes, including vapor [*22*], pH [*23*] and proteins [*24*]. Figure 4.1-2 shows a solution-gate FET in which graphene exhibits an ambipolar behavior, and the shift in the negative gate potential as a result of the pH change follows a supra-Nernstian response of 99 meV/pH [*23*]. To summarize, we can say that current graphene-based FET technology is in a similar place as SWCNT-based FETs or NWFETs were 5–7 years ago. Graphene-based FET devices have shown immense potential for sensing applications (some authors claim that these devices have lower electrical noise and

lower detection limits than those based on SWCNTs and nanowires [25]). However, suitable graphene functionalization strategies must be developed to achieve adequate selectivity. The successful application of graphene-based FETs to real samples remains a challenge for the future.

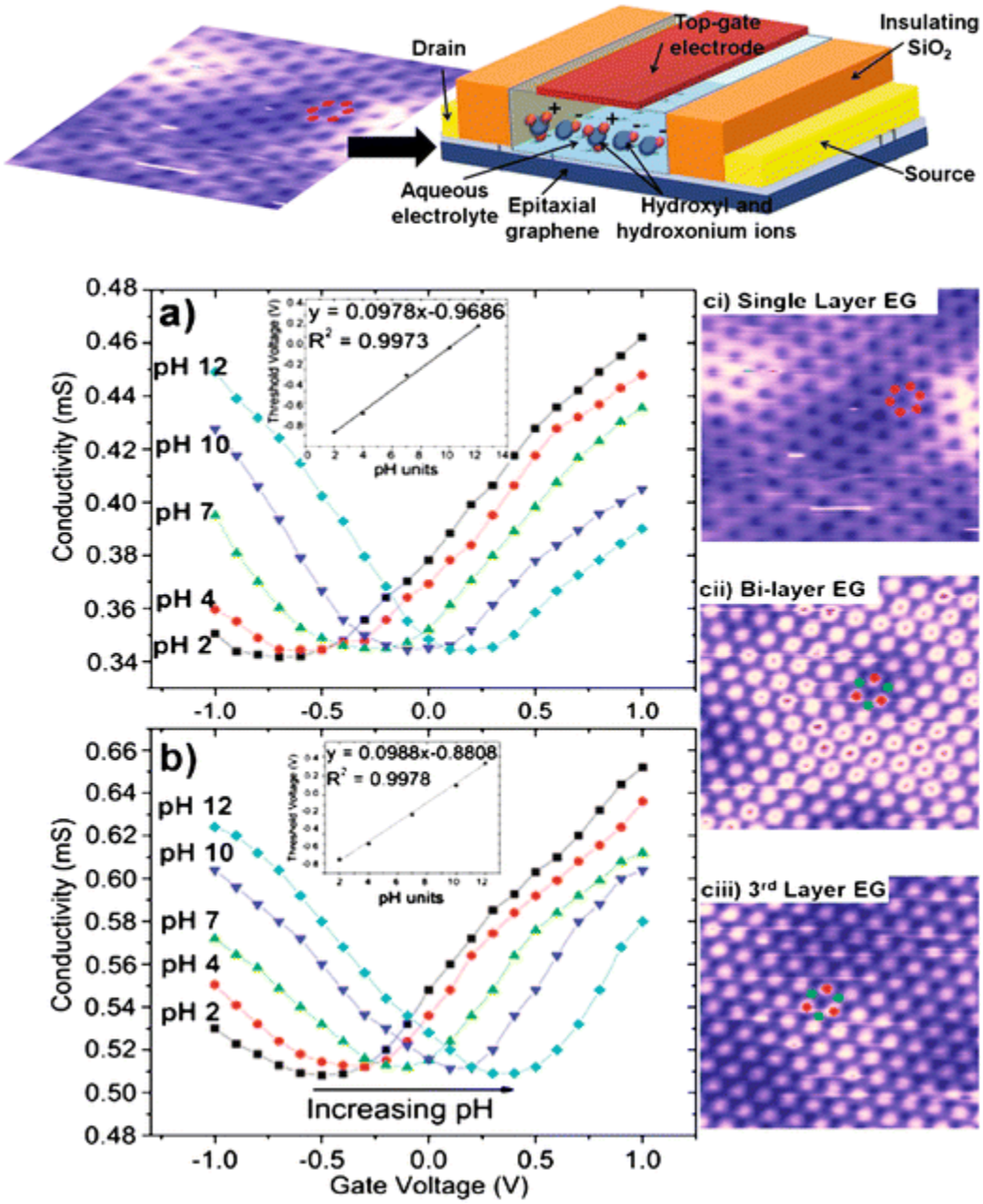

Figure 4.1-2 A solution-gated FET based on few layers of graphene (*top*). Hydronium (H_3O^+) and hydroxyl (OH^-) ions in the solution capacitively charge the surface of the graphene and thus induce an ambipolar charge transfer, characterized by a V-shaped conductivity versus gate potential curve (*bottom*). Scanning tunneling microscopy images of the graphene layers (*right*) [23]

From an operative point of view, the reduction in the size of FET devices made from nanostructured materials should be accompanied by the development of portable semiconductor analyzers so as to enable analysis in situ. Moreover, FETs require skilled and trained personnel to correctly select the potentials to be applied to the gate and to the conducting channel so as to record optimized measurements.

3.2.4.2.Ion-selective electrodes

The field of ISEs has recently been revitalized by several factors. The thorough understanding of the chemical and physical processes, especially the ion fluxes in the polymeric membranes (the sensing layer, which contains the ionophore that is the molecular receptor), has led to very low limits of detection and increased selectivities. Moreover, eliminating the undesired inner water layer has improved the performance of the electrodes [*26*, *27*].

One challenge remains which would complement these achievements: the miniaturization of the electrodes. The main motivation for miniaturization is to satisfy the need to obtain analytical information faster. Multitarget and/or multisample determinations would be highly desirable in potentiometry and the development of multianalyte electrodes would add substantial value to the already attractive characteristics of these electrodes. Miniaturization is a prerequisite for the development of multielectrodes. Pipette-type ISEs were miniaturized in a robust way by Gyurcsányi *et al* [*28*] and they have recently been multiplexed [*29*]. Although miniaturized electrodes based on the classic scheme of an inner filling solution and polymeric membranes have been in use for a long time, the development of microcavities and the electrical instabilities generated by the use of pulled-glass micropipette tips make these needle-type electrodes very cumbersome to fabricate and delicate to use.

Solid transducers are very attractive because they avoid the use of internal liquids, do not require maintenance, are easy to store, and do not display any risk of solution leakage. Moreover, all-solid-state electrodes can operate in any position or configuration. Many researchers have investigated new transducer materials to obtain solid-contact ISEs with stable electrode potential. To achieve this, it is necessary to have sufficiently fast and reversible ion-to-electron transduction in the solid state without any contribution from parasitic side reactions [*30*].

In the early 1990s, several components from the conducting polymer family were introduced as promising transducers because they showed an excellent ion-to-electron transducing ability that overcame the signal instability problems in coated-wire electrodes and triggered the new wave

of solid-contact ISEs [*31*, *32*]. The solid-contact concept has been widely accepted within the ISE community since the publication of the papers by Sutter *et al* [*33*, *34*] in 2004 which showed that the detection limit of all-solid-state ISEs could be extended to the subnanomolar range by using electropolymerized conducting polymers.

Different research groups have actively participated in determining the transduction mechanism in conducting polymers. Basically, conducting polymers behave as anion or cation exchangers and when ions approach or move away from the doped electroactive polymer backbone, redox processes are established and the ion-to-electron transduction takes place. Moreover, the high redox capacitance enables stable responses to be obtained from the solid-contact ISEs. Nevertheless, conducting polymers show some disadvantages, such as secondary reactions with redox interferences and high sensitivity to CO_2 and O_2. A recent study investigated the formation of a water film between the conducting polymer and the membrane because this is especially critical for measurements in the low limit of detection range and for the stability of the sensor [*26*]. Another drawback to conducting polymers is related to the light sensitivity of the semiconducting conducting polymers [*35*]. The difference in energy between the valence and conducting bands of most of these compounds matches the visible–near UV wavelengths of daylight, which clearly affects the measurements.

Nanostructured materials were initially introduced as new transducers in ISEs in an attempt to overcome the main drawbacks displayed by conducting polymers. Fouskaki and Chaniotakis [*36*] recently reported the first ISE which uses a layer of fullerenes as the transducing element. The authors attributed the charge-transfer mechanism to the ability of C_{60} to accept and donate electrons and to act as a solid electrolyte film between the membrane and the inner conducting support. Other nanostructured materials have also been assayed as transducing elements; these include three-dimensional ordered macroporous carbon [*37*], platinized porous silica [*38*], SWCNTs [*39*, *40*], multiwalled carbon nanotubes [*41*] and the composite material multiwalled CNT–poly(3,4-ethylene-dioxythiophene) [*42*].

Usually, the nanostructured material is deposited onto the conducting substrate in layers that are several micrometers thick. Fullerenes are deposited as crystalline layers, carbon nanotubes are randomly entangled, forming spaghetti-like films, and macroporous carbon is a monolith displaying an array of uniform spherical nanometric pores imbedded in a glassy carbon structure. In all cases the contact surface between the nanostructured material and the ion-selective membrane is very large and the transducing mechanisms seem to be very similar. The

high stability of the recorded potential exhibited by all the nanostructured materials is attributed to the large double-layer capacitance which results from their very large surface-to-volume ratio [37, 43]. Moreover, carbon nanotubes display a notable charge-transfer capability between heterogeneous phases. Recently, Crespo *et al* [43] graphically represented the different electrical contributions involved in the ion-to-electron transduction mechanism. Figure 4.1-3 displays these contributions, which, unlike in the transduction in conducting polymers, have a nonfaradaic character.

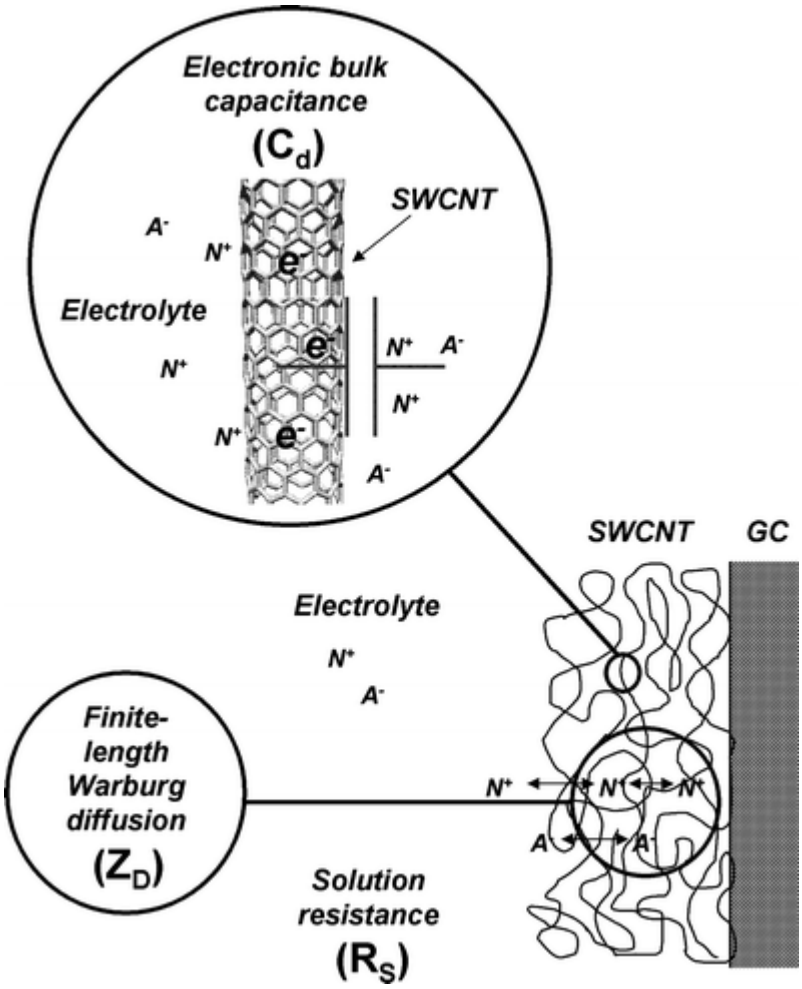

Figure 4.1-3 The ion-to-electron transduction process of the glassy carbon(*GC*)/single-walled carbon nanotube (*SWCNT*)/electrolyte system. The electronic bulk capacitance is generated at the asymmetric capacitor established between the SWCNT wall and the solution (this solution would be replaced by the ion-selective membrane in a solid-contact ion-selective electrode). N^+ cation, A^- anion, e^- electron

Unlike FETs, which need semiconducting nanorods or nanotubes, the transducing elements in ISEs do not need a nanostructured material with specific electrical characteristics. The large number of individual nanostructures (e.g., carbon nanotubes) involved in the transducing layers

means that the resulting devices are highly robust from a physical point of view. Moreover, their deposition is easily reproduced, providing highly precise instruments. Additionally, all carbon-based nanostructures display hydrophobicity, which is important for preventing water layers from forming between the ion-selective membrane and the transducing layer. Moreover, the risk of interferences is further reduced because they are insensitive both to light and to species displaying redox behavior. Therefore, although the nanostructured materials in ISEs are not in direct contact with the analytical targets (unlike in the majority of CNTFETs), they do have a series of unique characteristics that make them very valuable as substitutes for conducting polymers.

Zhu *et al* [*44*] went a step further by incorporating a transduction layer made of multiwalled CNTs into the polymeric membrane. However, 3 years earlier, Abbaspour and Izadyar [*45*] had reported the determination of Cr(III) in real samples using a coated wire electrode and a PVC membrane containing the same type of carbon nanotube. They used a very simple electrode preparation method to disperse the nanotubes into different polymeric ion-selective membranes, and demonstrated that the instrumental signal recorded was very stable and the performance characteristics were comparable to those of previously developed electrodes. However, the transducing mechanism of these ISEs has yet to be reported. Other nanostructures have also been used as components of the ion-selective membrane in ISEs; for example, PbO and PbS nanoparticles have been used in a cellulose acetate membrane [*46*] and in PVC membranes [*47*], respectively, to detect Pb(II). Nevertheless, in the latter case, the nanostructured material acts as an ionophore, that is, as the basic component of the sensing layer, and not as a transducing layer.

3.2.5. New potentiometric sensors using nanomaterials

The introduction of nanostructured material enables the development of a new type of potentiometric sensors in which the polymeric membrane has been replaced by receptors linked directly to the transducers. The functionalization of some of these materials, particularly carbon nanotubes, has been extensively studied of these reports, our group investigated the possibility of directly linking the receptor molecules to carbon nanotubes instead of entrapping them in the ion-selective polymeric membranes.

These types of sensors are very different from ISEs for different reasons: (1) the receptor is immobilized onto the walls of carbon nanotubes instead of being entrapped in a polymeric membrane; (2) the receptor is in direct contact with the target, and the recognition event is

based on an affinity process; (3) the targets are not necessarily small ions, but instead can be large multiionic species such as proteins or complex systems such as microorganisms; (4) the sensing mechanism is based on a superficial phenomenon, very different from the well-established phase-boundary potential model in ISEs; (5) the sensing mechanism is based on the potential generated by the different charged species in the chemical environment of the nanotubes, which in turn means that the calibration curves do not follow the classical Nernstian model; (6) the sensitivity of the new sensors is very low compared with that of ISEs, but it is high enough to enable the detection of the target as shown in the examples given below.

Düzgün *et al* [*48*] covalently linked a thrombin aptamer to a layer of carboxylated SWCNTs, thus developing the first aptasensor able to record a potentiometric signal that is directly proportional to the concentration of the target protein. The direct potentiometric signal can be easily recorded within 15 s and the method has a limit of detection of 80 nM. Fluorescence confocal microscopy results obtained with this labeled aptamer seem to confirm that the biosensing mechanism is based on the competition between the target analyte and the SWCNTs for the aptamer. The presence of the target protein induces a conformational change in the aptamer that separates the phosphate negative charges from the SWCNT side walls, thus inducing the subsequent increase of the recorded potential. This mechanism is similar to the one described by Levon's group [*49*], which used polyaniline as a transducer to monitor DNA hybridization.

Following this approach, Zelada-Guillén *et al* [*50*] demonstrated the feasibility of quantitatively determining the presence of very low levels of bacteria in a rapid and selective way using the hybrid material carbon nanotube–aptamer. Figure 4.1-4 shows a schematic representation of the interaction between the target bacteria and the hybrid aptamer–SWCNT system. Figure 4.1-4 also shows an environmental scanning microscope image obtained from an aptamer-functionalized SWCNT electrode after it had been exposed to *Salmonella typhi* (panel A) and the same electrode's two main performance parameters, sensitivity (panels B and C) and selectivity (panel D).

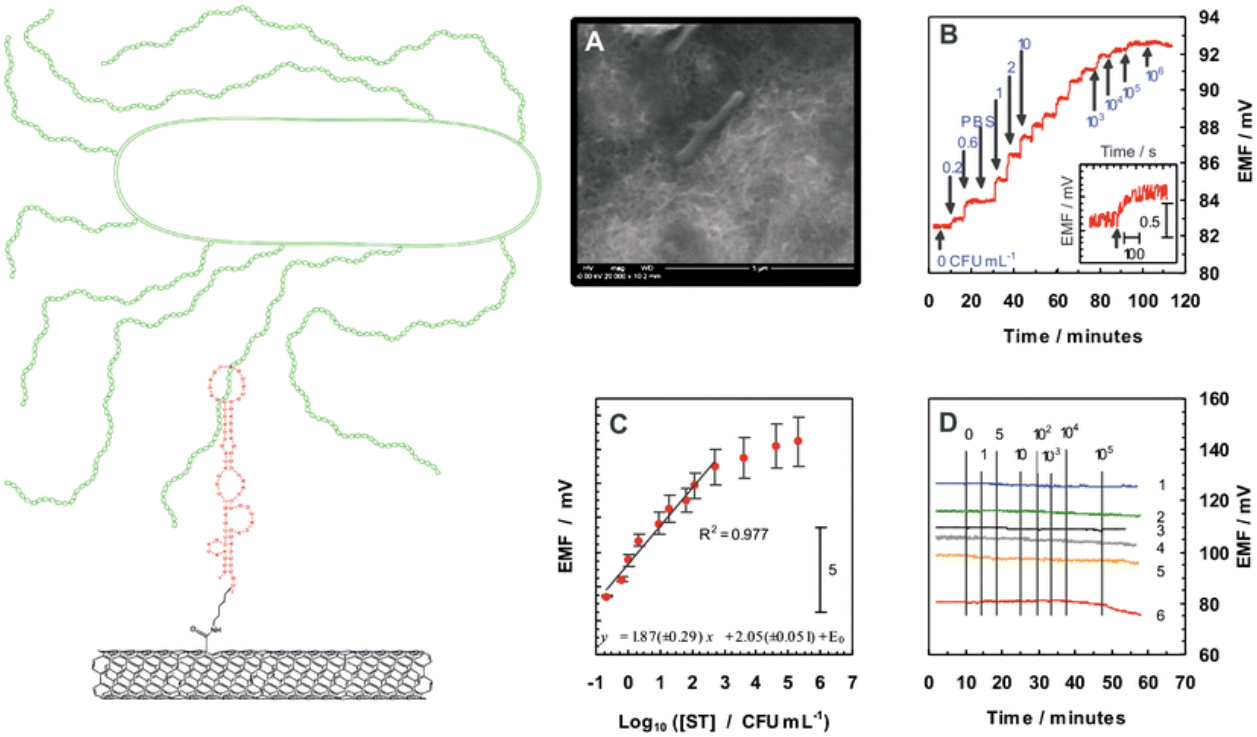

Figure 4.1-4 *Left*: The interaction between the target bacteria and the hybrid system aptamer–SWCNT. *Right*: Environmental scanning microscope image obtained from an aptamer-functionalized SWCNT electrode after exposure to *Salmonella typhi* (*A*) aptamer-functionalized SWCNT electrode exposed to stepwise increases of *Salmonella typhi* concentration (*B*), EMF response versus log of concentration of *Salmonella typhi* (*C*), and controls and selectivity assays (*D*) [*50*]

The low limit of detection achieved is probably due to the fact that many aptamers simultaneously link to the same bacterium, thus providing a clearly distinguishable signal. This new type of potentiometric sensor expands the field of potentiometry to include large charged species that cannot be analyzed using the classic ISEs because they are unable to be extracted in the polymeric membranes. However, some challenges still remain to be solved. One is the characterization problem. It is necessary to be able to correctly characterize the number of receptors linked to the nanotubes' surface to be able to optimize the devices. Moreover, the sensing mechanism should be clearly established. Although Düzgün *et al* [*48*] made some suggestions regarding the nature of the detection system, it still remains to be fully demonstrated. The new sensors also display some drawbacks. For instance, the devices have a rather narrow instrumental response range, which is probably because the electrostatic interactions on the sensor's surface are limited in their ability to generate large potential values. The ionic strength should be strictly controlled. All potentiometric sensors are sensitive to changes in the ionic strength but these devices, which are based on a superficial interaction, are more susceptible to ionic strength changes than ISEs. Finally, test samples containing charged

species that can approach the carbon nanotubes and undergo a charge transfer should be preprocessed so they can be eliminated.

3.2.6. Potentiometry as a tool for analyzing nanostructured materials

The improvements in ISE limits of detection have led to very promising applications in biochemical assays involving nanostructured materials. A cadmium ISE was used to quantify Cd^{2+} in a heterogeneous immunoassay. To do so, a microtiter plate format sandwich immunoassay was carried out on mouse IgG using CdSe quantum dot labels on a secondary antibody. The CdSe–quantum dot labels were dissolved in H_2O_2 and the response of the selective electrode was recorded [*25*]. Very recently, ISEs have also been used to characterize nanostructures and to monitor processes that involve nanostructured materials such as biometallization processes and nanoparticle growth. A copper ISE was used to monitor in real time the NADH-mediated reduction of copper in the presence of gold nanoparticle seeds [*51*]. Silver ISEs have been used in a glucose biosensor to monitor Ag^{+} generated from silver nanoparticles. These silver nanoparticles were oxidized by the H_2O_2 resulting from the oxidation of glucose by glucose oxidase [*52*]. Silver ISEs were also used to monitor the hydroquinone-induced precipitation of silver on gold nanoparticle seeds [*53*]. The growth dynamics of metal nanoparticles obtained from the potential–time recordings correlate well with classical optical measurements, and are useful because they are independent of sample turbidity. In these methods, ISEs are used as the detection device because of their extremely low detection limits. However, the steps involved in these methods must be carefully evaluated to determine the value of the potentiometric detection technique compared with that of the traditional techniques that use labels normally employed in biochemical assays.

3.2.6.1. Other potentiometric systems

The chemical interactions between species within nanopores offer interesting detection characteristics. Although all the interaction mechanisms have yet to be fully described, the basic idea is that the nanopore, and the interactions within it, modulates the transport characteristics of the target analytes. This offers the possibility of analyzing very small volumes of samples without using labels. Historically, nanopores have been classified into two groups, “biological” and “solid state”, depending on the techniques used to make them. In contrast to the development of biological nanopores, that of solid-state nanopores has grown rapidly in recent years owing to the implementation of nanoprocessing and nanofabrication techniques. High reproducibility, low cost, robustness, and flexibility in terms of size, shape, and material type of are some of the features of modern nanopores [*54*]. Shim *et al* [*55*] developed the first all-solid-

state ISE using glass nanopores with a diameter of 15–100 nm. In this case the nanopore was fabricated by sealing a conically etched platinum wire in a glass capillary and developing an AgCl/Ag electrode within the pore. The AgCl/Ag-layer-coated ISE was used in electrochemical microscope experiments to map the presence of the Cl^- ion by using the flux through the micropore. Very recently, Studer *et al* [56] reported the formation of nanopores using lipid bilayers. The diffusion of sodium ions across α-hemolysin channels was determined using ISEs. Small changes in the geometry of the nanopores resulted in large variations in the observable dynamic biomolecular processes. There is every chance that this area will offer interesting possibilities in the future for miniaturizing potentiometric sensors; however, in addition to solving the technical challenges inherent in manipulating nanopores, a thorough understanding of the theoretical aspects involved in the sensing process is still needed.

3.2.7. Outlook

Nowadays, potentiometric sensors have very attractive features, such as extremely low limits of detection and significant selectivity coefficients that complement favorable operational parameters such as simplicity, low cost, and labelless detection. However, multianalyte portable sensors should be available on the market to meet current analytical requirements. The future will therefore probably see the miniaturization of the potentiometric devices in response to the need for multiplexed in situ determinations. This envisaged miniaturization of all-solid-state electrodes will probably become a reality soon. Designing efficient solid ion-to-electron transducers that provide stable potential measurements is one of the key elements in the future development of robust arrays of potentiometric ultramicroelectrodes with diverse geometrical patterns. New nanostructured materials such as graphene that are being tested and compared with the available nanostructures will probably play an important role in this area. Solid-state miniaturized reference electrodes will be particularly important.

The wealth of studies on the functionalization of nanostructured materials has provided broad knowledge for the immobilization of different sensing layers. In this way, the different bioconjugation techniques, such as covalent and noncovalent bonding and entrapment or encapsulation of the receptors in the nanoparticles [57–61], nanotubes [62–65], nanowires [66–69], and other nanostructures [70, 71] that perform as transducers, will enable the development of new devices with different sensing mechanisms that complement the classic entrapment of ionophores within the polymeric structure of ion-selective membranes. The incorporation of new receptors will expand the range of analytes that can be determined using potentiometry to include entities such as DNA, proteins, viruses, and higher cellular organisms that are of

particular interest to biology and medicine. Nevertheless, the reader should be aware that all superficial interactions in potentiometry are limited by the screening of the ions in solution. Therefore, ionic strength must be strictly controlled.

Isolated nanostructures are the most sensitive; however, technical improvements are necessary to develop low-resistance, reproducible, and robust contacts between these nanostructures and the conducting material. Moreover, the use of micro- and nanofluids is necessary for the target analyte to encounter the receptor. Sensors that combine the characteristics of nanopores and electrochemical/potentiometric detection will be exhaustively explored in the future. Combining the chemical functionalization of these nanostructures with the needle-type ISE (with or without ion-selective membranes) will enable the development of even more sensitive instruments.

3.2.8. Acknowledgement

We thank the Spanish Ministry of Science and Innovation, MICINN, for supporting this work with project grant CTQ2007-67570.

3.2.9. References

1. Janata J (2004) Electroanalysis 16:1831–1835

2. Kong J, Franklin NR, Zhou C, Chapline MG, Peng S, Cho K, Dai H (2000) Science 287:622–625

3. Pretsch E (2007) Trends Anal Chem 26:46–51

4. Bakker E, Chumbimuni-Torres K (2008) J Braz Chem Soc 19:621–629

5. Janata J (2009) Principles of chemical sensors. Springer, Heidelberg

6. Krüger M (2001) Appl Phys Lett 78:1291–1294

7. Gansen EJ, Rowe MA, Greene MB, Rosenberg D, Harvey TE, Su MY, Hadfield RH, Nam SW, Mirin RP (2007) Nat Photon 1:585–588

8. Luo XL, Xu JJ, Zhao W, Chen HY (2004) Biosens Bioelectron 19:1295–1300

9. Haddon RC (1996) J Am Chem Soc 118:3041–3042

10. Kobayashi SI, Mori S, Lida S, Ando H, Takenobu T, Taguchi Y, Fujiwara A, Taninaka A, Shinohara H, Iwasa Y (2003) J Am Chem Soc 125:8116–8117

11. Bondavalli P, Legagneux P, Privat D (2009) Sens Actuators B 140:304–318

12. Cid CC, Jimenez-Cadena G, Riu J, Maroto A, Rius FX, Batema GD, Van Koten G (2009) Sens Actuators B 141:97–103

13. Kauffman DR, Star A (2008) Angew Chem Int Ed 47:6550–6570

14. Kauffman DR, Star A (2008) Chem Soc Rev 37:1197–1206

15. Villamizar RA, Maroto A, Rius FX, Inza I, Figueras MJ (2008) Biosens Bioelectron 24:279–283

16. Wijaya IPM, Nie TJ, Gandhi S, Boro R, Palaniappan A, Hau GW, Rodríguez I, Suri CR, Mhaisalkar SG (2010) Lab Chip 10:634–638

17. Cui Y, Wei Q, Park H, Lieber CM (2001) Science 293:1289–1292

18. Stern E, Vacic A, Reed MA (2008) IEEE Trans Electron Devices 55:3119–3130

19. Huang XJ, Choi YK (2007) Sens Actuators B 122:659–671

20. Xia F, Farmer DB, Lin Y, Avouris P (2010) Nano Lett 10:715–718

21. Tang YB, Lee CS, Chen ZH, Yuan GD, Kang ZH, Luo LB, Song HS, Liu Y, He ZB, Zhang WJ, Bello I, Lee ST (2009) Nano Lett 9:1374–1377

22. Dan Y, Lu Y, Kybert NJ, Luo Z, Johnson ATC (2009) Nano Lett 9:1472–1475

23. Ang PK, Chen W, Wee ATS, Loh KP (2008) J Am Chem Soc 130:14392–14393

24. Ohno Y, Maehashi K, Yamashiro Y, Matsumoto K (2009) Nano Lett 9:3318–3322

25. Bakker E, Pretsch E (2008) Trends Anal Chem 27:612–618

26. Fibbioli M, Morf WE, Badertscher M, de Rooij NF, Pretsch E (2000) Electroanalysis 12:1286–1292

27. Bobacka J, Ivaska A, Lewenstam A (2008) Chem Rev 108:329–351

28. Gyurcsányi RE, Nybäck A-S, Ivaska A, Tóth K, Nagy G (1998) Analyst 123:1339–1344

29. Anastasova-Ivanova S, Mattinen U, Radu A, Bobacka J, Lewenstam A, Migdalski J, Danielewski M, Diamond D (2010) Sens Actuators B 146:199–205

30. Lindner E, Buck RP (2000) Anal Chem 72:336A–345A

31. Bobacka J (2006) Electroanalysis 18:7–18

32. Michalska A (2006) Anal Bioanal Chem 384:391–406

33. Sutter J, Lindner E, Gyurcsanyi RE, Pretsch E (2004) Anal Bioanal Chem 380:7–14

34. Sutter J, Radu A, Peper S, Bakker E, Pretsch E (2004) Anal Chim Acta 523:53–59

35. Lindfors TJ (2009) Solid State Electrochem 13:77–89

36. Fouskaki M, Chaniotakis N (2008) Analyst 133:1072–1075

37. Fierke MA, Lai CZ, Buhlmann P, Stein A (2010) Anal Chem 82:680–688

38. Zhu Z, Zhang J, Zhu J, Lu W, Zi J (2007) IEEE Sens J 7:38–42

39. Crespo GA, Macho S, Rius FX (2008) Anal Chem 80:1316–1322

40. Ampurdanés J, Crespo GA, Maroto A, Sarmentero MA, Ballester P, Rius FX (2009) Biosens Bioelectron 25:344–349

41. Crespo GA, Gugsa D, Macho S, Rius FX (2009) Anal Bioanal Chem 395:2371–2376

42. Mousavi Z, Bobacka J, Lewenstam A, Ivaska A (2009) J Electroanal Chem 633:246–252

43. Crespo GA, Macho S, Bobacka J, Rius FX (2009) Anal Chem 81:676–681

44. Zhu J, Qin Y, Zhang Y (2009) Electrochem Commun 11:1684–1687

45. Abbaspour A, Izadyar A (2007) Talanta 71:887–892

46. Li S, Yang W, Chen M, Gao J, Kang J, Qi Y (2005) Mater Chem Phys 90:262–269

47. Song W, Wu C, Yin H, Liu X, Sa P, Hu J (2008) Anal Lett 41:2844–2859

48. Düzgün A, Maroto A, Mairal T, O'Sullivan C, Rius FX (2010) Analyst 135:1037–1041

49. Zhou Y, Yu B, Guiseppi-Elie A, Sergeyev V, Levon K (2009) Biosens Bioelectron 24:3275–3280

50. Zelada-Guillén GA, Riu J, Düzgün A, Rius FX (2009) Angew Chem Int Ed 48:7334–7337

51. Chumbimuni-Torres KY, Wang J (2009) Analyst 134:1614–1617

52. Ngeontae W, Janrungroatsakul W, Maneewattanapinyo P, Ekgasit S, Aeungmaitrepirom W, Tuntulani T (2009) Sens Actuators B 137:320–326

53. Chumbimuni-Torres KY, Bakker E, Wang J (2009) Electrochem Commun 11:1964–1967

54. Gyurcsányi RE (2008) Trends Anal Chem 27:627–639

55. Shim JH, Kim J, Cha GS, Nam H, White RJ, White HS, Brown RB (2007) Anal Chem 79:3568–3574

56. Studer A, Han X, Winkler FK, Tiefenauer LX (2009) Colloids Surf B 73:325–331

57. Sperling RA, Parak WJ (2010) Philos Trans R Soc Lond A 368:1333–1383

58. Giljohann DA, Seferos DS, Daniel WL, Massich MD, Patel PC, Mirkin CA (2010) Angew Chem Int Ed 49:3280–3294

59. Frasco MF, Chaniotakis N (2010) Anal Bioanal Chem 396:229–240

60. Knopp D, Tang D, Niessner R (2009) Anal Chim Acta 647:14–30

61. Huang CC, Chiang C-K, Lin Z-H, Lee K-H, Chang H-T (2008) Anal Chem 80:1497–1504

62. Yang W, Ratinac KR, Ringer SP, Thordarson P, Gooding JJ, Braet F (2010) Angew Chem Int Ed 49:2114–2138

63. Zhao Y-L, Stoddart JF (2009) Acc Chem Res 42:1161–1171

64. Wang J, Lin Y (2008) Trends Anal Chem 27:619–626

65. Tasis D, Tagmatarchis N, Bianco A, Prato M (2006) Chem Rev 106:1105–1136

66. Suspène C, Barattin R, Celle C, Carella A, Simonato J-P (2010) J Phys Chem C 114:3924–3931

67. Simpkins BS, Mccoy KM, Whitman LJ, Pehrsson PE (2007) Nanotechnology 18:355301

68. Park I, Li ZY, Pisano AP, Williams RS (2007) Nano Lett 7:3106–3111

69. Skinner K, Dwyer C, Washburn S (2006) Nano Lett 6:2758–2762

70. Sadik OA, Aluoch AO, Zhou A (2009) Biosens Bioelectron 24:2749–2765

71. Nicu L, Leichle T (2008) J Appl Phys 104:111101

3.3. Recent advances of nanostructured materials in potentiometry

3.3.1. Introduction

A detailed explanation of FETs and ISEs, with the concept theory and examples of different types of them, has already been given in chapters 3.2.4.1 and 3.2.4.2, respectively. Chapter 3.2.5 explained some different types of potentiometric sensors using nanomaterials and chapter 3.2.6 introduced recent works about the characterization of nanomaterials via potentiometry.

More detailed discussions regarding general nanoscience concepts and their possible applications in (bio)sensor technology have been recently reported in the literature [Reithmaier 2011, Li 2011].

Considering the recent trends in potentiometric sensing in different types of solid state sensors and biosensors, the following section introduces an update of the recent advances that have been appeared after the ones mentioned in chapter 3.2.

3.3.2. Field-effect transistors

Recently, Tian *et al* [Tian 2010] have managed to build a three dimensional pH FET, more specifically a nanoscale field-effect transistor (nanoFET) at the tip of an acute-angle kinked silicon nanowire, where connections are made by the arms of the kinked nanostructure, and remote multilayer interconnects allow three-dimensional (3D) probe presentation. The authors showed a near Nernstian response with ~58 mV/*p*H. Similarly, a leaf-like carbon nanotube/nickel (CNT/Ni) composite nanostructure is developed by Huang *et al* [Huang 2011] as the sensing membrane in an extended-gate field-effect transistor (EGFET) for the *p*H sensing using a nanocomposite plating technique. While sensing *p*H within a working range of 2-10, the leaf-like CNT/Ni EGFET exhibited a sensitivity of 59 mV/*p*H. This simple and low-cost sensing membrane can be applied in disposable biosensors. Hagen *et al* [Hagen 2011] reported zinc oxide field effect transistors (ZnO-FETs), covalently functionalized with single stranded DNA aptamers as a selective platform for label-free small molecule sensing. The sensor demonstrated selective detection of riboflavin down to pM levels in aqueous solution using the negative electrical current response of the ZnO-FET by covalently attaching a riboflavin binding aptamer to the surface. On another hand, Chen *et al* [Chen 2011] managed to obtain ultrahigh detection limit below attomolar level concentrations with their GaN nanowire (GaNNW) based EGFET

biosensor, capable of specific DNA sequence identification under label-free in situ conditions. Graphene based FETs, that are using graphene as the channel material, have also been used in the recognition of proteins (Ohno 2009), bacteria (Mohanty 2008), and single stranded DNAs (Lin 2010). Furthermore graphene based FETS are very recently used to detect glucose [Kwak 2012] by functionalization the CVD-grown graphene with linker molecules in order to immobilize the enzymes that induce the catalytic response of the sugar.

3.3.3. Ion-selective electrodes

Ciosek *et al* [Ciosek 2011] succeeded to classify amino acids and oligopeptides using 8 different classical potentiometric ISE arrays based on the increase of information gained during measurements of sensors' signals at various *p*H. In this way, they are able to capture more potentiometric data on interaction of amino acids and oligopeptides. Ghaedi *et al* [Ghaedi 2011] incorporated MWCNTs into their carbon paste electrodes including sodium tetraphenylborate (NaTPB), BHBAHMBP, Nujol, and graphite powder. Different amounts of MWCNTs (500/3.4/150/6.0/50 mg) were added to optimize the response against Pb^{2+} ions. At optimum values of variables, the proposed electrode response toward Pb^{2+} ion was linear in the range of 5.0×10^{-7} to 1.0×10^{-1} mol L^{-1} with slope of 29.50 mV per $decade^{-1}$ of Pb^{2+} ion concentration and detection limit of 2.5×10^{-7} mol L^{-1}. The electrode response was in the *p*H range of 2.7-4.0, while the response time of the electrode was ~ 40 s. Kisiel *et al* [Kisiel 2010] used polypyrrole microcapsules as a transducer for ion-selective electrodes to detect Ca^{2+} ions. They have managed to obtain a potentiometric response slope equal to 23.9 ± 0.1 mV/dec, and detection limit equal to $10^{-4.3}$ M. Addition of platinum and gold nanoparticles [Jaworska 2011a, 2011b] enabled to decrease the resistivity of polyacrylate ion-selective membranes, and to increase the potential reading stability on ISEs, respectively. Our group also recently reported several novelties: an ISE to determine Ca^{2+} ions in sap [Hernández 2010]; covalent immobilization of a new hybrid material, *i.e.* benzo-18-crown-6 covalently linked to MWCNTs, and its use in solid-state ion-selective electrodes both as a receptor and an ion-to-electron transducer for Pb^{2+} determination [Parra 2011]; solid-state classical and planar reference electrodes based on CNTs and polyacrylate membranes [Rius-Ruiz 2011a, 2011b]; and a potentiometric planar strip cell based on SWCNTs that aims to exploit the attributes of SC-ISEs for decentralized measurements [Rius-Ruiz 2011c].

Mousavi *et al* [Mousavi 2011] compared Multi-walled carbon nanotubes (MWCNTs) with poly(3-octylthiophene) (POT) as ion-to-electron transducer in all-solid-state potassium ion-selective electrodes with valinomycin-based ion-selective membranes using potentiometry and

electrochemical impedance spectroscopy. They found that the MWCNT-based electrodes have a more reproducible standard potential and a lower overall impedance than the electrodes based on POT. Both types of electrodes showed similar sensitivity to potassium ions and no redox sensitivity.

3.3.4. New potentiometric sensors using nanomaterials

Chirizzi *et al* [Chirizzi 2011] introduced a potentiometric urea biosensor based on urease (Ur) electrochemical immobilisation by poly(o-phenylenediamine) (PPD). Our group also reported a biosensor based on the same theory of functionalization of SWCNTs with aptamers to detect *Escherichia coli* (*E. coli*) CECT 675 in complex samples [Zelada-Guillén 2010] and sensors incorporating SWCNTs as both recognition and transduction elements to detect aromatic hydrocarbons in aqueous solutions [Washe 2010]. Moreover, a new sensor containing covalently functionalized SWCNTs with adenosine monophosphate as potential transducing and recognition elements in potentiometric sensors has recently been reported [Blondeau 2011].

3.3.5. Conclusions

As it can be seen from the very recent reports in the literature, both ISEs and FETs continue being an area of large scientific interest, where new techniques and nanomaterials are increasingly used due to their new and attractive properties. However, the new type of membraneless electrodes, based on the direct linking of the receptor to the carbon nanotubes, which creates the base of the current thesis, is yet to be widely studied and exploited. Improvements should be performed not only to develop robust and reliable sensors but to know the sensing mechanism as well.

3.4. References

Ahammad, A. J. S., Lee, J. -J., Rahman, M. A., Sensors 2009, 9, 2289-2319

Blondeau, P., Rius-Ruiz, F. X., Düzgün, A., Riu, J., Rius, F. X., Materials Science and Engineering: C 2011, 31, 1363-1368

Chen, C. -P., Ganguly, A., Lu, C. -Y., Chen, T. -Y., Kuo, C. -C., Chen, R. -S., Tu, W. -H., Fischer, W. B., Chen, K. -H., Chen, L. -C., Analytical Chemistry 2011, 83, 1938-1943

Chirizzi, D., Malitesta, C., in: G. Neri, N. Donato, A. d'Amico, C. Di Natale (Eds.) (Lecture Notes in Electrical Engineering), Springer Netherlands, 2011, p. 335-338

Ciosek, P., Jańczyk, M., Wróblewski, W., Analytica Chimica Acta 2011, 699, 26-32

Ghaedi, M., Shokrollahi, A., Montazerozohori, M., Mansouri, M., Khodadoust, S., Mousavi, A., Hossainian, H., Sensors Journal, IEEE 2011, 11, 2449-2457

Hagen, J. A., Kim, S. N., Bayraktaroglu, B., Leedy, K., Chávez, J. L., Kelley-Loughnane, N., Naik, R. R., Stone, M. O., Sensors 2011, 11, 6645-6655

Hernández, R., Riu, J., Rius, F. X., Analyst 2010, 135, 1979-1985

Huang, B. R., Lin, T. C., Applied Physics Letters 2011, 99, 023108

Jacobs, C. B., Peairs, M. J., Venton, B. J., Analytica Chimica Acta 2010, 662, 105-127

Jaworska, E., Kisiel, A., Maksymiuk, K., Michalska, A., Analytical Chemistry 2011a, 83, 438-445

Jaworska, E., Wójcik, M., Kisiel, A., Mieczkowski, J., Michalska, A., Talanta 2011b, 85, 1986-1989

Kwak, Y. H., Choi, D. S., Kim, Y. N., Kim, H., Yoon, D. H., Ahn, S. -S., Yang, J. -W., Yang, W. S., Seo, S., Biosensors and Bioelectronics 2012, 37, 82-87

Li, S., Singh, J., Li, H., Banerjee, I. A., "Biosensor Nanomaterials" Wiley-VCH (2011)

Lin, J., Teweldebrhan, D., Ashraf, K., Liu, G., Jing, X., Yan, Z., Li, R., Ozkan, M., Lake, R. K., Balandin, A. A., Ozkan, C. S., Small 2010, 6, 1150-1155

Mohanty, N., Berry, V., Nano Letters 2008, 8, 4469-4476

Mousavi, Z., Teter, A., Lewenstam, A., Maj-Zurawska, M., Ivaska, A., Bobacka, J., Electroanalysis 2011, 23, 1352-1358

Ohno, Y., Maehashi, K., Yamashiro, Y., Matsumoto, K., Nano Letters 2009, 9, 3318-3322

Parra, E. J., Blondeau, P., Crespo, G. A., Rius, F. X., Chemical Communications 2011, 47, 2438-2440

Reithmaier, P. R., Paunovic, P., Kulisch, W., Popov, C., Petkov, P., "Nanotechnological Basis for Advanced Sensors (NATO Science for Peace and Security Series B: Physics and Biophysics)", Springer (2011)

Rius-Ruiz, F. X., Kisiel, A., Michalska, A., Maksymiuk, K., Riu, J., Rius, F., Analytical and Bioanalytical Chemistry 2011a, 399, 3613-3622

Rius-Ruiz, F. X., Bejarano-Nosas, D., Blondeau, P., Riu, J., Rius, F. X., Analytical Chemistry 2011b, 83, 5783-5788

Rius-Ruiz, F. X., Crespo, G. A., Bejarano-Nosas, D., Blondeau, P., Riu, J., Rius, F. X., Analytical Chemistry 2011c, 83, 8810-8815

Shao, Y., Wang, J., Wu, H., Liu, J., Aksay, I. A., Lin, Y., Electroanalysis 2010, 22, 1027-1036

Tian, B., Cohen-Karni, T., Qing, Q., Duan, X., Xie, P., Lieber, C. M., Science 2010, 329, 830-834

Washe, A. P., Macho, S., Crespo, G. A., Rius, F. X., Analytical Chemistry 2010, 82, 8106-8112

Zelada-Guillén, G. A., Bhosale, S. V., Riu, J., Rius, F. X., Analytical Chemistry 2010, 82, 9254-9260

CHAPTER 4

EXPERIMENTAL SECTION

4.1. Introduction

This chapter describes in detail all the apparatus, materials, and reagents used along the experimental chapters of the thesis. Some useful references and development procedures are also introduced. Also, microscopic and electrochemical characterization techniques are described with their corresponding objectives.

4.2. Apparatus, materials, and reagents

4.2.1. Apparatus

A Keithley (U.K.) 6514 potentiometer, a Lawson (USA) multi-channel potentiometer and a Metrohm (Switzerland) Ag/AgCl reference electrode were used to perform the potentiometric experiments. A CHI Instruments (USA) electrochemical workstation was used for cyclic voltammetry (CV) experiments. A FEI Company (Netherlands) SEM-Quanta 600 is used to take the SEM image. Confocal images were acquired using a NIKON TE2000-E confocal laser scanning microscope. A Sutter 2000 puller machine was employed to make the teflon outer coatings for the glassy carbon rods.

4.2.2. Materials

The single walled nanotubes (SWCNT) were purchased from HeJi (China) in bulk form with > 90 % purity, 150 μm average length and 1.4-1.5 nm of diameter. 15-mer (5'-GGT TGG TGT GGT TGG-3')5'-NH_2-modified (with a 3-carbon spacer) thrombin binding aptamers (TBA), 15-mer (5'-GGTTGGTGTGGTTGG-3') 5'-SH modified (with a 3-carbon spacer) TBA, 35-mer (5'-TCT CTC AGT CCG TGG TAG GGC AGG TTG GGG TGA CT-3')5'-NH_2 (with a 3-carbon spacer) TBA and 3'-carboxyfluorescein (FAM) modified TBA were purchased from Eurogentec (Cultek, Spain). Human α-thrombin supplied by Haematologic Technologies (Vermount, USA). Gassy carbon (GC) rods were purchased from HTW (Germany).

4.2.3. Reagents

The reagents 1-ethyl-3-3(3-dimethylaminopropyl) carbodiimide hydrochloride (EDC), N-hydroxysuccinimide (NHS) and N-morpholinoethane sulfonic acid (MES) buffer were purchased from Acros Organics (Belgium). Phosphate buffer solution (PBS) is from Panreac Quimica (Spain). PBS was a mixture of 84 mL of 0.2 M NaH2PO4 and 16 mL 0.2 M Na2HPO4 in 100 mL of water to a final pH 7.5. Cetyl trimethylammonium bromide (CTAB) was purchased from Sigma-Aldrich (Spain). Aniline monomer (Aldrich) was distilled and kept cooled at 4 ºC. It was also kept in the dark to avoid any potential photooxidation. Sodium dodecyl sulphate (SDS) and sodium dodecyl benzene sulfonate (SDBS) (Aldrich) was used as purchased. $[Ru(NH_3)_6]^{3+}$ (RuHex, $Ru[(NH_3)_6]Cl_3$) were purchased from Sigma Aldrich (Spain).

4.3. Procedures

4.3.1. Pretreatment of carbon nanotubes

As the SWCNTs were purchased in bulk from, they need a two-step purification and carboxylation processes depending basically on the application required.

Firstly, oxidation of the amorphous carbon is achieved through a dry heating purification step to minimize the nanotubes's loss. Carbon nanotubes are heated up to 360 ºC under an oxygen atmosphere for 90 min [Furtado 2004]. 200 mg SWCNTs are put inside quartz tubular reactor (4 cm x 120 cm, Afora) and heated by a horizontal split tube furnace (HST/600, Carbolite). At the same time, a dry air current flows (100 $cm^3.min^{-1}$, Carburos Metálicos) through the tube.

Secondly, the SWCNTs were refluxed in 2.6 M nitric acid for 4 h for the carboxylation process and to further purify them by oxidizing the metallic impurities. The SWCNTs in nitric acid solution were then filtered and rinsed with Milli-Q water to remove the acid completely, and subsequently dried overnight at 80 ºC.

4.3.2. Deposition of carbon nanotubes

4.3.2.1.Spraying

SWCNTs were deposited onto the glassy carbon (GC) substrates by an optimized spraying technique derived from the report of Kaempgen et al [Kaempgen 2005]. 10 mg of SWCNTs were powdered via an agate mortar miller and dispersed in 10 ml of 1 % wt of sodium dodecyl sulphate (SDS). The dispersion was homogenized by tip-sonicator for 30 min (amplitude 60 %, cycle 0.5, Ultraschallprozessor UP200S, Dr. Hielscher). After a few seconds to settle, only the superior fraction is transferred to the compartment placed on the spray-gun. The electrodes are

placed at 30 cm in perpendicular line. The deposition was achieved in successive steps. After spraying the dispersion of SWCNTs for 2 seconds, the layer was dried by a hot-gun, thoroughly washed with water and dried again. The aim of this last step was to eliminate as much as possible the SDS on the electrode. The process was repeated 35 times obtaining a thickness around 35 μm (Figure 4.1).

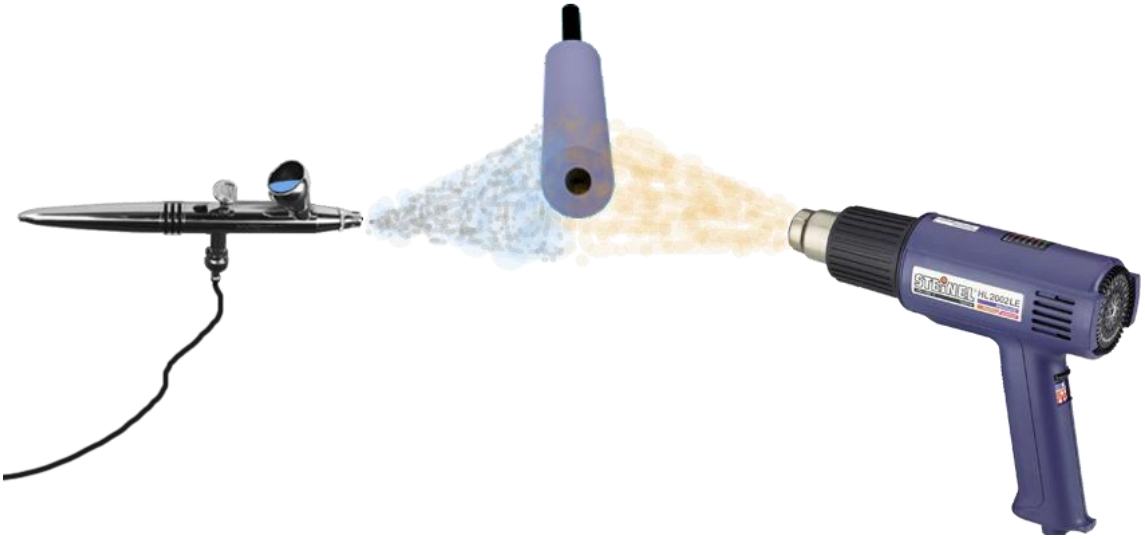

Figure 4.1 The scheme depicting the deposition of the CNTs by spraying technique onto the glassy carbon substrate.

4.3.2.2.Drop casting

1 mg of acid-purified SWCNT is dispersed in 1 ml of dimethyl formamyde (DMF) to form homogeneous dispersion. The glassy carbon rod covered with teflon is placed vertically onto the electric heater in such a way that the lower tip is in contact to the hot electric plate adjusted at 200 ºC. The solution of SWCNTs in DMF is drop casted onto the tip of the electrode by waiting 5 min after each drop. In this way the solvent is evaporated. The total numbers of the drops are 10.

4.3.2.3.Immersing in SWCNTink

In order to prepare the ink, we have used the SWCNTs and the SDBS, mixing them in water. The new solution is sonicated in the bath for 60 min. Later, the dispersion was further sonicated for 90 min in the tip sonicator.

4.3.3. Electrochemical deposition of polyaniline

Polyaniline films were electropolymerized onto the polished distal end of the glassy carbon rod via cyclic voltammetry with a three-electrode system that consisted of an Ag/AgCl reference electrode, a platinum wire as a counter electrode, and a GC rod as a working electrode. Prior to

electropolymerization, GC rods were pre-treated with 0.85 V potential during 10 s for the activation of the surface. Electropolymerization of aniline was carried out potentiodynamically on the GC rod within the potential range of -0.15 to 0.85 V by applying 50 potential cycles at a sweep rate of 100 mV/s.

4.3.4. Development of solid contact sensors

The GC rods were inserted by mechanical pressure into a hard teflon body. The electrical connections were directly made with a clamp in contact with the overhanging GC (teflon body: length 40 mm and external diameter 6 mm, Amidata SA).

4.3.5. Development of paper based sensors

Sensors were prepared by first dipping the rectangular cut (1 x 2 cm) filter papers into the nanoink for two days followed by rinsing in MilliQ water 24 hours.

4.3.6. Functionalization of aptamers

4.3.6.1.Covalent functionalization of aptamers

For SWCNTs based sensors, the carboxylic groups of the SWCNTs were activated with a solution containing 200 mM EDC and 50 mM NHS [Williams 2002] (dissolved in MES buffer, 50mM, pH 5.0). The GC surface containing the SWCNTs was dipped in this solution for 30 minutes. To covalently link the TBA to the walls of the SWCNTs through the nucleophilic attack of the amine to the activated carboxylic group, the sensor subsequently was dipped overnight in a solution containing 0.001 M PBS, 1 µM 5'-amine-TBA, as well as 0.2 mM of CTAB, a positively charged surfactant, added to facilitate the TBA immobilisation as the CTAB interacts with the remaining non-activated carboxylic groups (negatively charged) and avoids the electrostatic repulsion between these carboxylic groups and the TBA (also negatively charged at pH=7.5). Scheme 1 shows the steps of the covalent immobilisation of TBA.

For PANI based sensors, PANI modified GC probe is dipped into 5 μM TBA solution overnight for immobilization of the thrombin aptamer via aromatic substitution at the conducting polymer surface [Zhou 2009]

4.3.6.2.Non-covalent functionalization of aptamers

The GC surface containing the sprayed non-carboxylated SWCNTs was dipped in 5 µM solution of aptamers for overnight and rinsed 3 times with MilliQ water.

4.3.7. Microscopic characterization

4.3.7.1.Scanning electron microscopy

Environmental Scanning Electron Microscopy (ESEM) was used to characterize the CNT's layer deposited onto the electrodes by the spraying technique. The SWCNTs layer was attached to the support inside the E-SEM chamber. Parameters (potential, pressure and working distance) were characterized in each case to obtain the maximum resolution possible of the images.

4.3.7.2.Confocal laser electron microscopy

Confocal images were acquired using a NIKON TE2000-E confocal laser scanning microscope using 488 nm line from an argon laser for excitation. Images were recorded using an x100 oil immersion objective.

4.3.8. Electrochemical characterization

4.3.8.1.Potentiometry

A Keithley 6514 and Lawson multichannel high input resistance (10^{15} Ω) potentiometers were used to record electromotive forces (EMF). A double-junction Ag/AgCl/KCl (3 M) reference electrode (type 6.0729.100, Methrom AG) containing a 0.1-1 M LiAcO electrolyte bridge was used. The measurements were performed in stirred solutions at room temperature.

4.3.8.2.Cyclic voltammetry

Cyclic voltammetry experiments are conducted with a three-electrode system that consisted of an Ag/AgCl reference electrode, a platinum wire as a counter electrode, and a GC rod as a working electrode.

4.3.8.3.Electrochemical impedance spectroscopy

Electrochemical impedance spectroscopy experiments were performed in a preliminary attempt to elucidate the nature of the mechanism that may explain the increase of potential after the aptamer-protein interaction. The impedance spectra were recorded first with the sensors containing only a SWCNT layer, secondly after the aptamer functionalization, and finally after the interaction of the TBA functionalized SWCNTs.

4.4. References

Furtado, C. A., Kim, U. J., Gutierrez, H. R., Pan, L., Dickey, E. C., Eklund, P. C., Journal of American Chemical Society 2004, 126, 6095-6105

Kaempgen, M., Duesberg, G. S., Roth, S., Applied Surface Science 2005, 252, 425-429

Williams, K. A., Veenhuizen, P. T. M., de la Torre, B. G., Eritja, R., Dekker, C., Nature 2002, 420, 761-761

Zhou, Y., Yu, B., Guiseppi-Elie, A., Sergeyev, V., Levon, K., Biosensors and Bioelectronics 2009, 24, 3275-3280

CHAPTER 5

APPLICATIONS

5.1. Introduction

This chapter focuses on applications. The main aim is to develop two sensors to determine thrombin. In chapter 5.2, glassy carbon rod, covered with a Teflon jacket, is used as the sensor backbone while in chapter 5.3 a filter paper based CNTink aptasensor is described. Both chapters describe aptasensors that uses aptamers as recognition elements and SWCNTs as transduction elements to detect thrombin in aqueous solutions.

Recent advances in potentiometric protein determination using aptamer based sensors during and after the publications of the articles are also introduced and discussed in section 5.4.

5.2. "Solid-contact potentiometric aptasensor based on aptamer functionalized carbon nanotubes for the direct determination of proteins"

Analyst 2010, 135. 1037-1041

Ali Düzgün[a], Alicia Maroto[a], Teresa Mairal[b], Ciara O'Sullivan[bc] and F. Xavier Rius*[a]

[a]Department of Analytical and Organic Chemistry, Universitat Rovira i Virgili, 43007, Tarragona, Spain.

[b]Department of Chemical Engineering, Universitat Rovira i Virgili, 43007, Tarragona, Spain

[c]Institució Catalana de Recerca i Estudis Avançats, 08010, Barcelona, Spain

5.2.1. Abstract

A facile, solid-contact selective potentiometric aptasensor exploiting a network of single-walled carbon nanotubes (SWCNT) acting as a transducing element is described in this work. The molecular properties of the SWCNT surface have been modified by covalently linking aptamers as biorecognition elements to the carboxylic groups of the SWCNT walls. As a model system to demonstrate the generic application of the approach, a 15-mer thrombin aptamer interacts with thrombin and the affinity interaction gives rise to a direct potentiometric signal that can be easily recorded within 15 s. The dynamic linear range, with a sensitivity of 8.0 mV/log a_{Thr} corresponds to the 10^{-7}–10^{-6} M range of thrombin concentrations, with a limit of detection of 80 nM. The aptasensor displays selectivity against elastase and bovine serum albumin and is easily regenerated by immersion in 2 M NaCl. The aptasensor demonstrates the capacity of direct detection of the recognition event avoiding the use of labels, mediators, or the addition of further reagents or analyte accumulation.

5.2.2. Introduction

Potentiometric solid-contact electrodes display high selectivity, sensitivity, low limits of detection[1,2] and their miniaturizability and ease-of-use adds to their appeal. Since the first attempts in the mid-seventies many efforts have been devoted to replace the polymeric membranes and use the electromotive force generated by a direct interaction between the suitable receptor and the target molecule. As an example, an antibody-antigen interaction to directly detect proteins has been described.[3] However, the recorded signal was attributed later to secondary effects. Tang *et al*, have recently reported a potentiometric immunosensor for the detection of diphtheria antigens where the signal was large enough due to the building of sequential fields[4] and a selective direct potentiometric myoglobin and hemoglobin sensor was reported using a gold coated silicon chip.[5] Potentiometric monitoring of DNA hybridization has recently been demonstrated.[6]

Aptamers are able to bind to target proteins such as thrombin, a pluripotent serine protease, or other molecules with high affinity and specificity. Their small size, chemical simplicity, flexibility, reversible denaturation and use under non-physiological conditions, makes aptamers very advantageous with respect to other receptors such as antibodies, and consequently have been widely used to develop biosensors for protein detection.[7–10]

Carbon nanotubes (CNT) display extraordinary physical and electrical properties that are very beneficial for electrochemical detection,[11] and these characteristics have been taken advantage for the development of field effect transistors using the hybrid material SWCNT-nucleic acid.[12] Crespo *et al*[13] recently demonstrated that SWCNTs can act as efficient transducers in solid-contact ion selective electrodes. However, the presence of a selective polymeric membrane allowed the determination of small charged molecules but hindered the detection of large biomolecules. Therefore, a recognition layer of the sensor, directly linked to the transducing SWCNT, is a very attractive alternative.

In this report we describe the development of a solid-contact selective potentiometric sensor exploiting SWCNT as transducers, and aptamers as biorecognition elements, where the electrical potential following aptamer-target interaction is significantly changed to directly detect a protein target. The entrapment of the receptor into a polymeric membrane, routinely used in ion-selective electrodes, has been replaced by covalently linking the thrombin binding 5'-NH_2-functionalized 15-mer aptamer to the carboxylic groups of the SWCNT walls. In this way, aptamers assure selectivity towards the target molecule whilst the remarkable electronic properties of the SWCNT facilitate a significant potential change due to the charge distribution produced by the protein-aptamer binding process.

5.2.3. Experimental

5.2.3.1. Materials

SWCNT were purchased from HeJi (China) in bulk form with >90% purity, 150 μm average length and 1.4–1.5 nm diameter. 15-mer (5'-GGT TGG TGT GGT TGG-3')5'-NH_2-modified (with a 3-carbon spacer) thrombin binding aptamers (TBA) and 35-mer (5'-TCT CTC AGT CCG TGG TAG GGC AGG TTG GGG TGA CT-3')5'-NH_2 (with a 3-carbon spacer) and 3'-carboxyfluorescein (FAM) modified TBA were purchased from Eurogentec (Cultek, Spain). Human α-thrombin supplied by Haematologic Technologies (Vermount, USA).

The reagents 1-ethyl-3-(3-dimethylaminopropyl) carbodiimide hydrochloride (EDC), N-hydroxysuccinimide (NHS) and N-morpholinoethane sulfonic acid (MES) buffer were purchased from Acros Organics (Belgium). Phosphate buffer solution (PBS) is from Panreac Quimica (Spain). PBS was

a mixture of 84 mL of 0.2 M NaH_2PO_4 and 16 mL 0.2 M Na_2HPO_4 in 100 mL of water to a final pH 7.5. Cetyl trimethylammonium bromide (CTAB) was purchased from Sigma-Aldrich (Spain).

5.2.3.2. CNTs oxidation and purification

200 mg of as-purchased SWCNT were oxidized in a silica furnace chamber in order to selectively remove the amorphous carbon impurity, using the following conditions; T = 365 °C, air flow-rate = 100 cm^3 min^{-1}, t = 90 min. Subsequently, the SWCNTs were refluxed in 2.6 M nitric acid for 4 h to carboxylate them and to further purify them by oxidizing the metallic impurities.[14] The SWCNT in nitric acid solution were then filtered and rinsed with Milli-Q water to remove the acid completely, and subsequently dried overnight at 80 °C.

5.2.3.3. Sensor development

The solid contact sensor is prepared by placing a 3 mm diameter glassy carbon rod within a teflon body with an outer diameter of 7 mm. The tip is first polished using a Buehler p4000 paper, subsequently 25 µm and finally 3 µm grain size alumina powder to obtain a smooth surface prior to the spraying process. 25 mg of the purified and dried SWCNTs were powdered in a marble mill and then dispersed in 10 mL of Milli-Q water containing 100 mg of Sodium Dodecyl sulfate (SDS) to form the micelles and increase the solubility of SWCNT in water. The solution was sonicated for 30 min at 0.5 s^{-1} in order to achieve the maximum homogeneity of the dispersion. The sonicated solution was sprayed with approximately 1 bar pressure onto the glassy carbon surface under a high temperature (approx. 200 °C) air blower by spraying 35 times, dipping the surface into Milli-Q water under stirring conditions at intervals of 5 sprays so as to eliminate the SDS as its presence decreases the conductance on the SWCNT network.

We deposited a layer of about 30 µm thickness (measured with SEM) of purified SWCNT onto the polished tip of a glassy carbon (GC) surface.

5.2.3.4. TBA immobilisation process

The carboxylic groups of the SWCNT were activated with a solution containing 200 mM EDC and 50 mM NHS[15] (dissolved in MES buffer, 50 mM, pH 5.0). The GC surface containing the SWCNTs was dipped in this solution for 30 min. To covalently link the TBA to the walls of the SWCNTs through the nucleophilic attack of the amine to the activated carboxylic group , the sensor subsequently was

dipped overnight in a solution containing 0.001 M PBS, 1 µM 5'-amine-TBA, as well as 0.2 mM of CTAB, a positively charged surfactant, added to facilitate the TBA immobilisation as the CTAB interacts with the remaining non-activated carboxylic groups (negatively charged) and avoids the electrostatic repulsion between these carboxylic groups and the TBA (also negatively charged at pH = 7.5). Scheme 5.2-1 shows the steps of the covalent immobilisation of TBA.

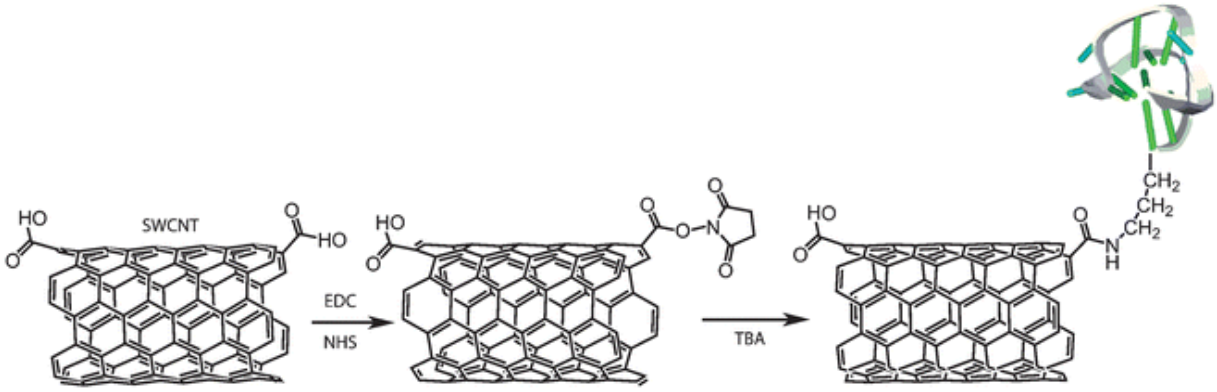

Figure 5.2-1 Steps of the covalent immobilization of TBA. Activation of the carboxylic groups using EDC and NHS, and subsequent covalent functionalization of 5'-NH_2-modified thrombin aptamer.

5.2.3.5. Setup and measurements

A Keithley (U.K.) 6514 potentiometer and a Metrohm (Switzerland) Ag/AgCl reference electrode were used to perform the experiments. A FEI Company (Netherlands) SEM-Quanta 600 is used to take the SEM image. Confocal images were acquired using a NIKON TE2000-E confocal laser scanning microscope. The 488 nm line from an argon laser was used for excitation. Images were recorded using an ×100 oil immersion objective.

Potentiometric measurements were conducted in 5 ml 1 mM PBS solution (pH = 7.5). The solution was stirred during the measurements at 1000 rpm. The two-electrode system consisted of an Ag/AgCl reference electrode and the developed GC sensor as the working electrode. Thrombin was spiked to the 5 ml solution to have a total concentration ranging from 0.5 nM up to 1 µM.

5.2.4. Results and discussion

Fig. 5.2-2 shows a scheme of the sensor together with a SEM image of the tip surface. This image shows the SWCNT onto the GC surface in a spaghetti form. The porous nature of the layer enlarges the number of the thrombin aptamers bound.

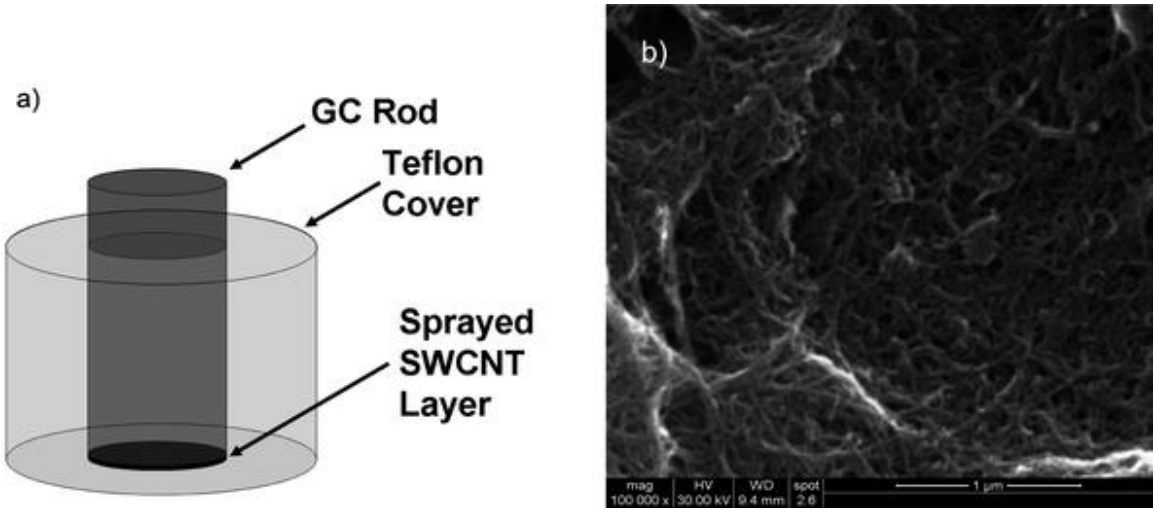

Figure 5.2-2 a) Scheme of the tip of the developed sensor. b) SEM image of the tip surface where the SWCNT have been deposited in a spaghetti form.

The time responses of the aptamer functionalized SWCNT solid-contact sensors for stepwise concentrations of thrombin from 5×10^{-10} to 10^{-6} M in 1 mM phosphate buffer solution (PBS) and pH 7.5 are shown in Fig. 5.2-3. The low ionic strength is necessary to avoid the screening effect of the electrolytes in the sample solution. Following addition of analyte, the signal rapidly plateaus to a very stable signal, with a response time of approximately 15 s, independent of analyte concentration, displaying a small negative average drift of 0.05 mV min^{-1}.

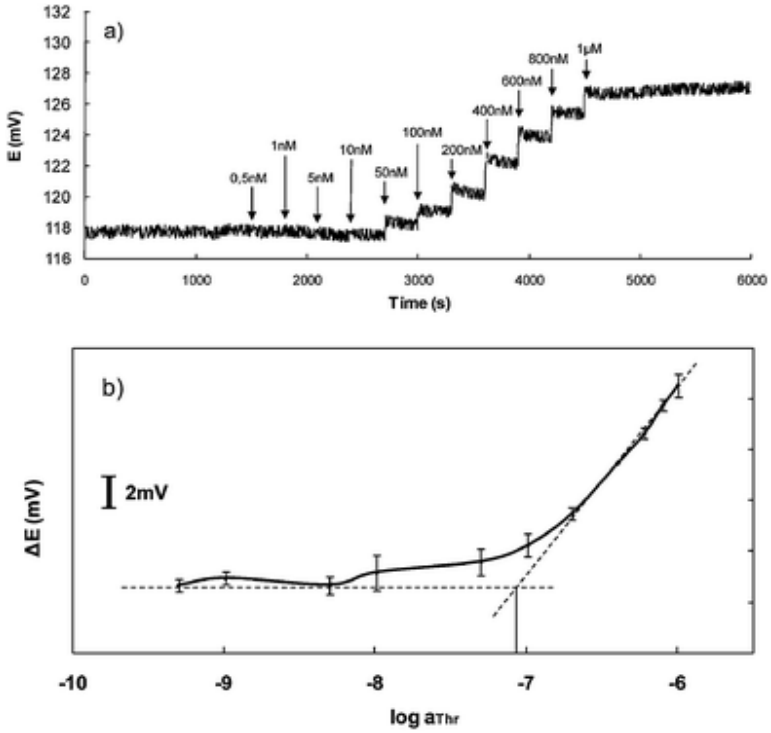

Figure 5.2-3 Calibration curve for the potentiometric aptasensor. a) Potential over time for a typical aptamer-SWCNT sensor for concentrations of thrombin in samples ranging from 0.5 nM up to 1 µM. b) Calibration curve obtained for three different sensors. The error bars represent the range of potential values obtained for each set of three measurements recorded.

Fig. 5.2-3b shows the calibration curve after subtracting the shift due to different standard potentials. The standard deviation of the standard potentials corresponding to three different sensors (each for 3 times, N = 9) is 2.1 mV. Two segments of very different slopes can be observed. The useful linear interval, with a sensitivity of 8.0 mV/log a_{Thr} corresponds to a range of thrombin concentrations between 1×10^{-7} and 8×10^{-7} M. At a working pH of 7.5 human thrombin is neutral (pI = 7.0–7.6),[16] therefore, the EMF recorded cannot be related to the activity of the charged analyte in a Nernstian way. It should be taken into account that this sensor differs from a potentiometric ion-selective electrode in the sense that it does not use a polymeric membrane, and the recorded response is related purely to the affinity between the aptamer and the target analyte. Therefore, it is a non-reversible sensor that could find valuable applications in disposable miniaturized devices. The limit of detection, defined for classical potentiometric sensors as the intersection of the two straight lines, is 80 nM. A value of 65.5 nM is obtained if the detection limit is computed according to the three sigma method. This value is close to the minimal physiological concentration levels of

thrombin. It is known that this level may increase up to a few µM levels when the clotting process is activated.[16] Regeneration of the aptasensor is achieved by dipping their tip into 2 M NaCl for 10 min. The standard deviation of the E_0 differences between regenerated and non-regenerated sensors (using seven regeneration cycles with the same sensor, n = 7) is 4.7 mV. The sensor is highly reproducible, with RSD = 5.8% for the slope obtained from the same sensor with individual measurements made on 14 days.

Two different control experiments were performed to assess that the increase of potential was only due to the interaction of thrombin with the SWCNT immobilized aptamers. In the first experiment, the purified SWCNT deposited onto the GC surface were not functionalized with the aptamers. The potential of the sensor was measured against thrombin using the same experimental conditions (*i.e.* from 5×10^{-10} M to 10^{-6} M in phosphate buffer solution (PBS). When carbon nanotubes are not functionalized with aptamers, a constant drift is observed. When this background drift of constant slope (10^{-2} mV s^{-1} in 1 mM PBS) is subtracted from the thrombin this results in a very slight potential increase (approximately 0.15 mV/log a_{Thr}) that can be attributed to the non-specific binding of the protein onto the surface of the non-functionalized carbon nanotubes. This drift appears to be related to the extreme sensitivity of CNT to their surrounding chemical environment and the ionic strength of the solution.[17] However, the signal due to non-specific adsorption of protein is negligible compared to the specific signal being just 0.64% for the lower concentration of 100 nM, and 4.94% for the higher concentration of 800 nM. This result indicated that the aptamer functionalized sensors had a much higher interaction ability to the thrombin molecules than the non-functionalized sensors.

In the second control experiment, all steps for the sensor development were followed except for the deposition of the SWCNT. In this way, the aptamers were functionalized directly onto the glassy carbon surface. A signal response of similar characteristic to that shown in Fig. 5.2-3 although with much lower sensitivity (approximately 3.8 mV/log a_{Thr}) was obtained. This result is not surprising if we consider that aptamers can be covalently linked directly to the surface of the glassy carbon through their carboxylated groups.[18,19]

Selectivity of the sensor was checked against two proteins; bovine serum albumin (BSA) and elastase, using two different experiments. In the first setup, the sensor response to each of the two mentioned proteins was checked separately. In the second setup the response against thrombin was

recorded in presence of BSA and elastase. BSA is a common plasma protein with a higher molecular weight compared to thrombin. Elastase is a serine protease enzyme with an isoelectric point and molecular weight similar to that of thrombin. As can be seen in Fig.5.2-4a, no significant potential increase is observed until the presence of 2 µM level for each interfering protein. Fig. 5.2-4b shows the TBA response of the sensor in presence of the two non-target proteins. Concentration of elastase was 3.2 nM, which is approximately the normal blood level.[20] Above this value, elastase starts to breakdown the thrombin, which explains the absence of the potential increase when a higher concentration of elastase is used (data not shown). However a similar behaviour was not observed for BSA which was present at a concentration 0.5 µM. Sensitivity of the sensor was 7.4 mV/log a_{Thr}. The reduced drop in the sensitivity value can be attributed to the presence of the non-specific target proteins in the solution. The sensor does not respond to a variation of type or concentration of inorganic electrolytes as long as the ionic strength is kept constant.

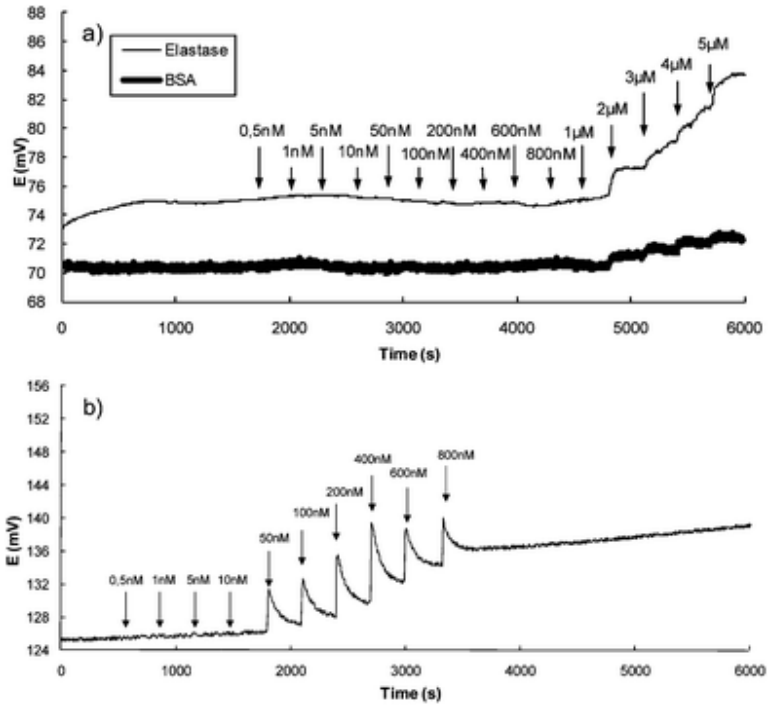

Figure 5.2-4 a) Responses of the aptamer functionalized SWCNT solid-contact sensors for stepwise concentrations of the non-specific targets elastase and BSA. b) Response against thrombin in presence of 3.2 nM elastase and 0.5 µM BSA. A sensitivity of 7.4 mV/log a_{Thr} is obtained.

Electrochemical impedance spectroscopy experiments were performed in a preliminary attempt to elucidate the nature of the mechanism that may explain the increase of potential after the aptamer

-protein interaction. The impedance spectra were recorded first with the sensors containing only a SWCNT layer, secondly after the aptamer functionalization, and finally after the interaction of the TBA functionalized SWCNT with 1 µM thrombin solution. 0.1 M of PBS is used as background electrolyte in all experiments. As shown in Fig. 5.2-5, the impedance spectra are dominated by a nearly 90° capacitive line, which extends down to low frequencies (0.3 Hz). At high frequencies, only a slight deviation from the capacitive line can be seen, indicating fast charge transfer at the glassy carbon/SWCNT/aptamer in solution interfaces as well as fast charge transport in the SWCNT layer. These results suggest that these glassy carbon sensors containing functionalized single-walled carbon nanotubes in contact with aqueous electrolyte and protein solution show a very small resistance and a large bulk capacitance that is related to a large effective double layer at the SWCNT /electrolyte interface.[21]

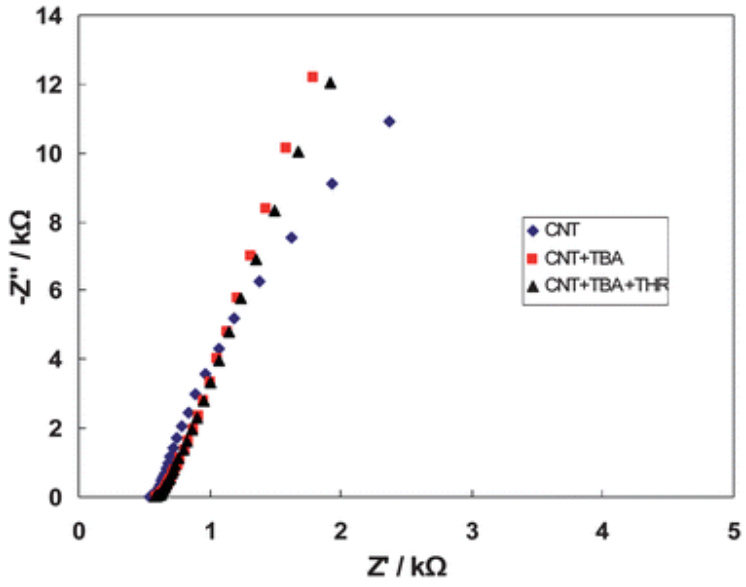

Figure 5.2-5 Complex plane impedance plots of the GC sensor containing only the SWCNT layer (◆), after TBA functionalization of the SWCNT layer (■) and after thrombin binding (▲).

The biosensing mechanism is based on the equilibrium competition between the target analyte and the SWCNTs to be linked to the aptamer. Johnson *et al*[22] have recently used molecular dynamics to demonstrate that aptamers are self-assembled to carbon nanotubes *via* π–π stacking interaction between the aptamer bases and the carbon nanotubes walls.[23] Since the phosphate groups of the aptamers are largely ionized at pH 7.5, these negative charges are transferred to the carbon nanotubes. This agrees with the decrease in the standard potential of the sensor measured

following functionalization of the SWCNTs with the aptamers. The presence of the target protein induces a conformational change in the aptamer that separates the phosphate negative charges from the SWCNT sidewalls[24,25] inducing the subsequent increase of the recorded potential. This mechanism is in agreement with the fluorescence confocal microscopy results obtained with the thrombin aptamer labeled with the fluorescein derivative FAM. In the absence of thrombin, the fluorescence is quenched by the proximity of the label to the carbon nanotube, whilst the presence of thrombin in the test solution results in the appearance of a fluorescent signal due to the competitive binding of the thrombin with the SWCNT for the aptamer, with a conformational change of the latter and the corresponding spatial displacement of the dye from the surface of the carbon nanotube.[26]Fig. 5.2-6 shows the confocal image of the tip sensor surface consisting of FAM labeled TBA linked to the SWCNTs. A very faint fluorescence is observed in the absence of thrombin while a strong fluorescence is observed after 30 min incubation of 45 µl of a 5µM thrombin solution followed by thorough washing.

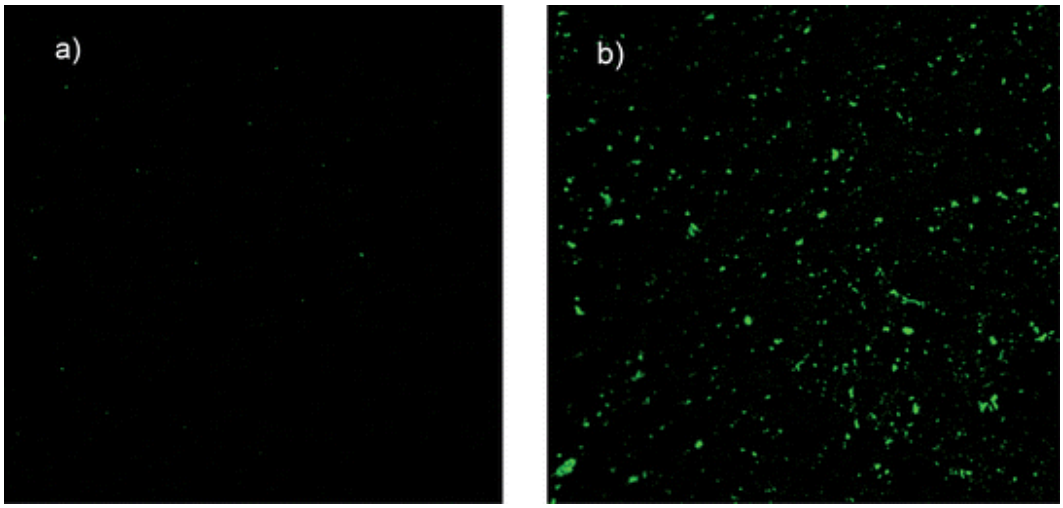

Figure 5.2-6 Fluorescence confocal image (area 127.3 µm × 127.3 µm) of tip sensor surface where SWCNTs have been modified with FAM-labelled thrombin aptamer. a) In absence of thrombin. b) After 30 min incubation of 45 µl of a 5 µM thrombin solution.

5.2.5. Conclusions

To summarize, we have reported on a generic method for aptasensing of proteins, where the simplicity of the selective potentiometric sensor, combined with its ability to directly detect a biorecognition event obviating the need for labels, mediators, the addition of further reagents or

analyte accumulation, highlight the promise of this electrochemical technique. In conclusion, we report on the use of SWCNTs as transducers in aptamer based potentiometric solid-contact sensors, with interaction between the TBA and the thrombin giving rise to a direct potentiometric signal that can be easily recorded in nearly real-time.

5.2.6. Acknowledgements

We thank the Spanish MICINN, for supporting the work through the project grant CTQ2007-67570. A. Maroto also would like to thank MICINN for providing her Juan de la Cierva fellowship.

5.2.7. Notes and references

1. E. Lindner and R. Gyurcsányi, J. Solid State Electrochem., 2009, 13, 51–68
2. E. Pretsch, TrAC, Trends Anal. Chem., 2007, 26, 46–51
3. J. Janata, J. Am. Chem. Soc., 1975, 97, 2914–2916
4. D. Tang and J. Ren, Electroanalysis, 2005, 17, 2208–2216
5. Y. Wang, Y. Zhou, J. Sokolov, B. Rigas, K. Levon and M. Rafailovich, Biosens. Bioelectron., 2008, 24, 162–166
6. Y. Zhou, B. Yu, A. Guiseppi-Elie, V. Sergeyev and K. Levon, Biosens. Bioelectron., 2009, 24, 3275–3280
7. G. Herzog and D. W. M. Arrigan, Analyst, 2007, 132, 615–632
8. A. Numnuam, K. Y. Chumbimuni-Torres, Y. Xiang, R. Bash, P. Thavarungkul, P. Kanatharana, E. Pretsch, J. Wang and E. Bakker, Anal. Chem., 2008, 80, 707–712
9. A. E. Radi, J. L. AceroSanchez, E. Baldrich and C. K. O'Sullivan, Anal. Chem., 2005, 77, 6320–6323
10. S. Tombelli, M. Minunni and M. Mascini, Biomol. Eng., 2007, 24, 191–200
11. I. Heller, A. M. Janssens, J. Mannik, E. D. Minot, S. G. Lemay and C. Dekker, Nano Lett., 2008, 8, 591–595
12. H. M. So, K. Won, Y. H. Kim, B. K. Kim, B. H. Ryu, P. S. Na, H. Kim and J. O. Lee, J. Am. Chem. Soc., 2005, 127, 11906–11907
13. G. A. Crespo, S. Macho and F. X. Rius, Anal. Chem., 2008, 80, 1316–1322
14. C. A. Furtado, U. J. Kim, H. R. Gutierrez, L. Pan, E. C. Dickey and P. C. Eklund, J. Am. Chem. Soc., 2004, 126, 6095–6105

15. K. A. Williams, P. T. M. Veenhuizen, B. G. de la Torre, R. Eritja and C. Dekker, Nature, 2002, 420, 761–761
16. M. Lee and D. R. Walt, Anal. Biochem., 2000, 282, 142–146
17. K. Maehashi, T. Katsura, K. Kerman, Y. Takamura, K. Matsumoto and E. Tamiya, Anal. Chem., 2007, 79, 782–787
18. H. Gunasingham and B. Fleet, Analyst, 1982, 107, 896
19. S.-i. Yamazaki, Z. Siroma, T. Ioroi, K. Tanimoto and K. Yasuda, Carbon, 2007, 45, 256–262
20. P. Mair, J. Mair, I. Seibt, W. Furtwaengler, D. Balogh and B. Puschendorf, The Journal of Thoracic and Cardiovascular Surgery, 1994, 108, 184–185
21. G. A. Crespo, S. Macho, J. Bobacka and F. X. Rius, Anal. Chem., 2009, 81, 676–681
22. R. R. Johnson, A. T. C. Johnson and M. L. Klein, Nano Lett., 2008, 8, 69–75
23. M. Zheng, A. Jagota, E. D. Semke, B. A. Diner, R. S. Mclean, S. R. Lustig, R. E. Richardson and N. G. Tassi, Nat. Mater., 2003, 2, 338–342
24. T. Hianik, V. Ostatná, M. Sonlajtnerova and I. Grman, Bioelectrochemistry, 2007, 70, 127–133
25. K. Padmanabhan, K. P. Padmanabhan, J. D. Ferrara, J. E. Sadler and A. Tulinsky, J. Biol. Chem., 1993, 268, 17651–17654
26. R. Yang, Z. Tang, J. Yan, H. Kang, Y. Kim, Z. Zhu and W. Tan, Anal. Chem., 2008, 80, 7408–7413

5.3. "Paper-based aptasensor for protein detection"

In preparation.

Ali Düzgün, Marta Novell, Francisco J. Andrade, Pascal Blondeau* and F. Xavier Rius

Department of Analytical and Organic Chemistry, Universitat Rovira i Virgili, 43007, Tarragona

E-mail: pascal.blondeau@urv.cat Fax: +34 977 558 446

5.3.1. Abstract

A new type of simple, disposable and low-cost potentiometric paper-based aptasensors is described in this work. A network of single-walled carbon nanotubes (SWCNTs), embedded in a filter paper, act as the transducing element of the sensor. Molecular recognition properties of the surface have been modified by covalently linking aptamers to the carboxylic groups of the SWCNTs. The useful linear interval, with a sensitivity of 7.33 mV/ log a_{Thr} corresponds to the 100 and 800 nM range of thrombin concentrations. The limit of detection (LOD) goes down to 82.57 nM thrombin concentration. Indeed, the analytical performances (sensitivity, selectivity, LOD) of the new paper-based sensor are comparable to the previously reported solid-contact potentiometric sensor while the stability improved with lower noise levels. Importantly, the construction of the sensor was considerably simplified involving painting and dip-coating processes which could be easily mass-manufactured. Using filter paper as a sensor backbone, we managed to build small, cheap and versatile sensors for highly selective detection of proteins.

5.3.2. Introduction

Sensors are usually designed to perform out of the laboratory. A further step consists not only in developing simple, cheap and portable sensors, which display relevant performance characteristics such as sensitivity and selectivity, but sensors that are integrated into flexible materials that can be embedded into everyday materials such as clothes, bandages, etc. The development of rapid, simple and inexpensive detection assays are also important to satisfy the increasing demand of diagnostic tools in isolated rural areas, as “point-of-care” [1-3] tests or for the expansion of telemedicine.[4, 5] Paper-based biosensors accomplish these requirements, targeting exciting new compounds and therefore, aiming to improve the quality of life world-wide. Thus, paper has become recently a popular base in flexible and low-cost sensor systems. Moreover, it is pollution-free due to its pure cellulose structure and it has the optimum thickness and hardness for manufacture. Several applications have been reported where functionalized paper-based sensors offer a great promise.[6] A new method for patterning microfluidics on a paper surface using plasma treatment has been demonstrated by Li et al..[7] The devices are capable of single- and multi-step tests, as well as reactions to be performed. Similarly, a microfluidic paper-based chemiluminescence analytical device (µPCAD) for glucose and uric acid was designed.[8] Cheng et al. used paper as the sensor substrate to perform enzyme-linked immunosorbent assays (ELISA) with a 96-microzone plate

(paper-based ELISA, or P-ELISA).[9] Liu et al. recently reported a self-powered paper based amperometric detection system for adenosine detection.[10]

Combination of flexible materials with aptamers, artificial nucleic acid oligomers that are able to bind to target proteins or other molecules[11], further improves the detection system by adding durability, selectivity and flexibility considering their small size and high affinity to the target. Biosensors for protein detection via aptamers have been widely studied and reported.[12-17]

Electrochemical techniques and specifically potentiometric methods are very adequate as detection systems in biochemical sensors because, in addition to displaying high selectivity, sensitivity and low limits of detection,[18] they can be miniaturized and are very easy to use.[19-21] A recent trend has emerged by the integration of nanostructured materials to potentiometric sensors.[22] Among these nanomaterials, carbon nanotubes (CNTs) display excellent physical and electrical properties that are very good candidates for electrochemical detection.[23] Crespo et al. showed that single-walled CNTs (SWCNTs) can act as efficient transducers in solid-contact ion selective electrodes.[24] Zelada-Guillén et al. used a hybrid transducing/biosensing material consisting of SWCNTs as ion-to-electron potentiometric transducers and aptamers as biorecognition molecules to detect bacteria.[25-27] The generated electromotive force (EMF) of this SWCNT-aptamer hybrid material derive from the SWCNT double-layer capacitance which have a remarkable ability to support charge transfer between the SWCNT-solution interface and surrounding ions. The extremely high surface-to-volume ratio of the nanotubes also enables sensing conformational changes in the linked aptamers during the target-recognition event that is thought switching the surface charge on the SWCNT layer.[28, 29]

There have been several attempts to incorporate CNTs to flexible materials.[30, 31] Immersing is one of the simplest and cheapest methods when an appropriate sensor backbone, e.g. filter paper, is used. It is also a less time consuming method compared to more complex methods such as electrochemical deposition or spraying, which has relatively more CNT loss during the process. Thus, we disperse SWCNTs in an aqueous suspension to generate the SWCNT ink and apply onto the paper surface. The paper becomes conductive, being among the simplest and low cost mass manufacturing methodologies.[32] Noteworthy, SWCNTs not only provide electrical conduction, but also make available the transduction layer of the potentiometric sensor thanks to their chemical

structure that enables chemical immobilization. The suitable receptors then immobilized onto the SWCNTs confer selectivity to the paper-based sensor.

We herein report a new type of simple and flexible solid-contact selective potentiometric paper-based aptasensor to detect proteins, which is based on the direct interaction between the aptamer receptor and the target protein. We chose the thrombin protein, a pluripotent serine protease enzyme that plays a central role in homeostasis following tissue injury that play important roles in subsequent inflammatory and tissue repair processes,[33] as a case study to show the uniqueness of the detection technique. SWCNTink based SWCNT act as the transducing element and thrombin binding aptamers (TBA) as the selective recognition elements. Importantly, we also compared the performance characteristics to our previously reported SWCNT based aptasensors where the sensor backbone is glassy carbon (GC) rods.[28]

5.3.3. Experimental

5.3.3.1. SWCNT ink preparation

The preparation of the SWCNT ink was achieved according to previous work using purified SWCNTs.[34, 35] Briefly, we have used 1.6 mg/ml purified and oxidized SWCNTs with 10 mg/ml SDBS, stirring them in MilliQ water. The obtained dispersion was sonicated in the bath for 60 min. and subsequently, 90 min. more in the tip sonicator (amplitude 60 %, cycle 0.5, Ultraschallprocessor UP200S, Dr. Hielscher).

5.3.3.2. Aptasensor development

Aptasensors are prepared by cutting 1 × 0.5 cm pieces of filter paper as substrate followed by first drop casting the SWCNT ink to the rectangular cut filter papers until the average resistance is as low as 0.3 kΩ. Figure 5.3-1 shows the chart where resistance is plotted versus the number of layers of carboxylated SWCNTs. In addition, the resistance of the non-carboxylated SWCNTs, previously developed in our group, was also shown for comparison. Interestingly, both SWCNT inks enable to reach a final resistance as low as 0.3-0.5 kOhms cm^{-1}. Although carboxylated SWCNTs afford similar resistance than non-carboxylated SWCNTs, a higher number of layers was necessary for the former (17 layers vs. 5 layers respectively). Nevertheless, the carboxylated SWCNTs display the advantage of being further functionalized by bioreceptors through covalent bonds.[34] As anchoring strategy for

the aptamer, we have selected covalent bonding instead of non-covalent immobilization because the first one enables better performances with potentiometric aptasensor and the resulting hybrid material is more stable in harsh conditions.[27]

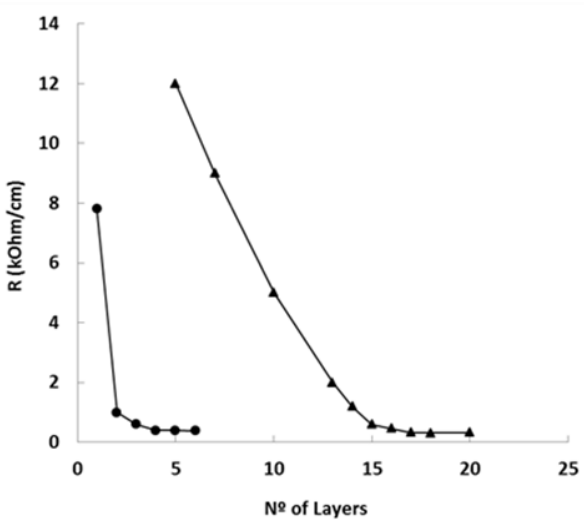

Figure 5.3-1 Resistance graph of non-carboxylated (•) and carboxylated (▲) SWCNTink covered filter paper surface as a function of the number of layers of SWCNT ink.

The SWCNT ink covered paper is then rinsed in MilliQ water for 24 hours. Conductance of the solution was monitored during this process to monitor the removal of the SDBS. Lastly, a PVC sticker with 3 mm diameter holes (active sensing area), used as a mask, is applied to the paper and coated with parafilm (excluding the sensing area) to avoid solution leakage which might cause drifts (See Scheme 5.3-1). The TBA immobilization was done according to a previous procedure.[28]

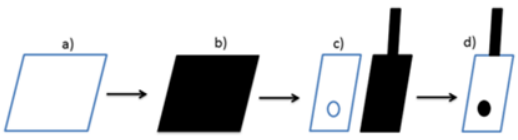

Scheme 5.3-1 a) Non-treated rectangle shaped filter paper. b) SWCNTink treated filter paper. c) PVC sticker mask and SWCNTink treated filter paper cut to final shape letting the active sensing area open. d) Final sensor containing a mask layer of parafilm (not visible).

5.3.3.3. Setup and measurements

The potentiometric measurements were made in 5 ml 10^{-3} M PBS solution (pH = 7.5). The solution was stirred during the measurements at 1000 rpm. The two-electrode system consisted of an Ag/AgCl reference electrode and the developed SWCNT ink sensor as the working electrode. Thrombin was spiked to the 5 ml solution to have a total concentration ranging from 0.5 nM up to 0.8 µM. Cyclic voltammetry (CV) was performed in a single-compartment classical 3-electrode electrochemical cell with a 10 mL volume. Supporting electrolytes and $[Ru(NH_3)_6]^{3+}$, were deoxygenated via purging with nitrogen gas for 10 min prior to measurements and nitrogen was bubbled during the experiments.

5.3.3.4. Cyclic voltammetry

Cyclic voltammetry (CV) was performed in a single-compartment classical 3-electrode electrochemical cell with a 10 mL volume. Supporting electrolytes and $[Ru(NH_3)_6]^{3+}$, were deoxygenated via purging with nitrogen gas for 10 min prior to measurements and nitrogen was bubbled during the experiments.

5.3.4. Results and discussion

5.3.4.1. Surface characterization experiments

The aim of these experiments is to know the surface ligand distribution/density in order to better understand the effectiveness of the SWCNT ink method compared to classical spraying method. By evaluating the amount of the immobilized aptamers and their concentration on the surfaces we should be able to compare the TBA surface density between the paper-based sensors and the GC sensor.

To characterize the active sensor surface, voltammetric Γ_{Ru}, a direct measure of the charge density (in mol/cm^2) of $[Ru(NH_3)_6]^{3+}$ forming ion-pairs with the phosphate groups of the TBA-modified sensors, can be calculated.[36-38] 1 mM stock $[Ru(NH_3)_6]^{3+}$ solution is added to the voltammetric cell starting from 1 µM up to 130 µM $[Ru(NH_3)_6]^{3+}$ in presence of 5 mM PBS until it is saturated as shown in Figure 5.3-2. For each successive step, one CV cycle is recorded after the addition of corresponding amount of $[Ru(NH_3)_6]^{3+}$ solution. Average of the total charge value, Γ_{RU} (mol/cm^2) is calculated as 3.21×10^{-11} mol/cm^2. The total charge (Q) was estimated by integration of

the average cathodic peaks starting from 1 µM to 130 µM in the cyclic voltammograms of the $[Ru(NH_3)_6]^{3+}$ and subsequently the total capacitance, C_T, is calculated. The area of the sensor is obtained by dividing the estimated total capacitance C_T, by the empirical reference value, C* (10 µF/cm^2), used for the capacitance of the unit true surface area of SWCNT. [39]

$$A = C_T / C^* \qquad (1)$$

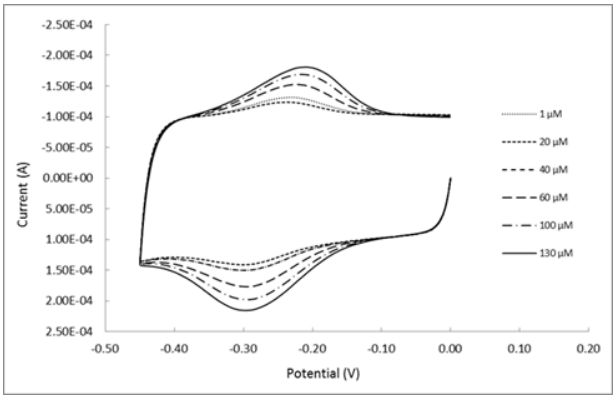

Figure 5.3-2 CV of the SWCNTink based aptasensor at different $[Ru(NH_3)_6]^{3+}$ concentrations.

The data in the Figure 5.3-2 shows that both sensors show reversible $Ru^{3+} \leftrightarrow Ru^{2+}$ reaction. Reduction of $[Ru(NH_3)_6]^{3+}$ takes place at -0,29 V. The area under the cathodic peak (subtracting the capacitive contribution) is related to the total amount of surface-confined $[Ru(NH_3)_6]^{3+}$ complex that is reduced. According to the areas obtained under the SWCNT ink peaks, there is a high charge accumulation on SWCNT. This result is most probably due to the large surface area of the carbon nanotubes and to the higher surface area density of the thrombin aptamer which is covalently linked to this surface.

Table 5.3-1 shows the calculated values for paper-based aptasensor in comparison in comparison with the GC rod based sensor with similar active surface, each in form of 3 mm diameter circle, that are in contact with the solution. Surface area total amount of immobilized aptamers of the paper-based SWCNT ink sensor are the highest while the aptamer density is comparable. The results indicate a considerable difference in the calculated active surface areas between the sensors: 190.92 cm^2 for SWCNT ink on paper, and 27.40 cm^2 for SWCNT on glassy carbon, i.e. a 7 fold increase. This difference is in good agreement with the increased total surface area of the three

dimensional porous structured filter paper compared to the two dimensional GC plane. Hence, the total charge on the surface is calculated as 5.73×10^{-4} C and 8.21×10^{-5} C for paper-based and GC rod based sensors, respectively. The results are also in accordance with the better sensor stability and lower noise levels for paper-based sensor (standard deviations of the noise are 0.072 mV and 0.167 mV, N=3, of SWCNTink and SWCNT based sensors, respectively). Although higher surface area was detected for the paper-based sensor, the TBA density was found comparable to the previous system (GC rod). Noteworthy, the type of surface does not affect the covalent linkage of the aptamer to the SWCNT.

Table 5.3-1 Surface characterization results of different sensor setups.

	A (cm^2)	Q (C)	Γ_{RU} (mol/cm^2)	Γ_{TBA} ($molecule/cm^2$)	N_{TBA}
Paper-based sensor	190.92	5.73×10^{-4}	3.21×10^{-11}	$3.87\times10^{+12}$	$7.15\times10^{+14}$
GC rod based sensor	27.4	8.21×10^{-5}	3.11×10^{-11}	$3.75\times10^{+12}$	$1.03\times10^{+14}$

5.3.4.2. Sensitivity experiments

Potentiometric response of the SWCNT ink based TBA sensors against thrombin is evaluated. The stabilization time where the initial EMF stabilizes to a quasi-constant value, which is required to start the thrombin additions, is approximately 30 minutes, which is comparable to the previously reported SWCNT sensor. Figure 3 shows the time responses of the aptamer functionalized SWCNTink-paper based sensors for stepwise concentrations of thrombin from 5×10^{-10} to 10^{-6} M in 1 mM phosphate buffer solution (PBS) at pH 7.5. The average sensitivity (N=3) is calculated as 7.33 mV/decade with a limit of detection of 82.57 nM (calculated according to the intersection between the extrapolated response function and the potential for the electrolyte background). A close value of 63.8 nM is obtained if the detection limit is computed according to the three sigma method. Slightly lower sensitivity against the previous SWCNT sensor (8,03 mV/decade vs. 7.33 mV/decade) suggests that the total sensing area does not affect the obtained EMF which coincides to the nature of potentiometry that is independent of the area. Instead, ligand distribution (ΓTBA) and efficiency of the TBA-thrombin interactions might be the main factor, as shown in Table 5.3-1.

In Figure 5.3-3, it is observed that after the initial signal jump corresponding to the thrombin addition, the signal tends to stabilize rapidly, with a response time of approximately 20 s, independent of analyte concentration. A control experiment is done using n-butylamine instead of TBA thanks to its structure that does not bind to thrombin while having the amine end for providing immobilization possibility similar that of the TBA. In this way, the SWCNT surface is highly blocked. A signal response with very different characteristics is obtained as shown in Figure 3. Considerably lower sensitivity (average 1.57 mV/log a_{Thr}, N=3) was obtained.

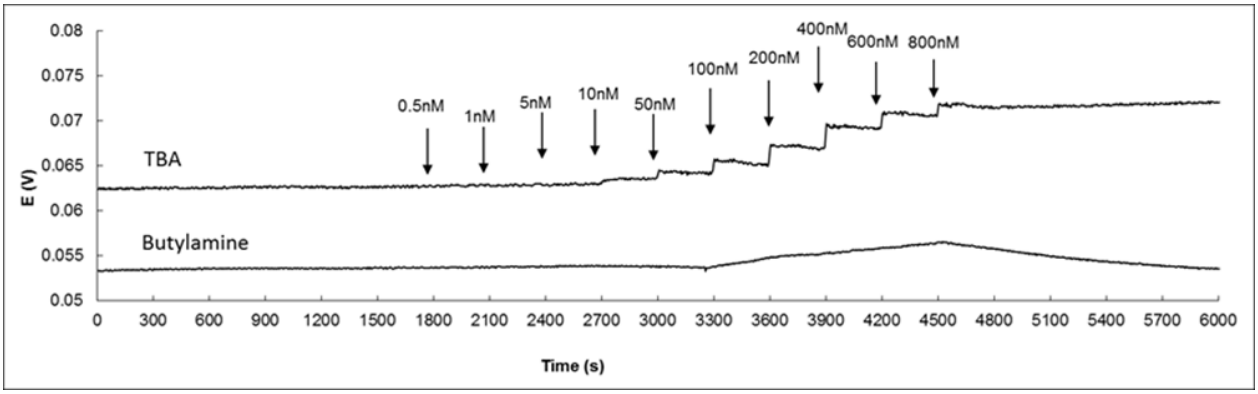

Figure 5.3-3 Potential over time graph for the butylamine functionalized CNTink sensor for concentrations of thrombin in samples ranging from 0.5 nM up to 1 µM.

Figure 5.3-4 shows the average (N=3) calibration curve after subtracting the shift due to different standard potentials. The standard deviation of the standard potentials corresponding to the sensors is 5.2 mV. This value is slightly higher than the previously reported SWCNT sensor (2.1 mV) although the noise levels of these standard potentials are lower in SWCNT ink based sensor as indicated above. Roughly, two segments of different slopes, first from 0.5 nM to 50 nM, and the second from 50 to 800 nM, can be observed. The useful linear interval, with a sensitivity of 7.33 mV/log a_{Thr} corresponds to a range of thrombin concentrations between 100 and 800 nM. It should be noted that this interval is in the range of the minimal physiological concentration levels of thrombin.[40]

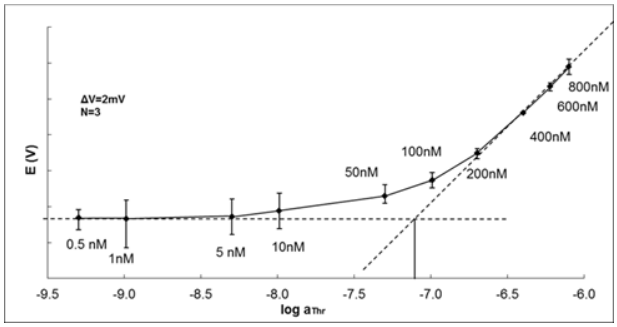

Figure 5.3-4 Calibration curve obtained for three different SWCNT ink sensors. The error bars represent the range of potential values obtained for each set of three measurements recorded.

5.3.4.3. Selectivity experiments

Selectivity of the sensor was evaluated against two proteins; bovine serum albumin (BSA), a common plasma protein with a higher molecular weight than thrombin and elastase, a serine protease enzyme with an isoelectric point and molecular weight similar to thrombin, in two different scenarios. In the first setup, the sensor response to each of the proteins was checked separately. In the second setup the response against thrombin was recorded in presence of both BSA and elastase. As can be seen in Figure 5.3-5, no noticeable increase of the potential is observed until the presence of 2 µM level for each interfering protein.

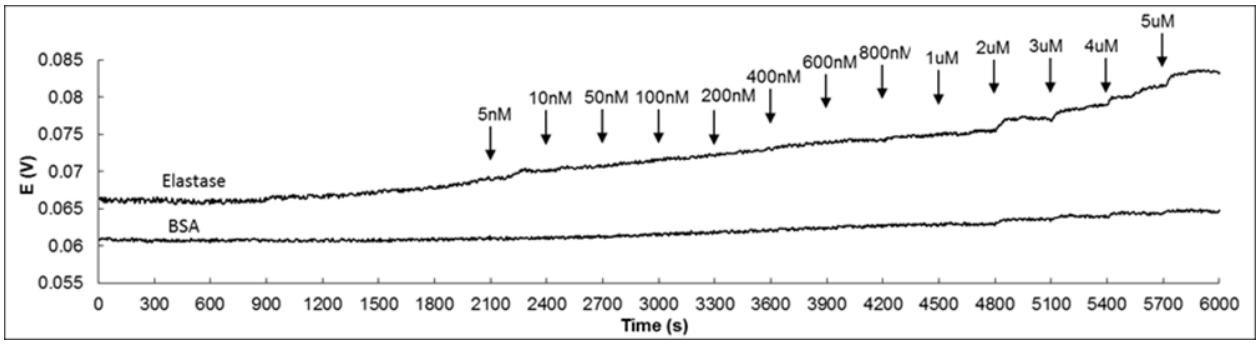

Figure 5.3-5 Responses of the TBA modified SWCNT ink sensors for stepwise concentrations of the non-specific targets; elastase and BSA.

Figure 5.3-6 shows the potentiometric response against thrombin in presence of the two non-target proteins. Concentration of elastase was 3.2 nM, which is approximately the normal blood level.[41] Higher concentration of elastase starts to breakdown the thrombin, which explains the

absence of the potential increase when a higher concentration of elastase is used (data not shown). BSA concentration was 0.5 µM. Sensitivity of the sensor was 5.9 mV/log a_{Thr} with a limit of detection of 107 nM. The reduced drop in the sensitivity value can be attributed to the presence of the non-specific target proteins in the solution. The sensor does not respond to a variation of type or concentration of inorganic electrolytes as long as the ionic strength is kept constant.

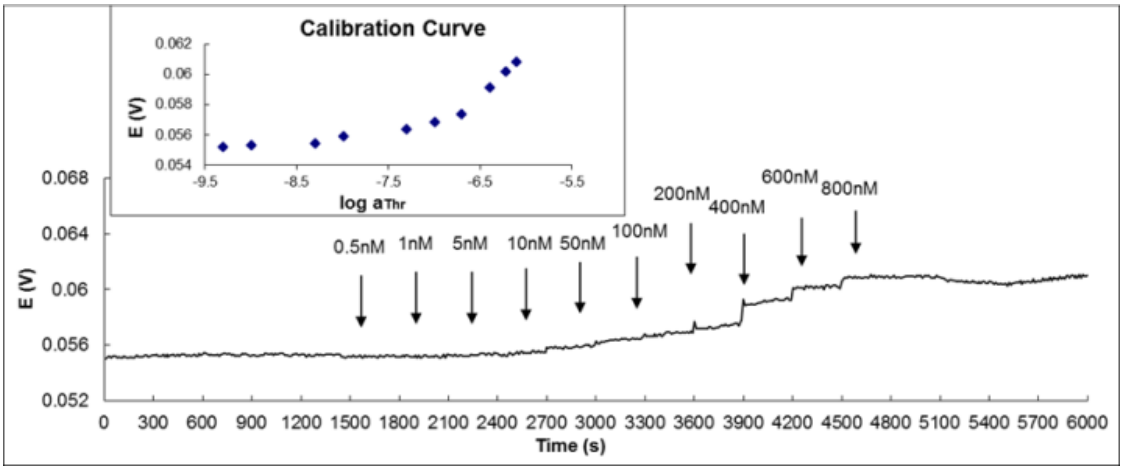

Figure 5.3-6 Potentiometric response against thrombin in presence of 3.2 nM Elastase and 0.5 µM BSA. Inset: calibration curve of the potentiometric response.

The electrochemical impedance spectra were recorded first with the sensors containing only a SWCNT ink layer, secondly after the aptamer functionalization to this layer, and finally after 1 µM thrombin interaction (see supporting information). The impedance spectra are dominated by a nearly 90° capacitive line, which extends down to low frequencies (0.3 Hz). At high frequencies, only a slight deviation from the capacitive line can be seen, indicating fast charge transfer at the SWCNT-aptamer solution interfaces as well as fast charge transport in the SWCNT ink based SWCNT layer.

5.3.5. Conclusions

We have shown that the SWCNT ink that is immobilized onto filter paper works as a transduction element of the potentiometric sensor. While sensors developed this way have comparable performance characteristics to our previously reported sensor (which uses SWCNT solution sprayed onto glassy carbon support) physical and economical aspects of the SWCNT ink based aptasensors are considerably enhanced. The advantages of this system are the flexibility, much lower cost, availability, lowered noise levels, and further miniaturization possibilities of the aptasensor which

widens the application areas thanks to the filter paper as the sensor support element. Additionally, the deposition of SWCNTs by using SWCNT ink enables avoiding any possible SWCNT loss and increased the total active sensor surface area.

In conclusion, we have further widened the application possibilities of our previously reported generic method for aptasensing of proteins with similar performance characteristics. The simplicity of the selective potentiometric sensor is further optimized, allowing a much versatile application possibilities thanks to its paper backbone. Future investigation is needed to increase the reproducibility of the sensor and correlate the performance characteristics with the surface ligand density. Different types of aptamers for different types of analytes are currently studied in our lab with this new optimized detection system.

5.3.6. Acknowledgements

Financial support from the Spanish Ministerio de Economia y Competitividad (Project CTQ2010-18717) is gratefully acknowledged.

5.3.7. References

1. C. P. Price, *Br. Med. J.*, 2001, **322**, 1285-1288.
2. P. Yager, G. J. Domingo and J. Gerdes, *Annu. Rev. Biomed. Eng.*, 2008, **10**, 107-144.
3. E. Aguilera-Herrador, M. Cruz-Vera and M. Valcarcel, *Analyst*, 2010, **135**, 2220-2232.
4. J. Polisena, D. Coyle, K. Coyle and S. McGill, *Int. J. Technol. Assess. Health Care*, 2009, **25**, 339-349.
5. J. Polisena, K. Tran, K. Cimon, B. Hutton, S. McGill and K. Palmer, *Diabetes, Obesity and Metabolism*, 2009, **11**, 913-930.
6. R. Pelton, *TrAC, Trends Anal. Chem.*, 2009, **28**, 925-942.
7. X. Li, J. Tian, T. Nguyen and W. Shen, *Anal. Chem.*, 2008, **80**, 9131-9134.
8. J. Yu, L. Ge, J. Huang, S. Wang and S. Ge, *Lab on a Chip*, 2011, **11**, 1286-1291.
9. C.-M. Cheng, A. W. Martinez, J. Gong, C. R. Mace, S. T. Phillips, E. Carrilho, K. A. Mirica and G. M. Whitesides, *Angew. Chem. Int. Ed.*, 2010, **49**, 4771-4774.
10. H. Liu, Y. Xiang, Y. Lu and R. M. Crooks, *Angew. Chem.*, 2012, DOI: 10.1002/ange.201202929.
11. C. O'Sullivan, *Anal. Bioanal. Chem.*, 2002, **372**, 44-48.
12. G. Herzog and D. W. M. Arrigan, *Analyst*, 2007, **132**, 615-632.

13. A. Numnuam, K. Y. Chumbimuni-Torres, Y. Xiang, R. Bash, P. Thavarungkul, P. Kanatharana, E. Pretsch, J. Wang and E. Bakker, *Anal. Chem.*, 2008, **80**, 707-712.
14. A. E. Radi, J. L. AceroSanchez, E. Baldrich and C. K. O'Sullivan, *Anal. Chem.*, 2005, **77**, 6320-6323.
15. S. Tombelli, M. Minunni and M. Mascini, *Biomol. Eng*, 2007, **24**, 191-200.
16. L. Li, H. Zhao, Z. Chen, X. Mu and L. Guo, *Anal. Bioanal. Chem.*, 2010, **398**, 563-570.
17. D. Rotem, L. Jayasinghe, M. Salichou and H. Bayley, *JACS*, 2012, **134**, 2781-2787.
18. E. Pretsch, *TrAC, Trends Anal. Chem.*, 2007, **26**, 46-51.
19. F. X. Rius-Ruiz, A. Kisiel, A. Michalska, K. Maksymiuk, J. Riu and F. Rius, *Anal. Bioanal. Chem.*, 2011, **399**, 3613-3622.
20. F. X. Rius-Ruiz, D. Bejarano-Nosas, P. Blondeau, J. Riu and F. X. Rius, *Anal. Chem.*, 2011, **83**, 5783-5788.
21. F. X. Rius-Ruiz, G. A. Crespo, D. Bejarano-Nosas, P. Blondeau, J. Riu and F. X. Rius, *Anal. Chem.*, 2011.
22. A. Düzgün, G. Zelada-Guillén, G. Crespo, S. Macho, J. Riu and F. X. Rius, *Anal. Bioanal. Chem.*, 2011, **399**, 171-181.
23. I. Heller, A. M. Janssens, J. Mannik, E. D. Minot, S. G. Lemay and C. Dekker, *Nano Lett.*, 2008, **8**, 591-595.
24. G. A. Crespo, S. Macho and F. X. Rius, *Anal. Chem.*, 2008, **80**, 1316-1322.
25. G. A. Zelada-Guillén, S. V. Bhosale, J. Riu and F. X. Rius, *Anal. Chem.*, 2010, **82**, 9254-9260.
26. G. A. Zelada-Guillén, J. Riu, A. Düzgün and F. X. Rius, *Angew. Chem. Int. Ed.*, 2009, **48**, 7334-7337.
27. G. A. Zelada-Guillén, J. L. Sebastián-Avila, P. Blondeau, J. Riu and F. X. Rius, *Biosens. Bioelectron.*, 2012, **31**, 226-232.
28. A. Düzgün, A. Maroto, T. Mairal, C. O'Sullivan and F. X. Rius, *Analyst*, 2010, **135**, 1037-1041.
29. P. Yáñez-Sedeño, J. M. Pingarrón, J. Riu and F. X. Rius, *TrAC, Trends Anal. Chem.*, 2010, **29**, 939-953.
30. S.-L. Chou, J.-Z. Wang, S.-Y. Chew, H.-K. Liu and S.-X. Dou, *Electrochem. Commun.*, 2008, **10**, 1724-1727.
31. S. H. Ng, J. Wang, Z. P. Guo, J. Chen, G. X. Wang and H. K. Liu, *Electrochim. Acta*, 2005, **51**, 23-28.

32. L. Gonzalez-Macia, A. Morrin, M. R. Smyth and A. J. Killard, *Analyst*, 2010, **135**, 845-867.
33. R. C. Chambers, P. Leoni, O. P. Blanc-Brude, D. E. Wembridge and G. J. Laurent, *J. Biol. Chem.*, 2000, **275**, 35584-35591.
34. M. Novell, M. Parrilla, G. A. Crespo, F. X. Rius and F. J. Andrade, *Anal. Chem.*, 2012, **84**, 4695-4702.
35. L. Hu, J. W. Choi, Y. Yang, S. Jeong, F. La Mantia, L.-F. Cui and Y. Cui, *PNAS*, 2009, **106**, 21490-21494.
36. B. Ge, Y.-C. Huang, D. Sen and H.-Z. Yu, *J. Electroanal. Chem.*, 2007, **602**, 156-162.
37. L. Su, C. G. Sankar, D. Sen and H.-Z. Yu, *Anal. Chem.*, 2004, **76**, 5953-5959.
38. H.-Z. Yu, C.-Y. Luo, C. G. Sankar and D. Sen, *Anal. Chem.*, 2003, **75**, 3902-3907.
39. S. Shiraishi, H. Kurihara, H. Tsubota, A. Oya, Y. Soneda and Y. Yamada, *Electrochem. Solid-State Lett.*, 2001, **4**, A5-A8.
40. M. Lee and D. R. Walt, *Anal. Biochem.*, 2000, **282**, 142-146.
41. P. Mair, J. Mair, I. Seibt, W. Furtwaengler, D. Balogh and B. Puschendorf, *J. Thorac. Cardiovasc. Surg.*, 1994, **108**, 184-185.
42. C. A. Furtado, U. J. Kim, H. R. Gutierrez, L. Pan, E. C. Dickey and P. C. Eklund, *J. Am. Chem. Soc.*, 2004, **126**, 6095-6105.

5.3.8. Supporting information

5.3.8.1. Chemicals and materials

A Keithley (U.K.) 6514 potentiometer and a Metrohm (Switzerland) double junction Ag/AgCl reference electrode with saturated KCl (3 M) as inner filling solution and a 1 M LiOAc as a bridge electrolyte were used to perform the potentiometry experiments. An Autolab (Netherlands) electrochemical workstation was used for cyclic voltammetry (CV) experiments. SWCNTs have been purchased from HeJi (China) in bulk form with > 90 % purity, 150 µm average length and 1.4-1.5 nm of diameter and were purified acording to a previous procedure.[28, 42] 15-mer (5'-GGTTGGTGTGGTTGG-3') 5'-NH2-modified (with a 3-carbon spacer) thrombin binding aptamers (TBA) have been purchased from Eurogentec (London, UK) and human α-thrombin is supplied by Haematologic Technologies (Vermount, USA). The reagents 1-ethyl-3-3(3-dimethylaminopropyl) carbodiimide hydrochloride (EDC), *N*-hydroxysuccinimide (NHS), the phosphate buffer solution (PBS) was a mixture of 84 mL of 0.2 M NaH_2PO_4 and 16 mL 0.2 M Na_2HPO_4 in 100 mL of water, 2-(N-

morpholino)ethanesulfonic acid (MES) buffer, cetyl trimethylammonium bromide (CTAB), sodium dodecylbenzenesulfonate (SDBS) and hexamine ruthenium chloride ($Ru[(NH_3)_6]Cl_3$) have been purchased from Sigma-Aldrich (Spain).

5.3.8.2. Electrochemical impedance spectroscopy

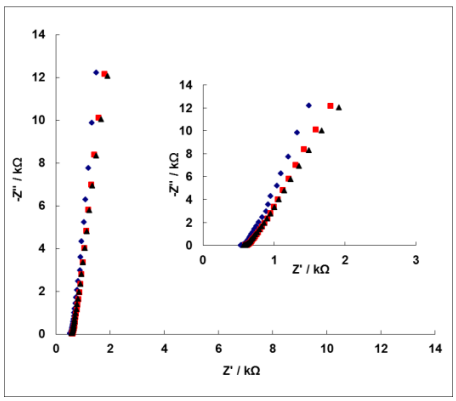

Figure 5.3-7 Complex plane impedance plots of the SWCNTink sensor containing only the SWCNT layer (◆), after TBA functionalization of the SWCNT layer (■) and after thrombin binding (▲). Inset shows a zoomed scale to distinguish the responses easier.

5.4. Recent advances

5.4.1. Introduction

A detailed explanation of solid-contact potentiometric sensors, with the concept theory and examples of different types of them, has already been given in chapters 5.2.2 and 5.3.2.

A very recent review discussed the use of carbon nanotubes and graphene in various types of sensors including biosensors [Pérez-López 2012]. Another detailed review by Liu et al. [Liu 2012] discussed recent advances in affinity and enzyme based biosensors for cell analysis and point-of-care testing. Hernandez and Ozalp have discussed graphene and other nanomaterial-based electrochemical aptasensors [Hernandez and Ozalp 2012].

Considering the recent trends in potentiometric sensing of large analytes in different types of solid state sensors and biosensors, the following section introduces an update of the recent advances that have been appeared after the ones mentioned in chapters 5.2 and 5.3.

5.4.2. Solid-contact (apta)sensors

Zelada-Guillén et al. very recently developed a hybrid transducing/biosensing material [Zelada-Guillén 2012] consisting of SWCNT as ion-to-electron potentiometric transducers and aptamers as biorecognition molecules for ultrasensitive and real-time detection of proteins in blood. They used the same aspects and the methodology of this thesis and optimized it to be able to make detection in complex samples.

A potentiometric label-free and substrate-free (LFSF) aptasensing strategy which eliminates the labeling, separation, and immobilization steps is described by Ding et al. [Ding 2012]. Using adenosine triphosphate (ATP) as a model analyte, they managed to detect ATP down to the sub-micromolar concentration range in HeLa cells.

Zhang et al. [Zhang 2012] have investigated the label-free electrochemical detection of tetracycline by an aptamer based nano-biosensor with a nano-porous structure. Electrochemical impedance spectroscopy (EIS) was used to analyze the behavior of the sensor. The specific binding of tetracycline to the aptamer biosensor led to a decrease in impedance. The corresponding impedance spectra (Nyquist plots) were obtained when serial concentrations of tetracycline were added into the system. An equivalent electrical circuit was used to fit the impedance data. The linear range of the sensor was 2.1–62.4 nM.

5.4.3. Flexible sensors

Cork et al. [Cork 2012] tested the commercial Vantix ® disposable sensor base to be able to detect to bovine herpes virus 1 (BoHV-1) antibodies comparable to standard ELISA method within 15 mins. The sensors consist of a working and reference electrode coated in the conductive polymer polypyrrole and covered in a protective plastic film. Biochemical or enzymatic activity taking place on the surface of the working electrode as a result of immunocomplexes built up on the electrode, causes electrochemical changes in the conductive polymer layer on and around the working electrode that generates the measurable change in electrical potential (measured in millivolts; mV) relative to the reference electrode.

Ibupoto et al. [Ibupoto 2012] developed a disposable potentiometric antibody immobilized ZnO nanotubes based sensor for the detection of C-reactive protein. They immobilized the monoclonal anti-C-reactive protein clone CRP-8 (mouse lgG1 isotype) with glutaraldehyde onto ZnO nanotubes

using simple physical adsorption method. They managed to detect the antibody in the concentration range of CRP from 1.0×10^{-5} mg/L to 1.0×10^{0} mg/L with sensitivity of 13.17 ± 0.42 mV/decade.

5.4.4. Conclusions

Detection of large molecules using flexible sensors continues being an area of large scientific interest, where new techniques and nanomaterials are increasingly used due to their new and attractive properties. However, improvements should be performed not only to develop robust and reliable sensors but to know the sensing mechanism as well.

5.5. References

Cork, J., Jones, R. M., Sawyer, J., Journal of Immunological Methods, 10.1016/j.jim.2012.10.007 (2012)

Ding, J., Chen, Y., Wang, X., Qin, W., Analytical Chemistry 2012, 84, 2055-2061

Hernandez, F. J., Ozalp, V. C., Biosensors 2012, 2, 1-14

Ibupoto, Z. H., Jamal, N., Khun, K., Willander, M., Sensors and Actuators B: Chemical 2012, 166–167, 809-814

Liu, Y., Matharu, Z., Howland, M., Revzin, A., Simonian, A., Analytical and Bioanalytical Chemistry 2012, 404, 1181-1196

Pérez-López, B., Merkoçi, A., Microchimica Acta 2012, 179, 1-16

Zelada-Guillén, G. A., Tweed-Kent, A., Niemann, M., Göringer, H. U., Riu, J., Rius, F. X., Biosensors and Bioelectronics, 10.1016/j.bios.2012.08.055 (2012)

Zhang, J., Wu, Y., Zhang, B., Li, M., Jia, S., Jiang, S., Zhou, H., Zhang, Y., Zhang, C., Turner, A.P.F., Analytical Letters 2012, 45, 986-992

CHAPTER 6

CHARACTERIZATION

6.1. Introduction

This chapter focuses on characterization of the SWCNTs based sensor by trying to determine the number of active aptamers on the surface. It also compares the developed carbon nanotube based sensor with a PANI based one in terms of characterization and sensitivity.

Recent advances in characterization of electrochemical sensors during and after the publications of the articles are also introduced and discussed in section 6.3.

6.2. "Protein detection with potentiometric aptasensors. A comparative study between polyaniline and single wall carbon nanotubes transducers" Submitted.

Ali Düzgün[a*], Hassan Imran[b], Kalle Levon[b], and F. Xavier Rius[a]

[a]Department of Analytical and Organic Chemistry, Universitat Rovira i Virgili, Campus Sescelades, Marcel·lí Domingo,Tarragona, 43007, Spain.

[b]Department of Chemical and Biological Sciences, Polytechnic Institute of New York University, Brooklyn, NY 11201, USA.

[*]Corresponding author at: Department of Analytical and Organic Chemistry, Universitat Rovira i Virgili, Campus Sescelades, Marcel·lí Domingo,Tarragona, 43007, Spain.

Tel.: +34 977 559 562; fax: +34 977 558 446

E-mail address: ali.duzgun@urv.cat

6.2.1. Abstract

A comparison study on the performance characteristics and surface characterization of two different solid-contact selective potentiometric thrombin aptasensors, one exploiting a network of single-walled carbon nanotubes (SWCNT) and the other polyaniline (PANI), both acting as a transducing element is described in this work. The molecular properties of both SWCNT and PANI surface have been modified by covalently linking thrombin binding aptamers as biorecognition elements. The two aptasensors are compared and characterized thorough potentiometry and electrochemical impedance spectroscopy (EIS) based on the voltammetric response of multiply charged transition metal cations (such as hexaammineruthenium; $[Ru(NH_3)_6]^{3+}$) bound electrostatically to the DNA probes. The surface densities of aptamers were accurately determined by integration of the peak for reduction of $[Ru(NH_3)_6]^{3+}$ to $[Ru(NH_3)_6]^{2+}$. The differences and similarities, as well as the transduction mechanism are also discussed. The sensitivity is calculated as 2.97 mV/decade and 8.03 mV/decade for the PANI and SWCNTs aptasensors respectively. These results are in accordance with the higher surface density of the aptamers in the SWCNT potentiometric sensor.

Keywords: Carbon nanotubes; Polyaniline; Potentiometry; Protein detection; Aptamers; Aptasensor.

6.2.2. Introduction

Biosensors based on electrochemical detection have been extensively used to detect proteins [1-3]. They offer, in addition to selectivity and sensitivity, the possibility to detect the target analytes in cloudy samples in a very simple and fast way. Even though the electrochemical techniques employed, such as amperometry, voltammetry or electrochemical impedance spectroscopy (EIS) provide these performance characteristics, the relative complexity of the detection procedures and the need for portable detectors enabling detection of the targets at the point of care, motivate the development of more rapid, cheaper and simpler detection techniques.

Potentiometry is one of the most simple electrochemical detection methods. Nanostructured biosensors based on field effect transistors (FETs) are considered members of this type [4, 5]. The miniaturized bio-FETs are able to detect nowadays large molecules such as plasma proteins or even bacteria [6, 7]. However, these devices display low physical robustness, large response times and poor reproducibility among individual sensors. Moreover, they are usually developed using microfabrication techniques and consequently they display high production costs. The appearance

of potentiometric all solid state aptasensors other than FETs made it possible to overcome most of these problems [8].

Aptamers enable the development of cheap and sensitive biosensors. Aptasensors, thanks to their relatively reduced nucleic acid based nature, display several advantages over the antibody counterparts developed for the same targets: higher heat, pH and ionic strength stability, smaller size, and in some cases higher selectivity [9]. Moreover, they can be synthesized at low cost. Electrochemical biosensors incorporating aptamers as recognition elements are extensively reported in the bibliography [10-14] although the translation to commercialized devices is very scarce [15].

Düzgün et al. recently demonstrated the feasibility to potentiometrically detect large analytes such as proteins using a nanostructured hybrid material (based on carbon nanotubes, CNT) that incorporate thrombin binding aptamers (TBA) [16]. The main advantages of this detection system are simplicity due to two electrode system used in potentiometry, low cost and real time detection which make it highly valuable for different types of applications. Zelada et al. showed that the same strategy could be applied to quantify bacteria in real samples [17, 18]. The biosensing mechanism is thought to be based on the superficial restructuration of the aptamers lying onto the surface of the single-wall carbon nanotubes (SWCNTs) when the target analyte, displaying a very high affinity constant with the aptamers, enter in contact with them. Johnson et al. [19] have recently demonstrated that aptamers are self-assembled to carbon nanotubes via π-π stacking interaction between the aptamer bases and the carbon nanotubes walls by using molecular dynamics. Since the phosphate groups of the aptamers are largely ionized at pH 7.5, these negative charges can be transferred to the carbon nanotubes. This agrees with the decrease in the initial potential of the sensor measured following functionalization of the SWCNTs with the aptamers. The presence of the target protein induces a conformational change in the aptamer that separates the phosphate negative charges from the SWCNT sidewalls [20] inducing the subsequent increase of the recorded potential. This mechanism is similar to the one reported by Levon's group in the development of a nucleic acid potentiometric biosensor based on the hybridization of the complementary DNA strands and using polyaniline (PANI) as transducer layer [21]. The sensing mechanism was assigned to a different interaction of the nucleic acid probes with the strongly cationic polyaniline substrate.

The conformational changes in the nucleic acid probes caused by the selective hybridization with the complementary strand provide the potential change that is monitored.

Due to the similarity of the proposed sensing mechanisms, it would be interesting to compare the performance of conducting polymers and SWCNTs as transducer elements in these potentiometric sensors. PANI and SWCNTs show different characteristics in terms of material nature, electrical conductivity, deposition procedures and thickness control of the transducing layer. Therefore it is worthwhile the comparison of their performance characteristics could provide us an advantage in terms of producing similar performance characteristics considering the relatively simple spraying method that is used for SWCNTs.

The characterization of the aptamer-SWCNT based aptasensors, basically the number of aptamers linked for unit length of carbon nanotube, is difficult due to the specific nature of the substrate and the small size of the nucleic acid segments attached to the carbon nanotube walls. Electrochemical techniques could provide a suitable methodology, although EIS studies cannot be applied directly to the system due to the reduced conductivity on the sensor surface made of semiconducting SWCNTs [22]. Surface ligand density calculation as a part of electrochemical characterization is a key factor in determining the source of the potentiometric signal, as classical Nernstian theory is not applicable due to the lack of a thermodynamic equilibrium at the sensor surface.

In this work, we conducted a comparative study of the aptasensors to determine protein using both SWCNT and PANI. We compared the sensitivity and the stability of the sensors using TBA as recognition layer and human alpha thrombin as target analyte. Furthermore, we characterized the solid surface by measuring the total surface aptamer density based on Cottrell equation [23, 24] assuming complete charge compensation of the DNA phosphate residues by redox cations.

6.2.3. Material and methods

6.2.3.1. Instrumentation and Reagents

A Lawson (USA) multi-channel potentiometer and a Metrohm (Switzerland) Ag/AgCl reference electrode were used to perform the potentiometric experiments. A Metrohm (Switzerland) laboratory type pH probe was used for the pH detection using 3 standards calibration. A CHI Instruments (USA) electrochemical workstation was used for cyclic voltammetry (CV) experiments. A FEI Company (Netherlands) SEM-Quanta 600 is used to take the SEM image. Aniline monomer,

$[Ru(NH_3)_6]^{3+}$ (hexaammineruthenium , $Ru[(NH_3)_6]Cl_3$) , and H_2SO_4 were purchased from Sigma Aldrich (Spain). Single walled carbon nanotubes (SWCNT) were purchased from HeJi (China) in bulk form with > 90% purity, 150 µm average length and 1.4-1.5 nm of diameter. 15-mer (5'-GGTTGGTGTGGTTGG-3') 5'-NH_2 and 15-mer (5'- GGTTGGTGTGGTTGG-3') 5'-SH modified (with a 3-carbon spacer) thrombin binding aptamers (TBA) were purchased from Eurogentec (Cultek, Spain) and Genemed Synthesis Inc. (USA), respectively. Human α-thrombin supplied by Haematologic Technologies (Vermount, USA). Elastase and BSA supplied by Aldrich. Phosphate buffer solution (PBS) is from Panreac Química (Spain). Glassy carbon (GC) rods were purchased from HTW (Germany). Aniline monomer (Aldrich) was distilled and kept cooled at 4 °C. It was also kept in the dark to avoid any potential photooxidation. Sodium dodecyl sulphate (SDS) (Aldrich) was used as purchased.

6.2.3.2. Sensor preparation

The solid contact sensors were prepared by placing a 3 mm diameter glassy carbon rod into a teflon body with the outer diameter of 7 mm. The tip was polished firstly using a Buehler p4000 paper. Subsequently, 6 µm diamond polish and 1 µm grain size alumina powder were used to obtain a smooth surface. Polished sensors were bath sonicated for 30 minutes in Milli-Q water to clean the alumina and diamond residues from the GC surface before the electropolymerization and spraying processes. The above mentioned steps were the same for both SWCNT and PANI modified sensors.

6.2.3.2.1. SWCNT sensor

25 mg of the purified and dried SWCNTs were powdered in a marble mill and then dispersed in 10 mL of Milli-Q water containing 100 mg of sodium dodecyl sulphate (SDS) to provide solubility of SWCNT in water. The solution was sonicated for 30 min at 2 s^{-1} in order to achieve the maximum homogeneity of the dispersion. The sonicated solution was sprayed with approximately 1 bar pressure onto the glassy carbon surface under a high temperature (approx. 200 °C) air blower by spraying 35 times, dipping the surface into milliQ water under stirring conditions at intervals of 5 sprays so as to eliminate the SDS as its presence decreases the conductance on the SWCNT network. We deposited a layer of about 30 µm thickness (measured with SEM) of purified SWCNT onto the polished tip of a glassy carbon (GC) surface. Lastly, to ensure the removal of the SDS, the SWCNT sprayed GC rods were placed into CVD furnace at 300 °C for 1 h under low air flow. The carboxylic groups of the SWCNT were activated with a solution containing 200 mM EDC and 50 mM NHS [25]

(dissolved in MES buffer, 50mM, pH 5.0). The GC surface containing the SWCNTs was dipped in this solution for 30 minutes. To covalently link the TBA to the walls of the SWCNTs through the nucleophilic attack of the amine to the activated carboxylic group, the sensor subsequently was dipped overnight in a solution containing 0.001 M PBS, 1 µM 5'-amine-TBA.

6.2.3.2.2. PANI sensor

Polyaniline films were electropolymerized onto the polished distal end of the glassy carbon rod via cyclic voltammetry with a three-electrode system that consisted of an Ag/AgCl reference electrode, a platinum wire as a counter electrode, and a GC rod as a working electrode. Prior to electropolymerization, GC rods were pre-treated with 0.85 V potential during 10 s for the activation of the surface. Electropolymerization of aniline was carried out potentiodynamically on the GC rod within the potential range of -0.15 to 0.85 V in 0.5 M H_2SO_4 solution by applying 50 potential cycles at a sweep rate of 100 mV/s. Finally, the PANI modified GC probe is dipped into 5 µM TBA solution overnight for immobilization of the thrombin aptamer via aromatic substitution at the conducting polymer surface [21], obtaining in this way the potentiometric PANI aptasensor.

Both types of sensors were washed out thoroughly with MilliQ water to get rid of non-covalently attached aptamers.

6.2.3.3. Measurements

Cyclic voltammetry measurements for both electropolymerization of PANI and ligand density calculations were performed in a single-compartment electrochemical cell with a 10 mL volume. Supporting electrolytes, H_2SO_4 and hexaammineruthenium, were deoxygenated via purging with nitrogen gas for 10 min prior to measurements and nitrogen was bubbled during the experiments. Potentiometric measurements were conducted in 5 ml 5mM PBS solution (pH = 7.5). This was important as to maintain physiological pH level for the aptamers and the thrombin. The solution was stirred during the measurements at 1000 rpm. The two-electrode system consisted of an Ag/AgCl reference electrode and the developed GC sensor as the working electrode.

6.2.3.3.1. Surface density measurements of TBA

The number of the probe TBA molecules that are covalently immobilized onto PANI was calculated from the number of cationic redox molecules of hexaammineruthenium forming ionic pairs with the anionic TBA backbone. Charge compensation is provided for the anionic phosphate groups in

TBA by cations, typically Na^+, K^+ and H^+. These cations readily exchange with other cations in the media [26] because the association constant between cations and TBA phosphate increases with the cation charge [27]. When a TBA sensor is placed in a low ionic strength electrolyte containing a multivalent cation, this latter cation exchanges with the native cation and becomes electrostatically trapped at that interface [28]. The trapped multivalent cation, hexaammineruthenium in our case, due to its oxidizing character can be readily reduced at the electrode as a surface-confined species. The resulting charge at the surface can easily be calculated from the cyclic voltammogram by integrating the suitable reduction peak. In saturation conditions, the amount of surface-linked hexaammineruthenium is proportional to the surface density of aptamers attached to the carbon nanotubes and PANI substrates. The objective was to characterize the electrode surface by determining the total number and density of the TBA in both sensor surfaces and to explain the sensitivity and stability differences that are observed between the two studied sensors.

6.2.3.3.2. Potentiometric setup

The EMF values recorded with TBA modified SWCNTs and PANI sensors were measured against the Ag/AgCl reference electrode with a Lawson multi-channel potentiometer in 5 mM PBS solution to maintain low ionic strength ($I = 5\times10^{-3}$). For the thrombin detection assay, the potentiometric cells were introduced in a solution in which successive aliquots of thrombin solutions were added giving rise to a total thrombin concentration starting from 0.5 nM up to 800 nM, which is the approximately the maximum physiological levels in blood [29, 30]. Assays were performed at solution temperatures of 37 °C.

6.2.4. Results and Discussion

6.2.4.1. Surface ligand density in functionalized PANI and SWCNTs

Voltammetric Γ_{Ru} is a direct measure of the charge density (in mol/cm^2) of $[Ru(NH_3)_6]^{3+}$ forming ion-pairs with the phosphate groups of the TBA-modified sensors [24, 31, 32]. It can be calculated from

$$\Gamma_{Ru} = Q / nFA \qquad (1)$$

where Q is the charge obtained by integration of the redox peaks in the cyclic voltammograms of the hexaammineruthenium coordination complex (see Fig. 1), *n* is the number of electrons in the

reduction reaction from Ru(III) to Ru(II), F is the Faraday constant and A is the area of the working electrode.

The calculated Γ_{Ru} value can be directly converted to the TBA surface density, Γ_{TBA}, in molecule/cm^2 using the relationship

$$\Gamma_{TBA} = \Gamma_{RU} (z/m) N_A \qquad (2)$$

where *m* is the number of nucleotides in the TBA, *z* is the charge of the hexaammineruthenium redox species, which is 3 in our case, and N_A is the Avogadro's number. In order to determine the surface ligand density, 1 mM stock hexaammineruthenium solution is added to the voltammetric cell starting from 1 µM up to 130 µM hexaammineruthenium in presence of 5 mM PBS until it is saturated as shown in Fig. 1. For each successive step, one CV cycle is recorded after the addition of corresponding amount of hexaammineruthenium solution without any further modification to the electrochemical cell. All of the CVs are overlaid and shown for PANI (Fig. 6.1-1a) and SWCNT (Fig. 6.1-1b).

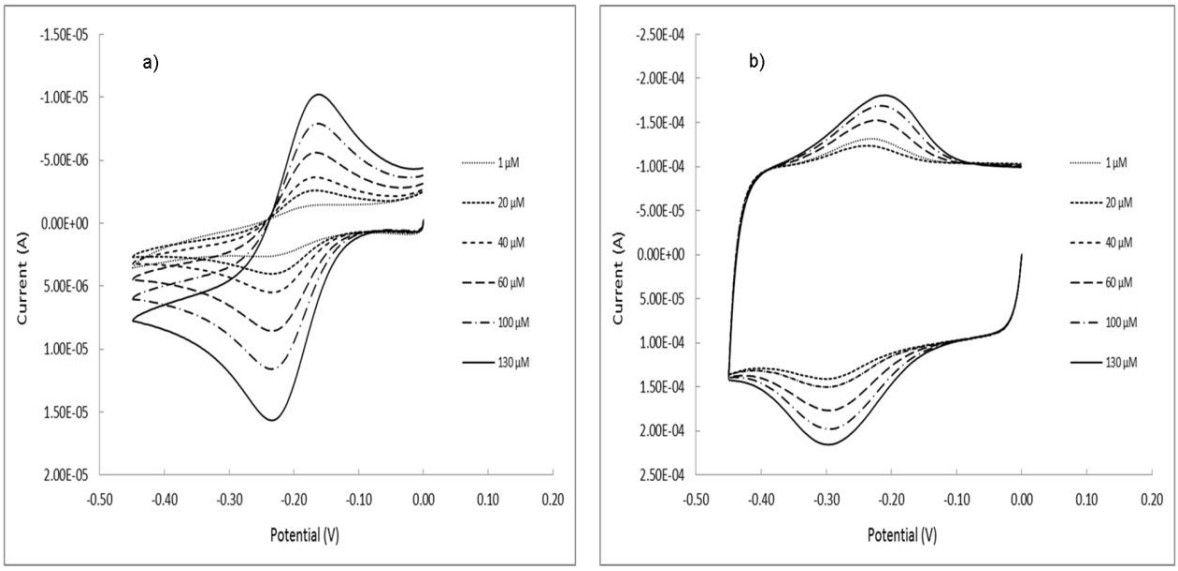

Figure 6.1-1 CV of the a) PANI b) SWCNT based aptasensors at different hexaammineruthenium concentrations. In all case the sweep rate was 0.1 V/s. The observed area under the average cathodic peak from 1 μM to 130 μM due to addition of hexaammineruthenium is used for calculations in (1) and (2).

According to the data in the Fig. 6.1-1, both sensors the CV has cathodic (reduction) and anodic (oxidation) peaks associated with hexaammineruthenium but the reduction peak shifted negatively

compared to hexaammineruthenium with TBA, supporting that the signal originates from hexaammineruthenium bound in the TBA[33]. Ideally, there should be no cathodic and anodic peak separation for a surface-confined molecule. Peak separation can be induced by kinetic control or interfacial electron-transfer rates comparable to the scan rate. Other reasons for apparent "nonideality" could be dissociation and association of $[Ru(NH_3)_6]^{3+/2+}$ that accompanies the electrochemical process due to different stochiometric PO_4^{3-}/hexaammineruthenium ratios when hexaammineruthenium is in the oxidized and reduced state[34]. These results also indicate that the hexaammineruthenium is slightly more present at PANI surface. The typical capacitive behavior of the carbon nanotube sensor is observed in Fig. 6.1-1b. The area under the cathodic peak (subtracting the capacitive contribution) is related to the total amount of surface-confined hexaammineruthenium complex that is reduced. According to the areas obtained under the PANI and SWCNTs peaks, there is a much higher charge accumulation on SWCNT. These results could be due to the larger surface area of the carbon nanotubes and to the higher surface area density of the thrombin aptamer covalently linked to this latter surface.

Average of the saturation charge value at 130 µM is used to calculate the hexaammineruthenium charge density, Γ_{RU} (mol/cm^2). This value is 5.18×10^{-12} mol/cm^2 and 5.19×10^{-12} mol/cm^2 for PANI and SWCNTs sensors, respectively. Placing this value in (2) gives the total surface aptamer density per cm^2. After estimating the approximate area of each sensor (see below) the aptamer density on the surface can be easily calculated.

According to IUPAC [35, 36], surface area of a non-metallic porous electrode surface can be estimated by determining the apparent total capacitance of the electrode surface and assuming that the double layer charging, i.e. the capacitive component, is the only process in the conditions that voltammetric curves are recorded. We have estimated the total charge (Q) by integration of the average cathodic peaks starting from 1 µM to 130 µM in the cyclic voltammograms of the hexaammineruthenium in Fig. 6.1-1 and subsequently calculated the total capacitance, C_T, by dividing it to the sweep rate following the expression $C_T = \delta Q/\delta E = I\,\delta t/\,\delta E = I/(\delta E/\delta t)$. The area of the sensor is obtained by dividing the estimated total capacitance C_T, by the empirical reference value, C* (10 µF/cm^2), used for the capacitance of the purified SWCNTs [37].

$$A = C_T / C^* \qquad (3)$$

Table 6.1-1 shows the values obtained from the addition of hexaammineruthenium to PANI and SWCNTs based aptasensors. The obtained results show considerable differences in the calculated surface areas for both sensors: 164.29 cm^2 for SWCNTs versus 11.27 cm^2 for PANI with standard deviations of 25.7 cm^2 and 2.16 cm^2 for SWCNTs and PANI, respectively (N=3). The area of the polished glassy carbon surface is 0.07 cm^2. The increase in the area of PANI sensor is thought to be due to the polymer chains conformation on the surface which is creating some slight roughness compared to bare GC surface. The area differences between PANI and SWCNTs sensors could result from the fact that the surface area to volume ratio of SWCNTs is much higher than the PANI chains deposited in the two dimensional plane of the sensor surface. Furthermore, spaghetti like formation [16] of the SWCNTs compared to very orderly distributed PANI chains also supports this result. The total charge on the surface are calculated 5.63×10^{-6} C for PANI, and 8.21×10^{-5} C for SWCNT based sensors with standard deviations of 1.08×10^{-06} C and 1.29×10^{-05} C for PANI and SWCNTs, respectively (N=3). Using equations (1) and (2), $6.23\times10^{+11}$ and $6.24\times10^{+11}$ TBA molecules are bound per cm^2 of PANI and SWCNT surface respectively which lead a total of $7.03\times10^{+12}$ aptamer molecules on PANI and $1.03\times10^{+14}$ aptamer molecules on SWCNT total sensor surface. All of the corresponding standard deviations are presented in Table 6.1-1.

Table 6.1-1 Calculated surface charge and ligand density values with corresponding standard deviations (N=3).

	A (cm^2)	**Q (C)**	**Γ_{RU} (mol/cm^2)**	**Γ_{TBA} (molecule/cm^2)**	**N_{TBA} at sensor surface**
PANI	11.27	5.63×10^{-06}	5.18×10^{-12}	$6.23\times10^{+11}$	$7.03\times10^{+12}$
SWCNT	164.29	8.21×10^{-05}	5.19×10^{-12}	$6.24\times10^{+11}$	$1.03\times10^{+14}$
PANI StDev	2.16	1.08×10^{-06}	9.94×10^{-13}	$1.20\times10^{+11}$	$1.00\times10^{+12}$
SWCNT StDev	25.7	1.29×10^{-06}	8.11×10^{-13}	$9.77\times10^{+10}$	$1.60\times10^{+13}$

6.2.4.2. Potentiometry

Potentiometric responses of PANI and SWCNTs based TBA modified sensors against thrombin are evaluated. Evaluation is done under consideration of that the sensing system is not based on equilibrium process, hence should not be explained by the Nernstian theory. The sensors do not

contain any membrane to provide the equilibrium process that is necessary for realizing the Nernstian theory, and it is similar to field effect transistors (FETs), which are also considered potentiometric sensors [4, 5]. Instead, our target is a neutral protein at where the isoelectric point is in the pH range of 7,0 – 7,6. What is thought is that the conformational change of the aptamer during binding event changes the capacitance value of the surrounding of the SWCNTs/PANI (the transducing elements) which leads to the detectable signal. Within this scenario, the response could be considered sensitive enough, at least for any type of semi-quantitative or qualitative detection since the target analyte is a protein that shows an illness above or below a critical level in blood.

The stabilization time for the PANI sensor is much longer (16 hours) than the approximately 30 minutes needed for the carbon nanotube sensor using the same experimental conditions. It might be related to the time needed to reach the equilibrium position of the nucleic acid segment onto the different surfaces and to the establishment of the interfacial double-layer in PANI sensor than the SWCNT sensor. This could also be attributed to relatively lower chemical stability and higher light sensitivity of PANI against SWCNTs. Fig. 6.1-2 shows the potentiometric responses obtained when increasing the total concentration of thrombin in the solution. Both sensors are kept without analyte until reaching a stable state and additions have been made simultaneously in both sensors for technical reasons. The sensitivity is calculated as 2.97 mV/decade and 8.03 mV/decade for the PANI and SWCNTs aptasensors respectively. These results are in accordance with the higher surface density of the aptamers in the SWCNT potentiometric sensor. Inset of the Fig. 6.1-2 shows average (N=3) calibration curves of the potentiometric response for both SWCNT and PANI.

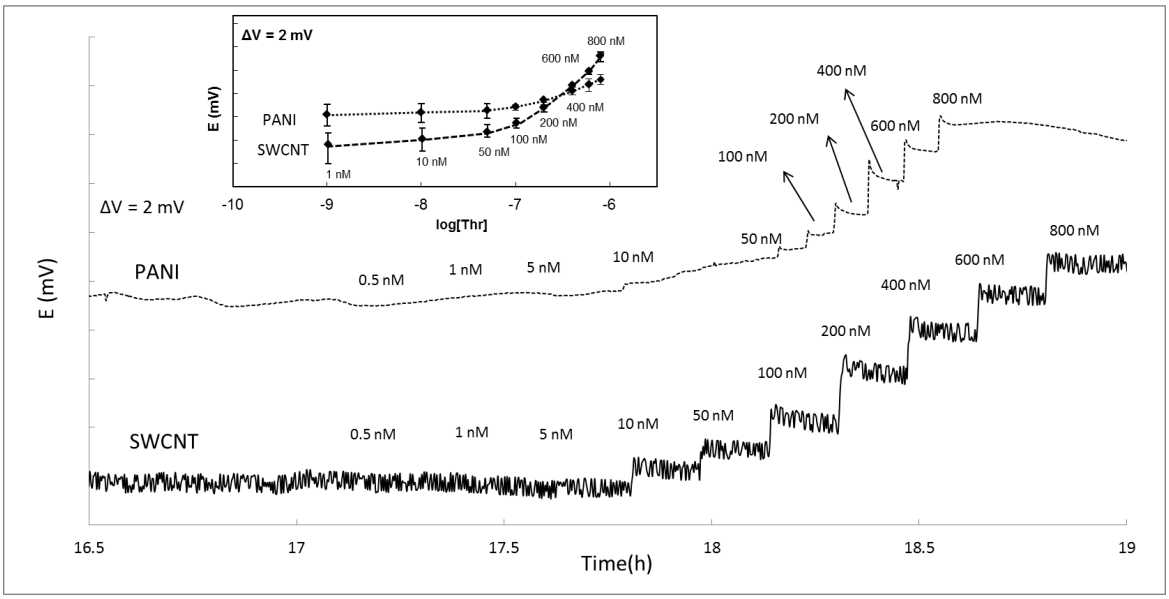

Figure 6.1-2 Potentiometric response of the TBA modified PANI and SWCNT based sensors to thrombin. Concentration range is 0,5 nM-800 nM in both cases. Inset; Average calibration curves for the PANI and SWCNTs potentiometric sensors against thrombin with corresponding error bars.

Selectivities of both sensors were measured against elastase and BSA separately. Both sensors did not show a noticeable response until 2 µM level. Additions were done first by ranging from 0.5 µM up to 800 nM as in the sensitivity experiments with no noticeable response. Later, the additions have been conducted by first 1 µM and later 2 µM of interfering proteins where they showed a noticeable signal.

Comparing the performance of PANI and SWCNTs as transducers in potentiometric aptasensors, the first aspect is that PANI can be deposited electrochemically onto the GC surface with a very high control on thickness. The same thickness control is difficult to reach with carbon nanotubes using any of the available deposition techniques [38]. Nevertheless, the produced sensor interface is very different in both sensors, while we obtain a quite homogeneous surface with PANI (area = 11.27 cm^2), the surface of the spaghetti-like deposited carbon nanotubes is very rough and inhomogeneous producing a very large superficial interface (area = 164.29 cm^2).

The chemistry used to covalently immobilize the thrombin aptamer onto the substrate gives very similar results in terms of surface density of the ligand (Γ_{TBA} is approximately $6.2\times10^{+11}$ molecule/cm^2

in both sensors). While the aromatic substitution involving a thiol group is used to link aptamers to PANI (See Scheme 6.1-1), the covalent bonds via carboxylic groups have been established between the receptors and SWCNTs. However, the very different available surface area in both substrates gives rise to large differences in the total ligand linked to the substrate (N_{TBA} = $7.03\times10^{+12}$ in PANI and $1.03\times10^{+14}$ in SWCNTs).

Considering that SWCNTs have a larger total surface area than the relatively planar PANI surface, a higher percentage of the immobilized and active aptamers is probably responsible of the differences in the observed sensitivity. Another reason for the higher sensitivity could be attributed to the relatively higher affinity that is caused by the covalent backbone of the carboxylic acid-amine interaction. Also there are some electrostatic interactions present which caused the phosphate backbone of the TBA and positively charged surface of PANI. These interactions must be higher than the ones between TBA and CNTs so that the total energy needed for the TBA to get its chair G-quartet formation is lower in case of CNTs which thought to be source of the potential response [39]. Further research is needed to be able to explain this difference considering the similarities and differences in both charge transfer mechanisms. However, both sensors have a similar limit of detection (LOD) (80 nM for SWCNT based sensor and 71 nM for PANI based sensor) values. Relatively lower noise level in PANI based sensor is thought to be the responsible for this slightly better LOD.

To conclude, using a redox molecule to determine the total charge on the surface of TBA modified sensor, and as a consequence, being able to calculate the surface ligand density can help in enhancing sensor's performance. However, the current method doesn't provide information on the formation and the distribution of the aptamer molecules on the SWCNT/PANI surface. Further investigation is needed to determine the correct formation of the aptamers to thoroughly understand the underlying phenomena of the generated EMF. In comparison to previously reported CNT based potentiometric sensor [16], PANI based sensor doesn't provide nor as good sensitivity, neither stability. However, both sensors responded to interfering proteins exhibiting a similar selective behavior.

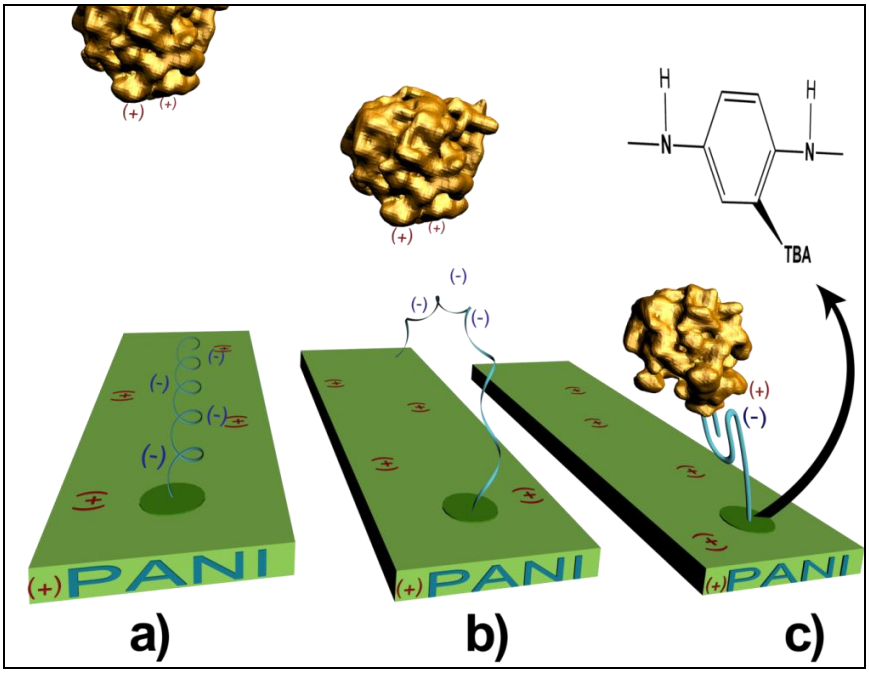

Scheme 6.1-1 The scheme depicting charge competition and TBA-thrombin binding. a) When the thrombin is not in the system, TBA tends to remain attached to PANI backbone due to charge attraction. b) TBA starts to dislocate from PANI surface through thrombin. c) Positively charged active site of the thrombin binds to the TBA which leads a potentiometric signal.

6.2.5. Acknowledgements

We thank the Spanish MICINN, for supporting the work through the project grants CTQ2010-67570.

6.2.6. References

[1] D. Cai, L. Ren, H. Zhao, C. Xu, L. Zhang, Y. Yu, H. Wang, Y. Lan, M.F. Roberts, J.H. Chuang, M.J. Naughton, Z. Ren, T.C. Chiles, Nat Nano, 5 (2010) 597-601.

[2] C.I.L. Justino, T.A. Rocha-Santos, A.C. Duarte, TrAC, Trends Anal. Chem., 29 (2010) 1172-1183.

[3] M.d. Vestergaard, K. Kerman, E. Tamiya, Sensors, 7 (2007) 3442-3458.

[4] X.P.A. Gao, G. Zheng, C.M. Lieber, Nano Lett., 10 (2009) 547-552.

[5] G. Zheng, X.P.A. Gao, C.M. Lieber, Nano Lett., 10 (2010) 3179-3183.

[6] K.G. Samit, et al., J. Phys. D: Appl. Phys., 44 (2011) 034010.

[7] L. Wang, P. Estrela, E. Huq, P. Li, S. Thomas, P.K. Ferrigno, D. Paul, P. Adkin, P. Migliorato, Microelectron. Eng., 87 (2010) 753-755.

[8] A. Düzgün, G. Zelada-Guillén, G. Crespo, S. Macho, J. Riu, F. Rius, Analytical and Bioanalytical Chemistry, 399 (2010) 171-181.

[9] C. O'Sullivan, Anal. Bioanal. Chem., 372 (2002) 44-48.

[10] T. Hianik, J. Wang, Electroanalysis, 21 (2009) 1223-1235.

[11] L. Lihong, F. Yingchun, X. Xiahong, X. Qingji, Y. Shouzhuo, Progress in Chemistry, 21 (2009) 724-731.

[12] A. Sassolas, L.J. Blum, B.D. Leca-Bouvier, Electroanalysis, 21 (2009) 1237-1250.

[13] B. Strehlitz, N. Nikolaus, R. Stoltenburg, Sensors, 8 (2008) 4296-4307.

[14] Y. Xu, G. Cheng, P. He, Y. Fang, Electroanalysis, 21 (2009) 1251-1259.

[15] G.S. Baird, Am. J. Clin. Pathol., 134 (2010) 529-531.

[16] A. Düzgün, A. Maroto, T. Mairal, C. O'Sullivan, F.X. Rius, Analyst, 135 (2010) 1037-1041.

[17] G.A. Zelada-Guillén, S.V. Bhosale, J. Riu, F.X. Rius, Anal. Chem., 82 (2010) 9254-9260.

[18] G.A. Zelada-Guillén, J. Riu, A. Düzgün, F.X. Rius, Angew. Chem. Int. Ed., 48 (2009) 7334-7337.

[19] R.R. Johnson, A.T.C. Johnson, M.L. Klein, Nano Lett., 8 (2008) 69-75.

[20] T. Hianik, V. Ostatná, M. Sonlajtnerova, I. Grman, Bioelectrochemistry, 70 (2007) 127-133.

[21] Y. Zhou, B. Yu, A. Guiseppi-Elie, V. Sergeyev, K. Levon, Biosens. Bioelectron., 24 (2009) 3275-3280.

[22] T.W. Odom, J.-L. Huang, P. Kim, C.M. Lieber, Nature, 391 (1998) 62-64.

[23] S.D. Keighley, P. Li, P. Estrela, P. Migliorato, Biosens. Bioelectron., 23 (2008) 1291-1297.

[24] H.-Z. Yu, C.-Y. Luo, C.G. Sankar, D. Sen, Anal. Chem., 75 (2003) 3902-3907.

[25] K.A. Williams, P.T.M. Veenhuizen, B.G. de la Torre, R. Eritja, C. Dekker, Nature, 420 (2002) 761-761.

[26] D.M. Rose, M.L. Bleam, M.T. Record, R.G. Bryant, Proc. Natl. Acad. Sci. U. S. A., 77 (1980) 6289-6292.

[27] M.M.T. Khan, A.E. Martell, J. Am. Chem. Soc., 89 (1967) 5585-5590.

[28] A.B. Steel, T.M. Herne, M.J. Tarlov, Anal. Chem., 70 (1998) 4670-4677.

[29] M. Lee, D.R. Walt, Anal. Biochem., 282 (2000) 142-146.

[30] Y. Xiao, A.A. Lubin, A.J. Heeger, K.W. Plaxco, Angew. Chem., 117 (2005) 5592-5595.

[31] B. Ge, Y.-C. Huang, D. Sen, H.-Z. Yu, J. Electroanal. Chem., 602 (2007) 156-162.

[32] L. Su, C.G. Sankar, D. Sen, H.-Z. Yu, Anal. Chem., 76 (2004) 5953-5959.

[33] A.B. Steel, T.M. Herne, M.J. Tarlov, Bioconj. Chem., 10 (1999) 419-423.

[34] M. Grubb, H. Wackerbarth, J. Wengel, J. Ulstrup, Langmuir, 23 (2006) 1410-1413.

[35] S. Trasatti, O.A. Petrii, J. Electroanal. Chem., 327 (1992) 353-376.

[36] S. Trasatti, O.A. Petrii, Pure & Appl. Chem., 63 (1991) 711-734.

[37] S. Shiraishi, H. Kurihara, H. Tsubota, A. Oya, Y. Soneda, Y. Yamada, Electrochem. Solid-State Lett., 4 (2001) A5-A8.

[38] P. Yáñez-Sedeño, J.M. Pingarrón, J. Riu, F.X. Rius, TrAC, Trends Anal. Chem., 29 (2010) 939-953.

[39] B.I. Kankia, L.A. Marky, J. Am. Chem. Soc., 123 (2001) 10799-10804.

6.3. Recent advances

6.3.1. Introduction

Recent trends in use of nanostructured materials have been discussed in detail in chapter 3. In chapter 6.2 we compared polyaniline and carbon nanotubes as transducing materials by characterizing the active surface areas of the sensors. This section focuses on newer reports on several transducing elements that display similar characteristics to carbon nanotubes and on the characterization of sensors using several instrumental techniques.

6.3.2. Transducers and characterization studies

Lange et al. [Lange 2012] proposed the use of conducting polymers, a polythiophene film as a case example, to monitor redox titrations potentiometrically without using electrolyte in the measurement solution, opening a way to perform electroanalytical measurements and in non-aqueous media. The approach was applied for redox titration. Equivalent points obtained by this titration in aqueous and organic solutions were identical. Then the approach was applied to the determination of bromine number by redox titration in non-conducting organic phase by using both conductimetry and redox potentiometry.

Marinina et al. [Marinina 2012] have investigated the behavior of polyfunctional properties ruthenium-titanium oxide film electrode (RTOE) in the absence of polarization in potentiometry. They checked the possibility of its application to the potentiometric detection of iron(III) titration with an ethylenediaminetetraacetic acid solution. They also have investigated mechanisms of reactions determining the potentials of electrodes by a number of methods.

Lakard et al. [Lakard 2012] have optimized the structural parameters of new potentiometric pH and urea sensors based on polyaniline and a polysaccharide coupling layer by using screen-printed

carbon electrodes. The resulting pH sensor exhibited a fast, reproducible and sensitive potentiometric response of approximately 59 mV per pH unit from pH 4 to 8. The sensitivity of polyaniline to pH variations was then used to design an enzymatic biosensor. For that purpose, urease was immobilized on a polyelectrolyte multilayer film (PEM), obtained by the alternate deposition of charged polysaccharides (layer-by-layer assembly), over the polyaniline film. Covalent grafting of the urease enzyme to the PEM film was also tested using carbodiimide coupling reaction. The potentiometric response of this assembly to pH variations was similar to the one of polyaniline films, and its response to urea, from 10^{-4} to 10^{-1} mol L^{-1}, exhibited a very high sensitivity combined to fast response, good lifetime and reproducibility. The number of polyelectrolyte layers composing the PEM film was also found to affect the response of the urea sensors.

6.3.3. Conclusions

Characterization of active surfaces of electrochemical sensors is very important to understand the underlying phenomenon of the generated signals. Recent reports include different transducing materials and mechanisms for electrochemical detection. However, proper characterization of the structure and mechanisms in the reported sensors remains as a challenge due to several reasons. New sensing methodologies and different sensor concepts usually lack of an appropriate characterization techniques. This is very usual in nanotechnology where the available techniques are usually expensive and difficult to use. More characterization techniques, and/or optimizations of the existing ones need to be developed to overcome most of these problems.

6.4. References

Lakard, B., Magnin, D., Deschaume, O., Vanlancker, G., Glinel, K., Demoustier-Champagne, S., Nysten, B., Bertrand, P., Yunus, S., Jonas, A. M., Sensors and Actuators B: Chemical 2012, 166–167, 794-801

Lange, U., Mirsky, V. M., Analytica Chimica Acta 2012, 744, 29-32

Marinina, G. I., Vasilyeva, M. S., Lapina, A. S., Journal of Analytical Chemistry 2012, 67, 550-554

CHAPTER 7

7.1. CONCLUSIONS

The main conclusion of this thesis is that with aptamer functionalized single-walled carbon nanotubes (SWCNTs), the classical polymeric ion-selective membrane (ISM) can effectively be eliminated to lead a membraneless potentiometric sensor which enables the determination of analytes larger than ions, such as proteins. For the first time, it has been demonstrated that this nanostructured composite material is able to compete with classical methods that usually require complex, expensive, and/or time consuming systems to detect large analytes.

This main conclusion can be detailed in a series of specific conclusions:

We have reported on a generic method for aptasensing proteins, where the simplicity of the selective potentiometric sensor, combined with its ability to directly detect a biorecognition event obviating the need for labels, mediators, the addition of further reagents or analyte accumulation, highlight the promise of this electrochemical technique.

We have also reported the use of SWCNTs as transducers in aptamer based potentiometric solid-contact sensors, with interaction between the TBA and the thrombin giving rise to a direct potentiometric signal that can be easily recorded in nearly real-time.

Potentiometric results demonstrated that an aptamer functionalized layer of single wall carbon nanotubes deposited onto a conducting substrate is able to transduce an ionic current into electronic current in SWCNTs based aptasensors.

The total charge on the surface of TBA modified sensor has been determined using the redox molecule, hexamine ruthenium chloride ($Ru[(NH_3)_6]Cl_3$) which enabled the calculation of the surface ligand density. This ligand density is related to the sensitivity of the sensor, therefore it is used to enhance the sensor's performance.

The biosensing mechanism is presumed to be based on the equilibrium competition between the target analyte and the SWCNTs to be linked to the aptamer. Since the phosphate groups of the

aptamers are largely ionized at pH 7.5, these negative charges may be transferred to the carbon nanotubes. This agrees with the decrease in the standard potential of the sensor measured following functionalization of the SWCNTs with the aptamers. The presence of the target protein induces a conformational change in the aptamer that separates the phosphate negative charges from the SWCNT sidewalls, inducing the subsequent increase of the recorded potential.

This mechanism is in agreement with the fluorescence confocal microscopy results obtained with the thrombin aptamer labeled with the fluorescein derivative FAM. In the absence of thrombin, the fluorescence is quenched by the proximity of the label to the carbon nanotube, whilst the presence of thrombin in the test solution results in the appearance of a fluorescent signal due to the competitive binding of the thrombin with the SWCNT for the aptamer, with a conformational change of the latter and the corresponding spatial displacement of the dye from the surface of the carbon nanotube.

Potentiometric responses of PANI and SWCNTs based TBA modified sensors against thrombin are evaluated. The stabilization time for the PANI sensor is much longer than the SWCNT sensor. This could be attributed to relatively lower chemical stability and higher light sensitivity of PANI against SWCNTs.

It should be noted that the developed electrodes have completely different sensing mechanism from the well-established ISEs. As long as the classical Nernstian theory is considered, the ideal sensitivity slope should be 59,2 mV/decade as a response for a single charged “ion” detection. However, the classical Nernstian theory is not applicable in our sensors since the sensors do not contain any membrane to provide the equilibrium process that is necessary for realizing the phase-boundary potential model. What is thought is that the affinity reaction between aptamer and the protein is causing a conformational change on the aptamer during the binding event, and changing the capacitance value of the surrounding of the SWCNTs/PANI (the transducing elements) which leads to the detectable signal. Although this theory is not well proved, we can speculate on the basis of the evidences collected. Within this scenario, the response could be considered sensitive enough, at least for any type of qualitative or semi-quantitative analysis where the target analyte could be a protein that indicates an illness when detected above or below a critical level in blood.

CNTs are known to be affected from the surrounding ions, which has a direct translation to reproducibility issues. Therefore, one of the most important development aspects is the proper blocking the surface of the CNTs without disturbing the surrounding aptamer in a way to enable the conformational change. We have made several attempts using surface blocking agents such as Tween 20 without high success. Strict controlling of temperature, pH and ionic strength is also necessary to avoid unforeseen effects such as drift and background noise. The ionic strength also should be as constant as possible to have an easily distinguishable signal.

Additionally to the proper blocking mentioned above, our production techniques could also be some of the reasons for decreasing reproducibility. Spraying of CNTs onto the conducting backbone, albeit is a fast and effective method, is very difficult to control. Therefore the thickness is not the same for all sensors in a batch. CNT loss is also another problem. To overcome these problems, we tried the immobilization of SWCNT ink to paper backbone, which enabled the control of the amount of CNTs on the active sensing area and the flexible management of the process, with similar performance characteristics as the glassy carbon backbones and minimal CNT loss.

Currently, there are no studies in the literature dealing with the detection of large analytes using potentiometric aptasensors with consistent experimental selectivity. The most similar sensors are the ones incorporating antibodies instead of aptamers and hence they have their specific drawbacks that are mentioned throughout the thesis. The original strategy shown in this work, with a systematic chemical functionalization of SWCNTs, could serve to open different pathways in order to obtain highly selective aptasensors useful for bacteria, protein, or polypeptide detection.

7.2. Acquisition of attributes and skills

During my PhD studies, in addition to acquiring scientific knowledge, I have also acquired certain attributes that will help me to develop my career in the future.

In this thesis I have outlined the development of my research project. Firstly, I have focused on learning the main features of what for me was a new and thus challenging field, nanotechnology, and how this field is related to analytical chemistry, which was my specific research area. To do this, I studied the literature extensively in order to understand the concepts and terminology involved. Secondly, I selected and reviewed the literature I found in order to obtain what was most useful for

my own work. This has helped me to develop critical reading skills for evaluating the relevant literature.

Moreover, I have acquired the ability to initiate research projects and to define the framework and variables involved.

These skills enabled me to perform my experimental work, which involved understanding what SWCNTs were, developing aptamer functionalized SWCNTs-based sensors for detecting a specific target analyte, and gaining the ability to critically evaluate my results, both within and across a changing disciplinary environment. The experimental work of this thesis has been conducted in collaboration with other members of the research group, and so I have learned to work as a member of a team.

I have taken several master's and doctorate courses after which I was awarded the official master's degree in Nanoscience and Nanotechnology. At the same time, I have attended several congresses where I had to present and discuss our scientific results. I also visited a foreign research group, and had the chance to observe differences and similarities of conducting science which also gained me some experience in collaboration strategies. Moreover, I have written up and published the results of our work in international scientific journals. Through these scientific contributions, I have acquired the ability to communicate results effectively both orally and in writing, and have gained an understanding of the relevance and value of my research to the national and international scientific communities.

ANNEXES

Annex 1. Glossary

Ω: resistance unit (Ohm)

ASS-ISE: all solid state ion selective electrode

CNTFET: carbon nanotubes field effect transistor

CNTink: carbon nanotube ink

CNTs : carbon nanotubes

COOH: carboxyl function

CTAB: cetyl trimethylammonium bromide

CV: cyclic voltammetry

CWE: coated wire electrode

DMF: dimethylformamide

EDC: 1-ethyl-3-3(3-dimethylaminopropyl) carbodiimide hydrochloride

EIS: electrochemical impedance spectroscopy

EMF: electromotive force

ESEM: scanning electron microscopy

F: Faraday constant (96485 C mol^{-1})

FET: field effect transistor

GC: glassy carbon rod

Hz: frequency unit (Hertz)

I: current unit (Ampere)

ISEs: Ion Selective Electrodes

IS-ISEs: internal solution ion selective electrodes

ISM: ion selective membrane

IUPAC: international union of pure and applied chemistry

LOD: limit of detection

MES: n-morpholinoethane sulfonic acid

MWCNTs: multiwall carbon nanotubes

N^-: anion with negative charge

N^+: cation with positive charge

NHS: n-hydroxysuccinimide

PANI: polyaniline

PBS: phosphate buffered saine

PVC: Poly(vinyl chloride)

R: molar gas constant (8.314 J K-1 mol-1)

rpm: revolutions per minute

R_s: solution resistance

SC-ISE: ion-selective electrodes with internal solid-contact

SDBS: sodium dodecyl benzene sulfonate

SDS: sodium dodecyl sulfate

SEM: scanning electron microscopy

SWCNT ink: single wall carbon nanotube ink

SWCNTs: single wall carbon nanotubes

T: absolute temperature (K)

TEM: transmission electron microscopy

V: voltage unit (Volt)

Z: impedance

Annex 2. Scientific contributions

Papers directly resulting from the Doctoral Thesis

1. "Paper-based aptasensor for protein detection" Ali Düzgün, Marta Novell, Fransisco J. Andrade, and F. Xavier Rius. In preparation
2. "Protein detection with potentiometric aptasensors. A comparative study between polyaniline and single wall carbon nanotubes transducers" Ali Düzgün, Hassan Imran, Kalle Levon, and F. Xavier Rius. Submitted
3. "Nanostructured materials in potentiometry" Ali Düzgün, Gustavo A. Zelada, Gastón A. Crespo, Santiago Macho, Jordi Riu, and F. Xavier Rius, Anal Bioanal Chem, 2011, 399, 171-181
4. "Solid-contact potentiometric aptasensor based on aptamer functionalized carbon nanotubes for the direct determination of proteins" Ali Düzgün, Alicia Maroto, Teresa Mairal, Ciara O'Sullivan and F.Xavier Rius, Analyst, 2010, 135, 1037-1041

Papers indirectly resulting from the Doctoral Thesis

1. "Immediate Detection of Living Bacteria at Ultralow Concentrations Using a Carbon Nanotube Based Potentiometric Aptasensor" Gustavo A. Zelada-Guillén, Jordi Riu, Ali Düzgün, and F. Xavier Rius, Angewandte Chemie, 2009, 121, 7470-7473
2. "Immediate Detection of Living Bacteria at Ultralow Concentrations Using a Carbon Nanotube Based Potentiometric Aptasensor" Gustavo A. Zelada-Guillén, Jordi Riu, Ali Düzgün, and F. Xavier Rius, Angew. Chem. Int. Ed., 2009, 48, 7334-7337
3. "Covalent functionalization of single-walled carbon nanotubes with adenosine monophosphate: Towards the synthesis of SWCNT–Aptamer hybrids" Pascal Blondeau, F. Xavier Rius-Ruiz, Ali Düzgün, Jordi Riu, and F. Xavier Rius, 2011, Article in Press, doi:10.1016/j.msec.2011.05.001